Identification of Claudin-8 Interaction Partners during Neural Tube Closure

Amanda Vaccarella

Department of Human Genetics

McGill University, Montreal, Canada

August 2019

A thesis submitted to McGill University in partial fulfillment of the requirements of the degree of Master of Science

Abstract

Claudins (Cldn) are a family of integral tight junction proteins that play a role in tight junction formation. Some members of the claudin family of integral tight junction proteins play important roles in neural tube closure. Removal of Cldn4 and Cldn8 from the neural ectoderm of chick embryos caused open neural tube defects (NTD) due to a failure of convergent extension and apical constriction. Protein localization at the neural ectoderm apical cell surface was disrupted in Cldn4/Cldn8-depleted embryos. Removal of only Cldn4 had no effect on neural tube closure, suggesting that Cldn8 is required for these events. The claudin cytoplasmic C-terminal tail interacts with signaling and cytoskeletal protein complexes at the tight junction cytoplasmic face. To test the function of the Cldn8 C-terminal domain, three variants at putative phosphorylation sites (S198A, S216A, S216I) and a fourth variant with a deleted PDZ binding domain (Cldn8ΔYV) were created in the C-terminal domain of Cldn8. Electroporation of wild type Cldn8, ΔYV, and S216A into chick embryos had no effect on neural tube closure. The S216I variant resulted in open NTDs ($p<0.002$) and two-thirds of these embryos showed convergent extension defects. S198A caused only NTDs ($p<0.002$). Based on these data, I hypothesize that protein-protein interactions with the Cldn8 cytoplasmic domain are required for its function during neural tube closure. The aim of my project was to identify proteins that interact with the Cldn8 cytoplasmic C-terminal domain. Using a GST-pulldown approach followed by mass spectroscopy, 227 potential interaction partners for the Cldn8 C-terminal domain were identified. *In silico* analysis was used to select the top 10 candidates based on the following criteria: proteins known to interact with other claudins, proteins associated with NTDs, proteins that interact with Cldn4, and proteins that were present only in Cldn8 samples versus control samples. These proteins were: ZO-1, MAPK1, SEC23A, SEC24C, Caspase-3, Afadin, PPP2R2A, PPP2CA, MAT1A, and CFR-p70. Functions

of these proteins included the apoptosis pathway, phosphorylation, and transport of proteins. My data indicate that proteins of many different functions interact with the C-terminal domain of Cldn8 and these interactions may be important for regulating processes during neural tube closure.

Résumé

Les claudines (Cldn) sont une famille de protéines transmembranaires impliquées dans les jonctions serrées. Certains membres de la famille des claudines jouent un rôle important dans la fermeture du tube neural. La suppression de la Cldn4 et de la Cldn8 de l'ectoderme neural d'embryons de poulet a provoqué des anomalies de fermeture du tube neural (AFTN) dues à une défaillance lors de l'extension convergente et de la constriction apicale. La localisation des protéines à la surface de la cellule apicale de l'ectoderme neural a été perturbée chez des embryons pour lesquels les Cldn4 et Cldn8 ont été déplétés. La suppression de la Cldn4 seulement n'a eu aucun effet sur la fermeture du tube neural, ce qui suggère que la Cldn8 est nécessaire dans ces processus. La queue C-terminale cytoplasmique de la claudine interagit avec les complexes protéiques de signalisation et du cytosquelette au niveau de la face cytoplasmique des jonctions serrées. Pour tester la fonction du domaine C-terminal de la Cldn8, trois variants potentiels au niveau des sites de phosphorylation (S198A, S216A, S216I) et un quatrième variant sans le domaine de liaison PDZ (Cldn8ΔYV) ont été créés dans le domaine C-terminal de la Cldn8. L'électroporation de Cldn8, YV et S216A de type sauvage dans des embryons de poulet n'a eu aucun effet sur la fermeture du tube neural. Le variant S216I a donné lieu à des AFTN ($p < 0,002$) et les deux tiers de ces embryons présentaient des défauts dans l'extension convergente. S198A n'a causé que des AFTNs ($p < 0,002$). En lien avec ces résultats, je suppose que des interactions protéine-protéine avec le domaine cytoplasmique de la Cldn8 sont nécessaires à sa fonction lors de la fermeture du tube neural. Le but de mon projet était d'identifier les protéines qui interagissent avec le domaine C-terminal cytoplasmique de la Cldn8. En utilisant la technique "GST-pulldown" suivie par une analyse par spectrométrie de masse, 227 partenaires d'interaction potentiels pour le domaine C-terminal Cldn8 ont été identifiés. Pour sélectionner les 10 meilleurs candidats, une analyse *In silico* a été effectuée selon les critères suivants: les protéines connues pour interagir

avec d'autres claudines, les protéines associées à des AFTD, les protéines interagissant avec la Cldn4 et les protéines présentes uniquement dans les échantillons de “GST-pulldown” de la Cldn8 par rapport aux échantillons contrôles. Les 10 candidats qui ont été obtenus suite à cette analyse étaient les protéines: ZO-1, MAPK1, SEC23A, SEC24C, Caspase-3, Afadin, PPP2R2A, PPP2CA, MAT1A et CFR-p70. Ces protéines sont impliquées dans l'apoptose, la phosphorylation et le transport des protéines. Mes résultats indiquent que des protéines de aux fonctions différentes interagissent avec le domaine C-terminal de la Cldn8 et que ces interactions peuvent être importantes dans la régulations des étapes de la fermeture du tube neural.

Table of Contents

Abstract 2

Résumé 4

List of Abbreviations 9

List of Figures 12

Acknowledgements 14

Format of the Thesis 16

Contribution of Authors 17

CHAPTER 1: Introduction 18

1.1. Neural Tube Defects (NTDs) 18

1.1.1 Types of NTDs 18

1.1.2 Causes of NTDs in Humans 19

1.2 Neural Tube Formation 20

1.2.1 Neural Plate Formation 21

1.2.2 Neural Plate Shaping 22

1.2.3 Bending of the Neural Plate and Elevation of the Neural Folds 23

1.2.4 Fusion of the Neural Folds 24

1.3 Tight Junctions 24

1.3.1 Formation of Tight Junctions 25

1.3.2 Tight Junction Proteins 26

1.3.2.1 Occludin 27

1.3.2.2 Junction Adhesion Molecules (JAMs) 28

1.3.2.3 Zonula Occludens Family of Tight Junction Proteins 28

1.3.2.4 MUPP1 30

1.4 Claudin (Cldn) Family of Tight Junction Proteins 30

1.4.1 Structure of Claudins 31

1.4.2 Claudin-Claudin Interactions 32

1.4.3 C-Terminal Domain of Claudins 33

1.4.4 Post-Translational Modifications of Claudins 34

1.4.4.1 Phosphorylation 34

1.4.4.2 Palmitoylation 35

1.4.5 Claudin-8 36

1.5 Using the Chick as an Animal Model to Study NTDs 36
1.6 *Clostridium Perfringens* Enterotoxin (CPE): A Tool Used to Study the Role of Claudins 37
1.7 Claudins Are Required During Neural Plate Shaping and Median Hinge Point Formation 38
1.8 Variants in the Cldn8 Cytoplasmic C-Terminal Domain Disrupt Neural Tube Closure 38
1.8.1 Residues in the Cldn8 Cytoplasmic C-Terminus Regulate Protein Localization in Neural Ectoderm Cells 39
1.9 Rationale and Hypothesis 40
CHAPTER 2: Materials and Methods 42
2.1 Transformation of BL21 *E. coli* 42
2.2 Preparation of Bacterially-Expressed GST Fusion Protein 42
2.3 SDS-PAGE Analysis 44
2.4 Collection and Lysis of Chick Embryos 44
2.5 GST-Pulldown Assay 45
2.6 Western Blot Analysis 46
2.7 Mass Spectrometry Analysis 46
CHAPTER 3: Results 48
3.1 Validation of a GST-Pulldown Approach to Isolate Cldn8 Interaction Partners 48
3.2 Validation of a GST-Pulldown Approach to Isolate Cldn14 Interaction Partners 51
3.3 Mass Spectrometry Data for GST, GST-Cldn8 C-Terminal Domain and GST-Cldn14 C-Terminal Domain GST-Pulldown Experiments 54
3.3.1 Overview of the Mass Spectrometry Analysis of GST and GST-Cldn8 C-Terminal Domain Pulldowns 55
3.3.2 Overview of the Mass Spectrometry Analysis of GST and GST-Cldn14 C-Terminal Domain Pulldowns 63
3.3.3 Validating the Efficiency of the GST-Pulldowns by Characterization of Claudin and ZO-1 Peptides Present in Cldn8 and Cldn14 C-Terminal Domain GST-Pulldowns 66
3.4 Prioritizing Cldn8 Interacting Partners for Further Analysis 68
3.5 The Top 10 Cldn8 Proteins Identified for Further Functional Analysis 78
CHAPTER 4: Discussion 82
4.1 Interactions that Occur Between ZO-1 and Cldn8 Are Important for TJ Assembly, Linking the TJ to the Actin Cytoskeleton and Formation of the TJ Cytoplasmic Plaque 84
4.2 COPII-Mediated Vesicle Transport Proteins Sec23A and Sec24C Are Known to Interact with Claudins and Sec23A Has Been Associated with NTDs 85

4.2.1 The Non-Canonical and Canonical Wnt/PCP Pathways, and the Regulation of Convergent Extension during Neural Tube Closure 86

4.3 The Association of Folic Acid and NTDs 87

4.4 Apoptosis May Be Necessary During Stages of Neurulation 88

4.5 Kinases and Phosphatases that Regulate Tight Junction Formation and the Phosphorylation Events that Mediate These Processes 90

4.6 Limitations of Using a GST-Pulldown Approach to Identify Cldn8 C-Terminal Domain Interacting Partners 92

4.7 A Proposed Model of Interactions that Occur at the C-Terminal Domain of Cldn-8 93

CHAPTER 5: Conclusions and Future Directions 96

5.1 Conclusions 97

5.2 Future Directions 98

CHAPTER 6: References 101

Appendix A: Permission to Reprint 115

Appendix B: Mass Spectrometry Data for Cldn8 C-Terminal Domain HH8 Samples 117

Appendix C: Mass Spectrometry Data for Cldn14 C-Terminal Domain HH8 and Day 4 Samples 130

List of Abbreviations

°C: Degrees Celsius

µg: Microgram

µL: Microliter

ATP: Adenosine tri-phosphate

BMP: Bone morphogenetic protein

BSA: Bovine serum albumin

Ca^{2+}: Calcium ion

Cl^-: Chloride ion

Cldn: Claudin

CPE: Clostridium perfringens enterotoxin

C-CPE: C- terminal domain of Clostridium perfringens enterotoxin

CRB: Crumbs

DLHP: Dorsolateral hinge point

DNA: Deoxyribonucleic acid

DTT: Dithiothreitol

FGFR: Fibroblast growth factor receptor

FWHM: Full width at half maximum

Grhl: Grainyhead-like

GST: Glutathione-S-transferase

GUK: Guanylate kinase

HCD: Higher energy collisional dissociation

HCV: Hepatitis C virus

HH: Hamilton and Hamburger

IPTG: Isopropyl β-D-galactopyranoside

JAM: Junctional adhesion molecule

kDa: Kilodalton

LB: Luria-Bertani broth

MAPK: Mitogen-activated protein kinase

MDCK: Madin-Darby canine kidney

MHP: Median hinge point

ml: Millilitre

MLC: Myosin light chain

MLCK: Myosin light chain kinase

mM: Millimolar

MUPP1: Multi-PDZ domain protein 1

N-: Amine-terminal region

Na^+: Sodium ion

NaCl: Sodium Chloride

ng: Nanogram

NTD: Neural tube defect

PALS: Protein associated with Lin-7

PATJ: Protein associated with Lin-7-associated tight junction

PAR: Partitioning defective

PBS: Phosphate buffered saline

PCP: Planar cell polarity

PDZ: Post-synaptic density 95/Drosophila discs large/Zonula occludens-1

pH: Potential of hydrogen

PKC: Protein kinase C

Rho: Ras homolog gene family

RNA: Ribonucleic acid

ROCK: Rho kinase

rpm: Revolution per minute

RT: Room temperature

SDS: Sodium dodecyl sulfate

SH3: Src-homology3

SHH: Sonic hedgehog

TER: Transepithelial electrical resistance

Wnt: Wingless integrated site

WT: Wild type

ZO: Zonula occludens

List of Figures

Figure 1: Neural Tube Formation in the Chick Embryo 21
Figure 2: Function of Tight Junctions 26
Figure 3: Tight Junction Proteins 30
Figure 4: Structure and Function of Claudins 32
Figure 5: Overexpressing S216I in Chick Embryos Result in NTDs and Convergent Extension Defects 39
Figure 6: Schematic of the Cldn8 C-Terminal Domain 41
Figure 7: Western Blot Analysis of GST and ZO-1 Localization in Unbound and Bound Fractions from GST-Pulldown Experiments to Identify Cldn8 C-Terminal Domain Interacting Partners 50
Figure 8: Western Blot Analysis of GST and ZO-1 Localization in Unbound and Bound Fractions from GST-Pulldown Experiments to Identify Cldn14 Interacting Partners 54
Figure 9: Proposed Model of Cldn8 C-Terminal Domain Interactions 96

List of Tables

Table 1: Total Proteins and Peptides Identified in Individual Samples of Cldn8 C-Terminal Domain Biological Replicates..... 58
Table 2: The Number of Chick Proteins Identified in Individual Cldn8 C-Terminal Domain Samples, and the Total Number of Proteins in Common Between Duplicate Samples 61
Table 3: The Total Number of Chick Proteins in Each Cldn8 C-Terminal Domain Sample Per Biological Replicate, and a Comparison Between Cldn8 C-Terminal Domain and GST Samples per Replicate..... 63
Table 4: The Total Number of Proteins and Peptides Identified in Cldn14 C-Terminal Domain HH8 and Day 4 Samples 65
Table 5: The Total Number of Chick Proteins Identified in Cldn14 C-Terminal Domain Samples and A Comparison of Cldn14 C-Terminal Domain Samples Vs GST..... 66
Table 6: The Criteria Used to Prioritize Cldn8 Interacting Partners..... 70
Table 7: The 40 Proteins Chosen for Further Analysis That Were Identified by Mass Spectrometry in Cldn8 C-Terminal Domain Samples 75
Table 8: Do the Cldn8 Interacting Partners Also Interact with Cldn14? 78
Table 9: The Top 10 Cldn8 Interacting Partners for Further Analysis 81

Acknowledgements

I would like to sincerely thank my supervisor, Dr. Aimee Ryan, for all her help, support, and patience over the past two years. No matter how extremely busy her schedule was, she always made the time to meet with me, go over my data and presentations and was always understanding. Thank you for always pushing me above my limit and for being an excellent role model.

I would like to thank the members of my supervisory committee, Dr. Colin Crist and Dr. Elena Torban, for all their innovative and valuable insights for my project, and to the Proteomics Platform at the RI-MUHC, specifically Dr. Lorne Taylor, for his countless hours helping me analyze my data. I would also like to thank Dr. Loydie Majewska, Dr. Indra Gupta, and all their lab members for their input and questions during lab meetings.

I am grateful to have been surrounded by such a great group of lab members throughout the past two years. Thank you to all my previous and current lab members: Amanda Baumholtz, Enrique Gamero Estevez, Jenna Haverfield, Simon La Charité-Harbec, Maria Laverde, Elizabeth Legere, and Dareen Almohammadi, for all their input during lab meetings, and for always taking their time to answer my questions, listen to presentations, and for all their support and discussions throughout the years.

I would especially like to thank Amanda Baumholtz, for sharing her knowledge with me, taking time out of her day to look at my presentations, and more importantly, for the friendship we have developed over the past two years. I would also like to thank Enrique Gamero Estevez for all the time he took to train me, and for mentoring me throughout the past two years. Thank you for answering all my questions, and for all the techniques that you showed me. Thank you to Vasikar

Murugapoopathy for all the time you took out of your day to challenge me by asking me questions on my project, and for being there for me when things weren't going as planned.

I would also like to thank my parents and my family for their unconditional love and support throughout the past two years. Thank you for understanding my hectic schedule and for being so understanding.

Format of the Thesis

This traditional master´s thesis was written according to the guidelines and format stated by Graduate and Postdoctoral Studies, McGill University.

Contribution of Authors

The candidate prepared and performed all the experiments presented here. The candidate, together with her supervisor, Dr. Aimée Ryan, participated in the experimental design, analyzed the data and edited all the content in this thesis.

CHAPTER 1: Introduction

My thesis research focuses on identifying the interacting partners of the Cldn8 C-terminal domain. Claudins are integral tight junction proteins that regulate paracellular permeability and apical-basal cell polarity. Their cytoplasmic C-terminal domain interacts with the actin cytoskeleton through adaptor proteins. When Cldn4 and -8 are simultaneously removed from tight junctions of the neural ectoderm, neural tube defects are seen in chick and mouse embryos and are caused by aberrant protein localization to the apical surface of neural ectoderm cells (Baumholtz et al., 2017). Removing only Cldn4 from tight junctions does not cause neural tube defects. Therefore, I hypothesize that Cldn8 plays a critical role in regulating neural tube closure through protein interactions at its cytoplasmic C-terminal domain. The introduction describes neural tube closure, the claudin family of tight junction proteins and the data from previous studies in the lab supporting my hypothesis that protein interactions that occur at the C-terminal domain of Cldn8 are important for the function of Cldn8 during neural tube closure.

1.1. Neural Tube Defects (NTDs)

Neural tube defects are a result of a failure of neural tube closure. They are the second most common birth defect, with an incidence of 1-2 per 2000 births in North America, and up to 20 per 1000 births in certain regions of China (Au et al., 2010; Zaganjor et al., 2016).

1.1.1 Types of NTDs

Open NTDs occur when there is a failure of neural tube closure in primary neurulation and occurs at any position along the anterior-posterior axis of the embryo (De Marco et al., 2011). A failure of secondary neurulation leads to closed NTDs which are covered by a layer of skin (Copp et al., 2013). The three types of open NTDs are myelomeningocele (spina bifida), which is failure of the neural tube in the spinal region, anencephaly, which is failure of the neural tube in the cranial

region, and craniorachischisis, the most severe NTD, which is when the brain and spinal region remain open (Botto et al., 1999; De Marco et al., 2011)

1.1.2 Causes of NTDs in Humans

Neural tube defects are a complex disease caused by both environmental and genetic factors which can interact together (Greene et al., 2014). Maternal malnutrition, such as having a low folate intake, has been linked to NTDs. Folic acid supplementation and fortification reduce up to 70% of NTDs (Blencowe et al., 2010). Other factors, such as maternal diabetes, may contribute to NTDs (Bell et al., 2012; Nikolopoulou et al., 2017) and it has been shown that mothers with diabetes that do not take folic acid supplementation have a two times greater risk of having babies with NTDs than diabetic mothers that do take folic acid supplementation (Correa et al., 2012).

It has also been shown that genetic factors can contribute to NTDs, and more than 200 genetic mouse models have been generated for NTDs, including folate-related genes, genes involved in cell death, and planar cell polarity (PCP) genes (Harris et al., 2010) . Families that have a child with a NTD have a 10-12-fold higher chance of having other children with NTDs (Pangilinan et al., 2012). While folic acid deficiency is considered an environmental factor that contributes to NTDs, mutations in genes in the folic acid pathway such as 5,10-methylene-tetrahydrofolate reductase (MTHFR) are genetic contributors to NTDs. A single nucleotide polymorphism in the MTHFR gene is associated with NTDs (Kibar et al., 2007; Pangilinan et al., 2012). Mutations in genes involved in the planar cell polarity (PCP) pathway, which is essential for proper neural tube closure, have also been associated with human NTDs (De Marco et al., 2011; Kibar et al., 2007). Mutations in other genes involved in cell-shaping events that are crucial during neural closure have also been associated with human NTDs, such as *SHROOM3*, which is an actin-binding protein involved in apical constriction, (Haigo et al., 2003; Hildebrand, 2005; Lee et al., 2007), Sonic

hedgehog (*SHH*), which is involved in the bending of the neural tube, and *PAR3*, which is involved in establishing apical-basal polarity (Chen et al., 2017).

1.2 Neural Tube Formation

Neural tube formation occurs in two phases - primary and secondary neurulation (Nikolopoulou et al., 2017). Primary neurulation forms the portion of the neural tube that gives rise to the brain and most of the spinal cord. Following completion of primary neurulation, the posterior neural tube is formed by secondary neurulation. Both primary and secondary neurulation are required to generate the complete neural tube of mammals, amphibians, and birds. This research will be identifying Cldn8 interaction partners during primary neurulation, which can be divided into four different stages: 1) neural plate formation (HH4), 2) neural plate shaping (HH6-9), 3) elevation of neural folds (HH8-10), and 4) fusion of neural folds (HH9-12) (Figure 1) (Moury et al., 1995). The events that occur at each of the four phases are as follows: Cells at the anterior end of the embryo thicken along their apical-basal axis to form a horseshoe shape called the neural plate. The neural plate then narrows and lengthens due to convergent extension movements. Apical constriction of cells at the midline of the neural plate forms the median hinge point, which enables the bending of the neural plate and elevation of the neural folds. Finally, epithelial remodeling unites the neural folds and separation occurs from the non-neural ectoderm, leading to a closed neural tube and an overlying layer of surface ectoderm (Colas et al., 2001; Pai et al., 2012).

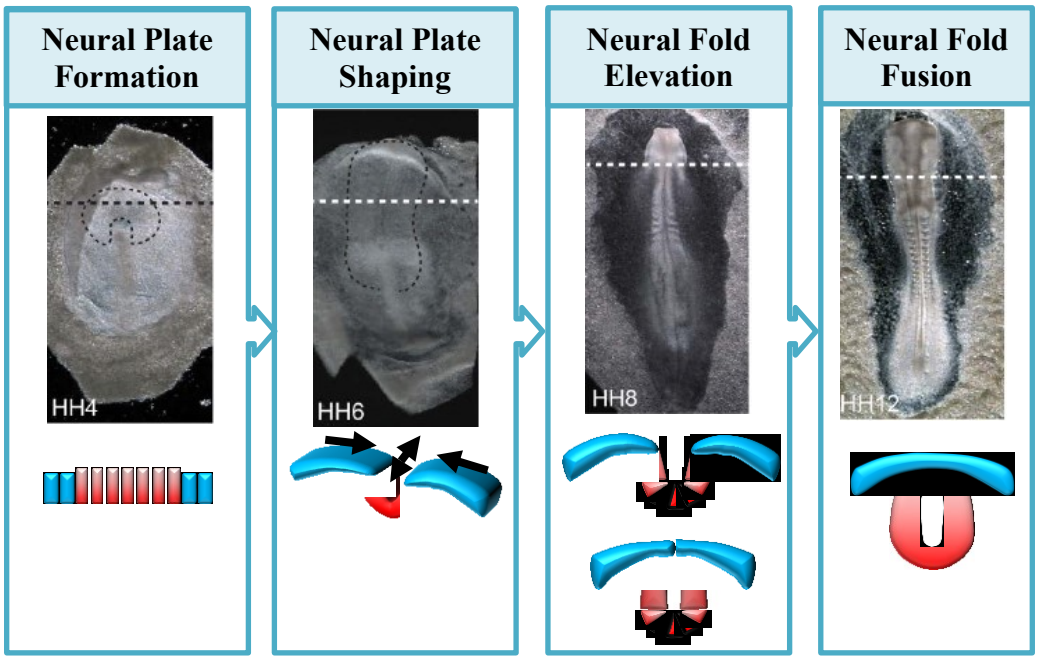

Figure 1: Neural Tube Formation in the Chick Embryo
The embryos (top) and cartoon images (bottom) in each panel show the different stages at which these events occur. Blue represents non-neural ectoderm, while the red represents neural ectoderm. A. Neurulation begins with induction of the neural plate. Cells in the neural plate thicken along their apical-basal axis. B. Convergent extension allows for the neural plate to narrow medio-laterally and elongate along the anterior-posterior axis. This morphologically distinguishes the neural ectoderm (red) from non-neural ectoderm (blue). C. Apical constriction occurs at the midline of the neural plate, which allows for the neural plate to bend and elevate, forming bilateral neural folds, which converge toward the midline, forming the median hinge point (MHP). Completion of neural tube closure involves fusion of the opposing neural folds to form a closed neural tube. D. Epithelial remodeling unites the lateral edges of the neural folds and separates them from the adjacent non-neural ectoderm to yield a closed neural tube and continuous layer of overlying surface ectoderm. Figure from Baumholtz, 2018.

1.2.1 Neural Plate Formation

After gastrulation has occurred, a flat epithelial sheet called the ectoderm covers the dorsal surface of the embryo and primary neurulation begins with the induction of the neural plate (Stern, 2005). Neural plate formation involves thickening of the neural plate along the apical-basal axis of the ectoderm, and this thickening distinguishes the neural ectoderm cells from the adjacent and flatter non-neural ectoderm cells (Schoenwolf et al., 1987). In chick and mouse, bone morphogenic protein (BMP) and fibroblast growth factor (FGF) signaling are required for neural induction

(Rodriguez-Gallardo et al., 1997; Rogers et al., 2011; Streit et al., 2000), while only BMP antagonists are sufficient to induce a neural fate in amphibians (Hawley et al., 1995; Rodriguez-Gallardo et al., 1997). At the end of this phase, the neural plate is made up of columnar epithelial cells, which already has apical-basal polarity. Apical-basal polarity is important for neural tube closure as the process of neurulation consists of apical-basal events such as apical constriction (Chen et al., 2017).

1.2.2 Neural Plate Shaping

During this phase, the neural plate thickens along the apical-basal axis and convergent extension causes the neural plate to narrow along its medio-lateral axis, and elongate along its anterior-posterior axis (Moury & Schoenwolf, 1995; Schoenwolf, 1988). Defects in the convergent extension process cause shortening and widening of the neural plate and, because of this, the neural folds do not come close enough to fuse (Davidson et al., 1999; Schoenwolf et al., 1989). The process of convergent extension is regulated by the non-canonical Wnt/planar cell polarity (PCP) pathway. This pathway is conserved from *Drosophila*, where it was first identified, to higher vertebrates (Devenport, 2016; Nikolopoulou et al., 2017). PCP-dependent convergent extension is also required in *Xenopus*, and in the absence of the PCP genes, the neural plate is wide and short, and the neural folds do not elevate enough to appose or fuse to each other (Wallingford, 2002). Mice carrying mutations in PCP genes also have cranial and spinal neural tube defects (Curtin et al., 2003; Kibar et al., 2001; Murdoch et al., 2014; J. Wang et al., 2006; Y. Wang et al., 2006). These data suggest that convergent extension and components of the PCP pathway are important for proper neural tube closure. Humans with mutations in the PCP pathway also have NTDs (De Marco et al., 2013; De Marco et al., 2012; Kibar et al., 2009; Robinson et al., 2012).

1.2.3 Bending of the Neural Plate and Elevation of the Neural Folds

During this phase of neural tube closure, the neural plate begins to bend and elevate, creating bilateral neural folds that converge towards the midline. Through a process called apical constriction, the neuroepithelial cells at the midline of the neural plate constrict at the apical surface and these cells go from being columnar to a wedge shape. This forms the median hinge point (MHP) and this change in cell shape is what allows the neural folds to elevate and for the neural groove to form (Schoenwolf et al., 1984; Smith et al., 1994). MHP formation is induced by the secretion of Sonic hedgehog (Shh) and BMP antagonist's chordin and noggin from the notochord underlying the neural tube (Patten et al., 2002; Ybot-Gonzalez et al., 2007). It is important to note that neural tube closure is a continuous process, and that convergent extension and apical constriction are occurring together.

Both intrinsic and extrinsic forces are required for the morphogenetic movements associated with bending and elevation of the neural plate (Moury & Schoenwolf, 1995; Schoenwolf & Alvarez, 1989). Intrinsic forces are responsible for neural plate bending and are generated by the formation of the median hinge point (MHP), which is formed through apical constriction, and the paired dorsolateral hinge points (DLHPs). Folding around the DLHPs results in neural fold convergence. Extrinsic forces are generated by cell-shape changes and position of non-neural ectoderm cells and contributes to neural fold elevation.

The bending and narrowing of the neural plate and the process of apical constriction are also mediated by the PCP pathway (Nishimura et al., 2012). The PCP protein Celsr1 interacts with the proteins DAAM1, Dishevelled and RhoGEF, and these interactions upregulate Rho kinase (ROCK). This, in turn, causes actomyosin contraction and promotes apical constriction. The activation of myosin light chain (MLC) is crucial for apical constriction (Escuin et al., 2015;

Kinoshita et al., 2008), and the interactions between the PCP pathway and RhoA-ROCK signaling at the apical surface lead to the phosphorylation of MLC, along with actin-myosin contraction. These events are what cause the apical surface of the cells to constrict (Nishimura et al., 2012). When chick embryos were treated with the ROCK inhibitor Y27632, the neural folds did not elevate. When chick embryos were exposed to a RhoA inhibitor, C3, the MHP did not form (Escuin et al., 2015).

1.2.4 Fusion of the Neural Folds

The final phase of neural tube closure is the fusion of the apposed bilateral neural folds. Before fusion occurs, the non-neural ectoderm and the neural ectoderm are in direct contact (Schoenwolf, 1979). Epithelial remodeling unites the lateral edges of the neural folds and separates them from the adjacent non-neural ectoderm to yield a closed neural tube and continuous layer of overlying surface ectoderm. Separation of the non-neural and neural ectoderm results in formation of two epithelial layers: the underlying neural tube and the non-neural or surface ectoderm. Not much is known about the mechanism behind epithelial remodeling; however, apoptosis is thought to be a consequence of neural fold fusion, and cells that lose cell-cell adhesion undergo apoptosis during epithelial remodeling. Inhibiting or knocking-out pro-apoptotic genes in chick (Weil et al., 1997) and mouse (Cecconi et al., 1998) causes NTDs.

1.3 Tight Junctions

Epithelial cells are connected by junctional complexes zona occludens (tight junctions), zonula adherens (adherens junctions) and basal macula adherens (desmosomes). Tight junctions (TJs) were first identified in epithelial tissues of rat and guinea pig in the 1960s by Farquhar and Palade, through transmission electron microscopy (Farquhar et al., 1963).

Tight junctions are the most apical cell-cell junction between adjacent epithelial and endothelial cells, defining the boundary between the apical and basolateral area of the cell and regulate gene expression, cell proliferation and differentiation, and also maintain apical-basal polarity (Guillemot et al., 2008). They have various functions serving as both a fence and as a gate. Tight junctions serve as a fence within the same cell to prevent movement of proteins from the apical and basolateral surfaces and maintain apical-basal polarity. They serve as a gate between adjacent cells, regulating the paracellular movement of certain molecules and ions between apical and basolateral surfaces. Tight junctions form a tight seal between neighboring cells (Balda et al., 1996), and are composed of different types of transmembrane proteins including: occludin, claudins, junctional adhesion molecules (JAMs) and Multi-PDZ domain protein 1 (MUPP1) (Furuse et al., 1998; Furuse et al., 1993; Martin-Padura et al., 1998).

1.3.1 Formation of Tight Junctions

Tight junction formation is linked to two complexes that drive the apical-basal polarization of epithelial cells: The Crumbs polarity complex, and the partitioning defective (PAR) complex. The Crumbs polarity complex is composed of Lin Seven 1 (PALS1), PALS1-associated tight junction homologue (PATJ), and Crumbs (CRB) (Campanale et al., 2017). This complex was first discovered in *Drosophila melanogaster*, and is found at the apical membrane and border between epithelial cells, (Tepass et al., 1990), where it plays a role in apical-basal polarity (Campanale et al., 2017).

The Par complex is composed of Par3, Par6, and atypical protein kinase C (αPKC) (Campanale et al., 2017). These proteins were first identified in *C. elegans* (Kemphues et al., 1988). Both the Par3 and Par6 proteins have PDZ binding domains, which are described in further detail below (Hung et al., 1999). The Par proteins interact with Cdc42, a small Rho GTPase that modulates cell

polarity (Qiu et al., 2000). Par6 binds to Par3, αPKC, Cdc42 and also to PALS1 and CRB3 from the Crumbs polarity complex (Hurd et al., 2003; Qiu et al., 2000). These interactions are what link both polarity complexes to each other and establishes apical-basal polarity. Then, tight junctions are positioned at the apical membrane once epithelial cells are polarized, thus preventing the mixing of apical and basolateral proteins (Figure 2).

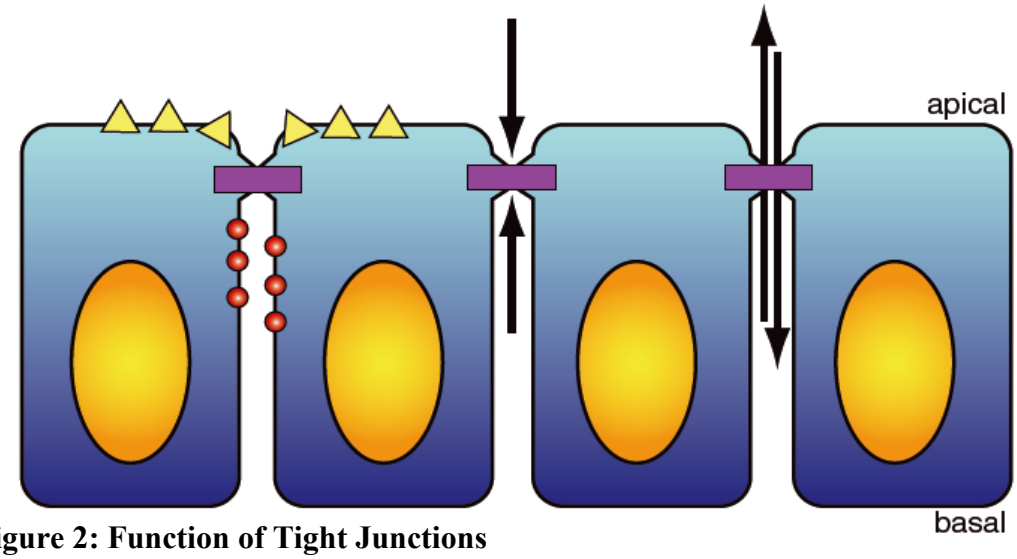

Figure 2: Function of Tight Junctions
Tight junctions (purple rectangles) are the most apical cell-cell junction and regulate the paracellular movement of ions and select for size and charge of ions. They have multiple functions, such as serving as a gate and fence. Tight junctions serve as a fence by separating proteins at the apical surface (yellow triangles) from proteins at the basal lateral surface (red circles). The arrows represent the movement of ions and small molecules through the paracellular space. Figure from Gupta and Ryan, 2010.

1.3.2 Tight Junction Proteins

Tight junctions are composed of transmembrane and cytoplasmic proteins. Transmembrane proteins include claudins, occludin, JAMs and MUPP1 (Figure 3). These proteins interact with scaffolding proteins at the cytoplasmic plaque including Zonula Occluden proteins (ZO-1, ZO-2, and ZO-3) (Figure 3). The interactions between scaffolding proteins such as ZO-1 and transmembrane proteins such as claudins are what link the tight junction to the actin cytoskeleton (Fanning et al., 1998; Wittchen et al., 1999). Some transmembrane proteins that are a functional

component of tight junctions have a PDZ domain, which stands for PSD-95/discs-large/Zonula occludens-1 (PDZ) domain. Some transmembrane domains instead have a PDZ biding domain or binding motif. Some interactions between transmembrane proteins occur between the PDZ domain and the PDZ biding domain or motif. PDZ binding motifs are conserved in most claudins and the last few amino acids at the end of the C-terminal domain are part of this PDZ-binding motif. Although this thesis focuses on claudins, and specifically on Cldn8, the other tight junction proteins at the cytoplasmic plaque are important, as they form interactions directly or indirectly with claudins, and these interactions are what regulate and form the tight junction.

1.3.2.1 Occludin

Occludin was the first integral tight junction membrane protein identified (Furuse et al., 1993). It is composed of cytoplasmic N- and C- termini, four transmembrane domains, and two extracellular loops (Furuse et al., 1994), and has a molecular weight of 60-65 kDa. Occludin was determined to be endogenously expressed and localize to tight junctions in MDCK cells (Balda et al., 1996), an epithelial cell line that endogenously forms tight junctions. Occludin was found to bind to the zonula occludens proteins (ZO-1, ZO-2, and ZO-3) through its C-terminal domain, linking occludin to the actin cytoskeleton (Furuse et al., 1994). The C-terminal cytoplasmic domain of occludin is needed for its localization to the tight junction (Furuse et al., 1994).

As stated previously, tight junctions regulate the paracellular permeability of selective ions, and occludin was shown to increase this paracellular permeability when there was an overexpression of truncated C-terminal domain of occludin in epithelial cells (Balda et al., 1996). Expression of wild-type and mutant occludin increased transepithelial resistance (TER) in MDCK type 2 cell lines. Paracellular flux measures transport capabilities over a period of time, while TER measures the tightness. When occludin is knocked-down in cell lines, tight junctions still form (Yu et al.,

2005). Overall, the data show that occludin is not required for tight junction formation but is important for cell adhesion properties of tight junctions.

1.3.2.2 Junction Adhesion Molecules (JAMs)

JAMs are part of the immunoglobulin superfamily and are composed of one transmembrane domain, two immunoglobulin-like extracellular loops, and a C-terminal domain that contains a PDZ-binding domain (Martin-Padura et al., 1998). This PDZ binding domain interacts with proteins at the tight junction cytoplasmic plaque such as ZO-1, MUPP1, and Par3, which is part of the Par polarity complex (Bazzoni et al., 2000; Ebnet et al., 2004). The family of JAMs is composed of three proteins: JAM-A, JAM-B, and JAM-C, which are enriched at tight junctions of epithelial cells (Ebnet et al., 2004; Martin-Padura et al., 1998). It has been shown that JAMs regulate cell polarity. Unlike claudins, it has been shown that JAMs are not required for tight junction formation, but they still play a role in the function of tight junctions such as barrier formation (Ebnet et al., 2003; Laukoetter et al., 2007). When JAM-A was ectopically expressed in fibroblasts, tight junction strands did not form (Itoh et al., 2001).

1.3.2.3 Zonula Occludens Family of Tight Junction Proteins

Zonula occludens (ZO) proteins ZO-1, ZO-2, and ZO-3 are located at the cytoplasmic plaque of tight junctions and are composed of three PDZ domains, a Src-3 homology 3 (SH3) domain, and a Guanylate Kinase (GUK) homology domain, which binds to occludin. All ZO proteins are part of the Membrane Associated Guanylate Kinase (MAGUK) family of proteins (Willott et al., 1993). The ZO proteins interact with each other through their second PDZ domain (Utepbergenov et al., 2006), while their first PDZ domain interacts with the C-terminal domain of transmembrane proteins such as claudins, occludin, and JAMS (Itoh et al., 1999). All ZO proteins bind directly to the actin cytoskeleton at their C-terminal regions (Itoh et al., 1999; Wittchen et al., 1999).

ZO-1 is ~225 kDa and was the first tight junction associated protein to be identified (Stevenson et al., 1986). ZO-1 interacts with components of the planar cell polarity (PCP) and Wnt-signaling pathways, which will be discussed in further detail below (Van Itallie et al., 2013). ZO-2 is 160 kDa and was identified when it co-immunoprecipitated with ZO-1 (Gumbiner et al., 1991). ZO-3 is 130 kDa and was later identified when it co-immunoprecipitated with ZO-1 (Balda et al., 1993). ZO-3 has been shown to bind to ZO-1 and occludin, but not ZO-2 (Haskins et al., 1998).

ZO proteins have a role in tight junction assembly, specifically through their PDZ domains. (Umeda et al., 2006). When ZO-1 is knocked out and ZO-2 is knocked down in epithelial cells, these epithelial cells are polarized but do not form tight junctions (Umeda et al., 2006). This suggests that ZO-1 and ZO-2 can mark the location of tight junctions and can determine where claudins are polymerized. The exogenous expression of ZO-1 and ZO-2 rescues tight junction formation, while ZO-3, which is not expressed in these epithelial cells, does not (Umeda et al., 2006). ZO proteins are also required for embryonic development. Deficiency in ZO-1 causes an embryonic lethal phenotype in mice with extensive cell death in epithelial tissues (Katsuno et al., 2008). ZO-2 null mice have increased apoptosis and decreased proliferation and die shortly after implantation (Xu et al., 2008). ZO-3, however, is dispensable, as mice lacking ZO-3 show no phenotype. These data show that ZO proteins have different roles in embryogenesis.

1.3.2.4 MUPP1

MUPP1 is a scaffolding protein that contains 13 PDZ domains, and is localized at the tight junction cytoplasmic plaque (Guillemot et al., 2008). It was first identified as a protein that interacts with serotonin (Ullmer et al., 1998), and was also identified to interact with the C-terminal domain of Claudin-1 (Hamazaki et al., 2002). MUPP1 interacts with other adaptor and transmembrane proteins through its PDZ domain; however, it is not required for tight junction formation.

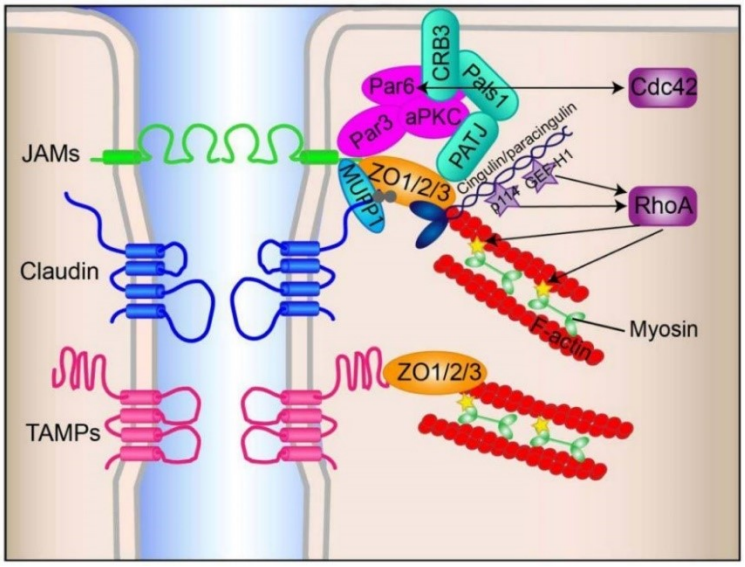

Figure 3: Tight Junction Proteins
The tight junction is made up of transmembrane proteins, including claudins, occludin, and JAMS. These interact with the scaffold proteins zonula occludens (ZO-1, ZO-2, and ZO-3), and these interactions are what link the tight junction to the actin cytoskeleton. Two complexes, the Crumbs polarity complex (turquoise) and the Par polarity complex (pink), are involved in the formation of tight junctions. Figure from Baumholtz, 2018.

1.4 Claudin (Cldn) Family of Tight Junction Proteins

Claudins are a family of integral tight junction proteins. The word claudin is derived from the Latin word “claudere” which means “to close”, as claudins are the principle barrier-forming proteins in tight junctions. Claudins were first discovered when re-examining junction fractions from chicken liver, which were used to isolate occludin (Furuse et al., 1998). Two proteins other

than occludin were identified, and these proteins also had four transmembrane domains and were present in the tight junctions in the chicken liver. These proteins did not have any sequence homology to occludin but did co-localize with occludin at tight junctions. These proteins were named “claudin-1” and “claudin-2” (Furuse et al., 1998).

1.4.1 Structure of Claudins

*CLDN*s encode proteins of molecular weights between 20-27 kDa (Furuse et al., 1998). There are 24 known claudins in humans, and 19 in the chick (*gallus gallus*). They are comprised of two extracellular loops (EL), four transmembrane domains, and cytoplasmic N- and C-termini (Figure 4) (Furuse et al., 1998). Little is known about the N-terminal domain; however, it is composed of two to seven amino acids. The first extracellular loop determines the size and charge selectivity of tight junctions. This is due to the combination of charged amino acids present in this first loop, which is composed of roughly 50 amino acids that vary considerably between claudins (Piontek et al., 2017).

The second extracellular loop participates in *trans*-interactions with claudins in adjacent cells (Piontek et al., 2008) and in *cis*-interactions with claudins in the same cell (Suzuki et al., 2014). The second extracellular loop is smaller than the first extracellular loop, being composed of 16-33 amino acids. The transmembrane domains are also involved in *cis*-interactions with neighboring claudins and required for correct folding and assembly of claudins (Rossa et al., 2014). The C-terminal domain has the most sequence variability between claudin family members. The C-terminal domain interacts with different adaptor and scaffold proteins, such as ZO-1, and these interactions are what link the tight junction to the actin cytoskeleton. The C-terminal domain can be post-translationally modified, including phosphorylation and palmitoylation (D’Souza et al., 2005, Van Itallie et al., 2005). Claudins have also been categorized as either cation barriers (Cldn1,

-5, -8, -11, -14, -19), cation pores (Cldn2, -10b, -15, 16), anion barriers (Cldn6 and -9) or anion pores (claudin-10a) (González-Mariscal et al., 2012).

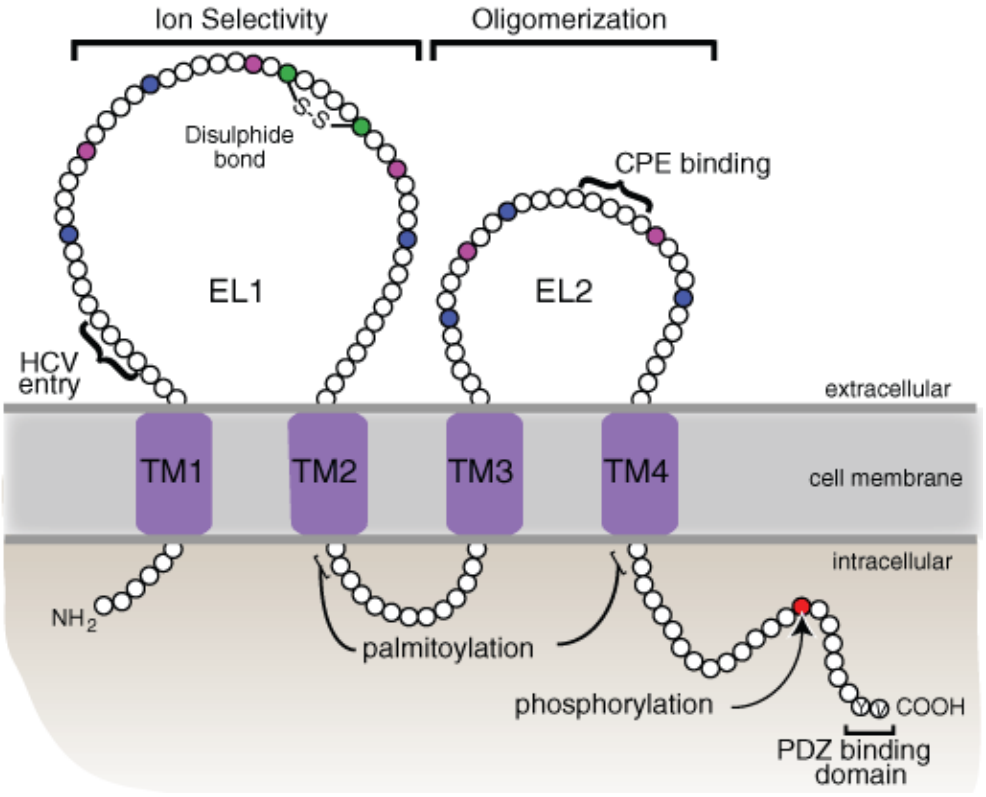

Figure 4: Structure and Function of Claudins
Claudins are composed of cytoplasmic N and C-termini, two extracellular loops (EL), and four transmembrane domains (TM). Most claudins have a conserved YV residue at the end of the C-terminal domain, which is part of the PDZ binding domain. This domain interacts with proteins such as ZO-1, linking the tight junction to the actin cytoskeleton. From Gupta and Ryan, 2010.

1.4.2 Claudin-Claudin Interactions

When like claudin family members interact with one another, this is known as a homophilic interaction and when different claudin family members interact with one another, it is known as a heterophilic interaction. The second extracellular loop of claudins interact in *trans*- with claudins in apposing cells, and participate in *cis*-interactions with claudins in the same cell (Piontek et al., 2008; Suzuki et al., 2014). Not all claudins interact with one another. For example, Cldn4 interacts

with Cldn3 and -8 but not with Cldn7 or with itself (Gong et al., 2015), and although Cldn4 can interact with Cldn3 through *cis* interactions, it cannot interact with Cldn3 through *trans* interactions (Daugherty et al., 2007).

Interactions between different claudin family members are important for integration into tight junctions. Cldn4 and -8 are present in the neural ectoderm in the chick during neurulation. Although this thesis focuses on Cldn8, the interactions that occur between Cldn4 and -8 may be of importance. It has been shown that the assembly of Cldn4 into tight junction strands in collecting duct cells of kidneys requires interaction with Cldn8 (Hou et al., 2010). When there was a depletion of Cldn8, there was a loss of paracellular chloride conductance through a mechanism involving recruitment of Cldn4 (Hou et al., 2010). In Cldn4 knockout mice, there is also a reduced localization of Cldn8 to tight junctions in the kidney (Fujita et al., 2012). In Cldn8 knockout mouse kidneys, there is no Cldn4 localization (Gong et al., 2015). These interactions that occur between claudins within a cell and between cells give the ability to generate tight junctions.

1.4.3 C-Terminal Domain of Claudins

The C-terminal domain is the most variable domain between different claudin family members, ranging in size between 21 to 63 amino acids (Ruffer et al., 2004). The last two amino acids in the C-terminal domain (YV) are conserved, except in Cldn12 and -23 (Collins et al., 2013). The YV amino acid residues are part of the PDZ- binding motif, which interacts with other proteins at the cytoplasmic plaque of tight junctions, such as ZO-1 and MUPP1 (Guillemot et al., 2008).

Although the sequences important for proper tight junction targeting in Cldn1 and -5 (aa 188 ± 207 in Cldn1 and 182 ± 196 in Cldn5) are conserved between species, they do not show similarities to one another (Ruffer & Gerke, 2004). The importance of the PDZ-binding motif in regulating claudin localization to the tight junction differs between family members. While it is not required

for Cldn1 localization to the tight junctions (Kobayashi et al., 2002), it is critical for the ability of Cldn16 to localize to tight junctions (Muller et al., 2003). When looking at residues in the C-terminal domain of Cldn1 and -5, it was shown that residues between the PDZ-binding sequence and the fourth transmembrane domain were indispensable for proper tight junction localization (Ruffer & Gerke, 2004).

As stated earlier, Cldn4 and -8 are present in the neural ectoderm during neurulation, and the presence of both these claudins together has been looked upon in various studies. In a study published by Fredriksson et al., proteins that interact with the Cldn4 C-terminal domain and occludin were identified through mass spectrometry (Fredriksson et al., 2015). Proteins shown to interact with the Cldn4 C-terminal domain were enriched in signaling and trafficking proteins. The PDZ binding motif in Cldn4, -5, and -8 interact with MUPP1 (Jeansonne et al., 2003). This finding is important because MUPP1 is a scaffold protein, and interactions that occur at the C-terminal domain of claudins, such as with scaffolding proteins, are predicted to link the tight junction to the actin cytoskeleton and signaling events such as cell shaping, which are important during morphogenesis (Gupta et al., 2010).

1.4.4 Post-Translational Modifications of Claudins

Post-translational modifications, including phosphorylation and palmitoylation, occur to claudins, and these modifications affect protein stability and localization.

1.4.4.1 Phosphorylation

Many proteins are phosphorylated in mammalian cells, and phosphorylation regulates aspects of protein function and structure, such as protein folding, protein-protein interactions, and stability (Nishi et al., 2011; Van Itallie et al., 2004). The C-terminal domains of claudins are enriched in

serine, threonine, and tyrosine residues (Van Itallie et al., 2018), which can be phosphorylated and this can affect the protein interactions that occur at the C-terminal domain of claudins, and at the tight junction (Tanaka et al., 2005).

Thr-203 in the C-terminal domain of Cldn1 is phosphorylated by mitogen activated protein kinase (MAPK) (Fujibe et al., 2004). Phosphorylation of this site enhances the barrier function of Cldn1 at tight junctions. Cldn3 and -4 are phosphorylated in ovarian cancer cells but are phosphorylated by different kinases (D'Souza et al., 2005). Cldn3 is phosphorylated by PKA at Thr-192, also located in the C-terminal domain. This study suggested that phosphorylation of Cldn3 at this site may disrupt tight junctions in ovarian cancer. It has been shown that ephrin signaling can play a role in claudin phosphorylation. EphA2 binds to the first extracellular loop of Cldn4. When this occurs, the C-terminal domain of Cldn4 is phosphorylated, specifically at Tyr-208 (Tanaka et al., 2005). This phosphorylation event reduces the association between Cldn4 and ZO-1 and leads to reduced localization of Cldn4 to the tight junction (Tanaka et al., 2005). Cldn5 is a major component of the blood-brain barrier (BBB) and it regulates BBB permeability in mice (Nitta et al., 2003). When Cldn5 was phosphorylated by Rho kinase (ROCK) and myosin light chain kinase (MLCK), there was increased permeability of the BBB (Haorah et al., 2005; Persidsky et al., 2006).

1.4.4.2 Palmitoylation

The process of palmitoylation occurs when fatty acids such as palmitic acid bind to cysteine residues. All members of the claudin family have conserved cysteines near the second and fourth transmembrane domains. It has also been shown that palmitoylation of cysteine residues in the C-terminal domain of claudins is required to target claudins to the membrane (Van Itallie et al., 2005). When palmitoylation of Cldn14 is inhibited, there is a deficiency in its localization (Van Itallie et

al., 2005). Preventing palmitoylation decreased the amount of Cldn14 at tight junctions domains (Van Itallie et al., 2005). When cysteines were mutated to serine residues, there was a decrease in TER.

1.4.5 Claudin-8

Cldn8 and the protein-protein interactions that occur at its C-terminal domain are the focus of this thesis. In humans, *CLDN8* is located on chromosome 21and in chick, it is located on chromosome 1. Cldn8 is a cation barrier and is 224 amino acids long in chick, and 225 amino acids long in humans. Cldn8 interacts in *cis* with multiple claudins, including Cldn3, -4, and -7 (Hou et al., 2010). Cldn8 conditional deletion in the collecting duct in mice causes renal salt wasting of Na^+, Cl^- and K^+ (Gong et al., 2015).

Cldn8 is enriched in the neural plate and in open neural folds (Collins et al., 2013). Cldn8 is present in the neural ectoderm, along with Cldn4, in early stages of neurulation in the chick (Baumholtz et al., 2017). Cldn4 and -8 have been known to participate in interactions with each other. For example, they have been shown to interact in collecting ducts in mice kidney, and the interactions between Cldn4 and -8 is important for Cldn4 localization to tight junctions (Hou et al., 2010). MUPP1 binds to Cldn8 through its PDZ9 domain, which was identified through yeast two-hybrid screening (Jeansonne et al., 2003). When Cldn8 interacts with MUPP1, the paracellular conductance is reduced in epithelial cells (Jeansonne et al., 2003).

1.5 Using the Chick as an Animal Model to Study NTDs

To study neural tube closure, our lab uses the chick embryo as a model organism, as the process of neurulation has been well-studied and the morphogenetic events that occur during neural tube closure in chick highly resemble those of the human embryo (Colas & Schoenwolf, 2001). Using

the chick as our model organism has many benefits over using other animal systems: the chick system is easy to manipulate, has a low cost, and has a short period of embryogenesis. The chick is also a great model to study protein-protein interactions. The Hamburger Hamilton (HH) system is used to categorize the distinct stages of embryonic development, including the phases of neural tube closure (Hamburger et al., 1951). The process of neural tube closure occurs over a short period of time (around 48 hours), enabling our lab to collect embryos in a short time frame and at various stages of neural tube closure. Fertilized eggs are grown in a 39ºC incubator and are available year-round to the lab. Each chicken claudin clusters more with its human or mouse ortholog than with other claudin family members (Collins et al., 2013), and the genome organization of claudins in chick is similar to that of humans and mice.

1.6 *Clostridium Perfringens* Enterotoxin (CPE): A Tool Used to Study the Role of Claudins

Our lab uses C-terminal domain of the *Clostridium perfringens* enterotoxin (CPE) to study the role of claudins during morphogenesis. Full-length CPE is cytotoxic but the C-terminal domain binds to the second extracellular loop of claudins and removes them from tight junctions without killing cells. This enterotoxin has a molecular weight of approximately 37 kDa (Wieckowski et al., 1994), and removes a subset of claudins simultaneously from the tight junction, specifically Cldn3, -4, -6, -7, -8, and -14 (Fujita et al., 2000; Katahira et al., 1997; Shrestha et al., 2013; Winkler et al., 2009). In the chick, C-CPE only removes Cldn-3, -4, -8, as -6 and -7 are not present in the chick genome. C-CPE does not affect the transcription or translation of claudins and does not affect the localization of claudins that are not C-CPE sensitive.

1.7 Claudins Are Required During Neural Plate Shaping and Median Hinge Point Formation

Previous studies from our lab have shown that using C-CPE to remove Cldn3, -4, and-8 from tight junctions in the neural (Cldn4 and -8) and non-neural ectoderm (Cldn3 and -4) during neurulation resulted in open NTDs in chick embryos (Baumholtz et al., 2017). Although Cldn14 is expressed during neurulation, it remained localized to tight junctions in C-CPE treated embryos. These NTD phenotypes were observed after embryos were treated with C-CPE, during the neural plate shaping stage and during the bending and elevation of the neural folds. Absence of Cldn4 and -8 from the neural ectoderm results in defects in apical constriction and convergent extension, which are both morphogenetic events that regulate neural tube closure (Baumholtz et al., 2017). Embryos treated with C-CPE^{LSID}, a variant that removes Cldn4 from tight junctions, did not exhibit NTDs. However, an increase in Cldn8 at the tight junction was observed, suggesting Cldn8 compensates for Cldn4 when removed, and this is why NTDs may not be seen when only Cldn4 is removed. The data support that the presence of Cldn4 is not essential for neural tube closure.

1.8 Variants in the Cldn8 Cytoplasmic C-Terminal Domain Disrupt Neural Tube Closure

Sequence analysis of claudin coding regions in a neural tube cohort (Spina Bifida Center of the Gaslini Hospital, Genova, Italy) identified two CLDN8 variants located at the C-terminal domain, S217I and P216L (Baumholtz et al., submitted). This cohort consisted of 152 patients that had myelomeningocele (open spina bifida). The P216L variant did confirm by sanger sequencing, but the S217I variant was not confirmed. As part of the functional analysis of these variants, three additional variants were generated at two putative serine phosphorylation sites in the chick Cldn8 C-terminal tail, at S198 and S216. The three variants generated were S198A, S216A, and S216I.

The chick S216I variant corresponds to the human S217I variant. Another variant, ΔYV had the C-terminal PDZ-binding domain deleted.

Chick embryos were injected and electroporated at the neural plate stage with expression vectors encoding either wild-type human or chick Cldn8 or their variants (Baumholtz, 2018). Analysis of these embryos 24 hours later revealed that overexpression of human and chick wild-type Cldn8 had no effect on neural tube closure. Similarly, embryos overexpressing Cldn8 S216A and Cldn8ΔYV chick variants also had closed neural tube, suggesting that these variants did not affect neural tube closure. However, overexpressing the S198A variant caused open NTDs but did not affect convergent extension, while overexpressing the S216I variant caused both NTDs and convergent extension defects (Figure 5). Overexpressing the human P216L variant also caused NTDs in chick embryos.

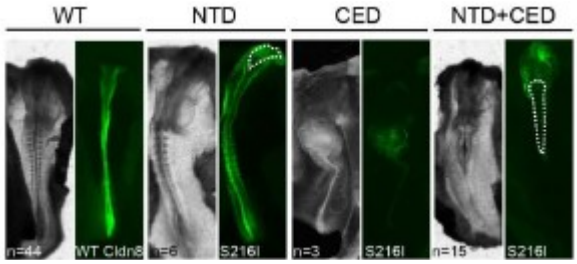

Figure 5: Overexpressing S216I in Chick Embryos Result in NTDs and Convergent Extension Defects
Images show dorsal views of chick embryos overexpressing S216I. The first panel shows a closed neural tube, the second panel an NTD, the third panel a convergent extension defect, and the last panel a NTD and convergent extension defect. Dashed lines are open neural tubes. Figure from Baumholtz, 2018.

1.8.1 Residues in the Cldn8 Cytoplasmic C-Terminus Regulate Protein Localization in Neural Ectoderm Cells

When Cldn4 and -8 were removed from the neural ectoderm at HH4 and analyzed during the bending and elevation of the neural plate (HH8) of C-CPE treated embryos, there was reduced localization in RhoGTPases Cdc42 and RhoA at the apical surface (Baumholtz et al., 2017). In

embryos overexpressing wild-type Cldn8, Cdc42 and RhoA partly co-localized with ZO-1 in neural ectoderm cells. Embryos overexpressing the S198A variant result in loss of Cdc42 from tight junctions in the neural ectoderm. In embryos overexpressing the S216I variant, 60% of embryos had increased Cdc42 localization and reduced RhoA localized in 50% of embryos. This data suggests that residues in the C-terminal domain of Cldn8 interact with different proteins that potentially regulate cell shape changes and morphogenetic movements during neural tube closure.

1.9 Rationale and Hypothesis

The Cldn8 data suggest that residues in the C-terminal domain of Cldn8 participate in interactions with proteins at the tight junction cytoplasmic plaque that regulate cell shape changes during neural tube closure and may have distinct interaction partners that regulate different morphogenetic events during neural tube closure. When the wild-type Cldn8 C-terminal domain is overexpressed, the necessary protein-protein interactions occur at positions S198 and S216 (Figure 6), and these interactions can contribute to proper neural tube closure. However, when variants are generated at these positions, these protein-protein interactions may not occur, leading to NTDs. This can be due to lack of phosphorylation or even a change in protein conformation and folding. S198 is a putative serine phosphorylation site and when this position is mutated to S198A and overexpressed in chick embryos, a NTD phenotype is observed Variants generated at S216 give different phenotypes, with overexpression of S216A resulting in no NTD phenotype and overexpression of S216I resulting in NTDs and convergent extension defects. Isoleucine is hydrophobic and is also larger than serine, which can cause a change in protein shape and folding. Overexpressing human P216L, although not conserved in chicks, also resulted in NTDs. Proline is hydrophobic and is known to change protein folding.

Hypothesis: These findings have led me to the hypothesis that protein-protein interactions that occur at the Cldn8 cytoplasmic tail are required and important for Cldn8 function during neural tube closure.

Objective: The objective of this project has been to identify the interacting partners that interact with the Cldn8 C-terminal domain.

Figure 6: Schematic of the Cldn8 C-Terminal Domain
This is a schematic of the Cldn8 C-terminal domain, with the orange dot representing position S198, which was mutated to S198A, the red dot representing S216, which was mutated to S216A and S216I, and YV in blue, which had the PDZ-binding motif removed.

CHAPTER 2: Materials and Methods

2.1 Transformation of BL21 *E. coli*

BL21 *E. coli* cells were transformed with pET14b plasmid vector that encoded either GST or a GST-fused to the C-terminal domain of Cldn8 or Cldn14. Briefly, competent BL21 *E. coli* cells were thawed on ice and 100 ng plasmid DNA was added to 50 µL of the thawed cells in 15 mL snap-cap tubes. The DNA-bacterial cell mixture was incubated on ice for 30 minutes. The DNA-bacterial cell mixture was then heat-shocked for 45 seconds at 42°C, and then incubated on ice for two minutes. 250 µL of the pre-warmed Luria-Bertani (LB) was then added to the transformation and they were incubated at 37°C with shaking at 250 rpm for one hour. 50 µL of the transformed cells were spread onto LB-agar plates that contained 50 µg/mL ampicillin and 34 µg/mL chloramphenicol and incubated overnight at 37°C.

2.2 Preparation of Bacterially-Expressed GST Fusion Protein

A single transformed BL21 *E. coli* colony was added to 4 mL of LB broth with 50 µg/mL ampicillin and 34 µg/mL chloramphenicol in a 15 mL snap-cap tube incubated overnight at 37°C, with shaking at 250 rpm. The 4 mL overnight culture was added to a 2L flask containing 395 mL of LB with 50 µg/mL ampicillin and 34 µg/mL chloramphenicol and incubated at 37°C with shaking at 250 rpm for approximately 2-2.5 hours until OD_{600} was between 0.4-0.6. To induce expression of the fusion protein, IPTG (0.4mM final concentration) was added to the culture and it was incubated for four hours at 37°C, with shaking at 250 rpm. The bacterial cell culture was centrifuged at 5000 rpm for 15 minutes at 4°C. The supernatant was removed, and the pellet was stored in the -80°C freezer. Aliquots prior to IPTG treatment and of the induced sample were analyzed by SDS-PAGE to ensure that the GST-fusion protein was expressed prior to completing the next steps of the purification.

Pellets were thawed on ice for 30 minutes and then resuspended in 5 mL of 50mM Tris-HCl, pH 8.0; 150mM NaCl, 0.1mM EDTA, and protease inhibitors (10 µg/µL Aproptonin, 10 µg/µL Leupeptin, 1 mg/ml Pepstatin A and 1.74 mg/ml PMSF). The bacterial cell resuspension was transferred to a 15 mL falcon tube and lysozyme (10 mM final concentration) was added. This was then incubated on ice for 20 minutes. Sodium deoxycholate was then added to achieve a final concentration of 0.2%. This mixture was sonicated at an amplitude of 30A for three thirty seconds pulses, with a rest of one minute in between each pulse. Insoluble cell debris was removed from this mixture by centrifugation for 30 minutes at 4°C at 15,000 rpm in microcentrifuge 5417C. The supernatant was filtered through a 0.45 µm syringe filter. Aliquots of the filtered supernatant and of the pellet were kept for SDS-PAGE analysis to estimate concentration of induced fusion proteins as compared to BSA standards loaded on the same gel. Based on the estimated fusion protein concentration, washed glutathione sepharose 4B beads (GE Healthcare) were added to the GST-fusion protein supernatant at a ratio of 125 µL of 50% slurry per 500 µg fusion protein. The fusion protein extract was incubated on a rocker overnight at 4°C.

The next day, the beads and GST-fused protein were either centrifuged for two minutes at 1000 x *g* for batch purification or transferred to a column. An aliquot of the supernatant containing unbound protein was kept for SDS-PAGE analysis. The beads were washed with resuspension buffer (without EDTA) for batch purification or with at least 10 volumes of buffer for column purification until no protein was remaining in the wash supernatant, as determined by Bradford assay. The glutathione sepharose beads loaded with GST fusion protein were kept on ice until use. Aliquots of unbound protein, bound protein (bound to beads) and different amounts of BSA concentrations (0.5,1, and 5 µg) were loaded onto an SDS-PAGE gel.

2.3 SDS-PAGE Analysis

Both 7% and 10% separating gels were used for SDS-PAGE analysis, and the gels were both made with: 4X separation buffer (Tris base, SDS and distilled water) (pH 8.8), 30% Acrylamide/Bis solution from Bio-Rad, 10% Ammonium persulfate (APS), Temed, and distilled water. The only difference between the different percentage gels was the volume of acrylamide and APS added. For a 7% gel, 2.33 mL 30% acrylamide and 100 µL 10% APS were added, while 3.3 mL 30% acrylamide and 87.5 µL of 10% APS were added per 10% gel.

Stacking gels were made as follows: 4X stacking buffer (Tris base, SDS, and distilled water), pH 6.8, 30% Acrylamide, 10% APS, Temed, and distilled water. 1X running buffer (10X stock made with Tris base, glycine, SDS, and water) was used for SDS-PAGE analysis. Running buffer was either made fresh or stored for three to four days at 4°C. Electrophoresis was performed for 1-1.5 hours at 100 volts. The gel was then stained for 10 minutes using Coomassie blue staining (0.25% Coomassie brilliant blue, 50% methanol, 10% acetic acid, and 39.75% distilled water), and then destained (50% H_2O, 40% of 100% MeOH, and 10% Acetic acid) until bands appeared. The gel was then covered in water, placed in a tray covered by aluminum foil and left rocking overnight at 4°C.

2.4 Collection and Lysis of Chick Embryos

Fertilized white leghorn chicken eggs (Ferme GMS, Holstein, Quebec) were incubated for approximately 36 hours (for HH8) or for 4 days (for Day 4) in a 39°C egg incubator. Dissected embryos were washed in ice-cold PBS, staged and then centrifuged at 12,000 rpm for 10-15 seconds in a microcentrifuge to remove the PBS, flash frozen in liquid nitrogen and then stored at -80°C.

Embryos were resuspended in 1 mL of lysis buffer (20 mM Tris-HCl, pH 7.4, 10mM NaCl, 0.2% SDS, 1% NP40, and 50 mM NaF) plus protease inhibitors (10 µg/µL Aproptonin, 10 µg/µL Leupeptin, 1 mg/ml Pepstatin A and 1.74 mg/ml PMSF) per 1mg tissue. Approximately 98 HH8 or 48 Day 4 embryos were used per Cldn14 GST-pulldown experiment, and 30-40 HH8 chick embryos were used per Cldn8 GST-pulldown experiment. HH8 chick embryos were resuspended in lysis buffer using a 1 mL syringe attached to a 21G needle until homogenized, while Day 4 chick embryos were lysed using a homogenizer and then passed through a 21G needle. The homogenized chick lysates were then incubated on ice for 10 minutes and then centrifuged at 15,000 rpm at 4°C for 15 minutes. Protein concentration was determined by Bradford assay, using Bio-Rad protein assay. The specific concentration of HH8 chick lysate per Cldn8 experiment were as follows: 4.04 µg/µL for experiment 1, 7.43 µg/µL for experiment 2, and 5.63 µg/µL for experiment 3. The specific concentration of Day 4 chick lysate for the Cldn14 experiment was determined to be 15.5 µg/µL, and the concentration of HH8 chick lysate used for the Cldn14 experiment was 8.25 µg/µL.

2.5 GST-Pulldown Assay

1 mg of HH8 chick embryo lysate was added to 10-20 µL of sepharose beads containing 400 µg of GST or GST-fusion protein. When using batch purification, the chick lysate was added to GST or GST-Cldn8 beads in an Eppendorf tube, and when using column purification, chick lysate was added to beads over a closed column. The next day, the beads were washed with resuspension buffer without EDTA. The beads were washed until the flow-through (unbound) had an absorbance of zero at a wavelength of 595 nm, and this was done by using a Bradford. Aliquots of the unbound were kept to later load onto an SDS-PAGE gel, and an aliquot of the beads mixed in 50% slurry was also kept for loading alongside the unbound samples on the SDS-PAGE gel. The

remainder of the proteins bound to GST, GST-Cldn8, or GST-Cldn14 beads (between 10-15 µL) were stored at -80°C.

2.6 Western Blot Analysis

50 µg from unbound protein, HH8 or Day 4 whole embryo protein extracts, and bound protein from the GST-pulldown were separated by 10% SDS-PAGE for immunoblotting with GST antibody or 7% SDS-PAGE for immunoblotting with ZO-1 antibody. Proteins were transferred to polyvinylidene difluoride (PVDF) membrane in 1X Transfer buffer with methanol added, for a final concentration of 20% and ran for 1-1.5 hours at 100V on ice. The membrane was blocked for one hour in PBST with 5% carnation dry milk powder. Membranes were incubated with 1:10,000 dilution of mouse αGST antibody (Invitrogen) or 1:500 dilution of rabbit αZO-1 (Invitrogen 40-2200) in PBST overnight at 4°C. The membranes were washed three times with 1X PBST for 30 minutes and then incubated with a 1:7500 dilution of goat αMouse or goat αRabbit secondary antibody conjugated to horseradish peroxidase (Jackson Immuno Research) in PBST. The membranes were again washed three times with PBST for 20 minutes each and then revealed with Clarity™ Western ECL substrate (BIO-RAD) and imaged on Amersham Imager 600.

2.7 Mass Spectrometry Analysis

Washed beads bound to GST, GST-Cldn8 C-terminal domain and GST-Cldn14 C-terminal domain protein were sent to the Proteomics Platform at the McGill University Health Centre (MUHC) – Glen Site. After running a single SDS-PAGE stacking gel band containing all proteins for each sample, the proteins were reduced with DTT, alkylated with iodoacetic acid and digested with trypsin. The resulting peptides were re-solubilized in 0.1% aqueous formic acid and loaded onto a Thermo Acclaim Pepmap (Thermo, 75 µM ID X 2 cm C18 3 µM beads) precolumn and then onto an Acclaim Pepmap Easyspray (Thermo, 75 µM X 15 cm with 2 µM C18 beads)

analytical column separation using a Dionex Ultimate 3000 uHPLC at 250 nl/min with a gradient of 2-35% organic (0.1% formic acid in acetonitrile) over two hours. Peptides were analyzed using a Thermo Orbitrap Fusion mass spectrometer operating at 120,000 resolution (FWHM in MS1) with HCD sequencing at top speed (15,000 FWHM) of all peptides with a charge of 2+ or greater. The raw data were converted into *.mgf format (Mascot generic format) for searching using the Mascot 2.6.2 search engine against combined chick and *E. coli* protein sequences (UniProt, 2019). The database search results were loaded onto Scaffold Q+ Scaffold_4.9.0 (Wilson et al., 2019) for statistical treatment and data visualization.

Scaffold allows for common peptides and proteins to be compared between samples, and allows for the comparison between biological relevance, molecular function and organelles. The amino acid sequence of the proteins identified are present for viewing, and the unique peptides of a protein can be identified, along peptides that are common to multiple proteins. Protein sequences can also be BLASTED. Different significance tests such as Fisher's exact and t-test can be performed, along with looking at the fold change between samples.

CHAPTER 3: Results

3.1 Validation of a GST-Pulldown Approach to Isolate Cldn8 Interaction Partners

To identify proteins that interact with the Cldn8 C-terminal domain, a GST-pulldown approach was used. HH8 whole chick embryo protein extracts were used as the source of Cldn8 C-terminal domain interacting partners, as it is the first stage in which NTDs were observed in Cldn3/4/8-depleted chick embryos (Baumholtz et al., 2017). This stage also yields a substantial amount of protein per embryo. Using an earlier stage of development would not have been practical for the amount of protein needed for these assays.

For the GST-pulldowns, three experiments were conducted. GST was used in all experiments to control for non-specific binding partners in the GST-pulldown. For the first experiment, 200 µg of GST or GST-Cldn8 C-terminal domain fusion protein loaded on 10 µL of glutathione sepharose beads were incubated with 500 µg or 1 mg of HH8 whole chick extract. For the second and third experiments, GST and GST-Cldn8 C-terminal domain beads containing 400 µg of GST or GST -Cldn8 C-terminal domain fusion protein loaded on 20 µL of glutathione sepharose beads were incubated with 1 mg of HH8 whole chick extract, and GST-pulldowns were conducted in duplicate.

Western blot analysis was conducted using a GST antibody to confirm the presence of GST-fusion protein. The results for the first experiment are shown in Figure 7A. As expected, a ~26kDa band that corresponded to the GST or the GST-Cldn8 C-terminal tail fusion protein was detected in the bound GST and bound Cldn8 C-terminal domain lanes but not in the unbound GST, unbound Cldn8 C-terminal domain, or HH8 chick extract lanes (top image). Although one would expect that the GST-Cldn8 C-terminal tail fusion protein would migrate slower than the GST only protein, that does is not what we observed (Figure 7A). When cloning the Cldn8 C-terminal domain (100

basepairs) into the pET14b plasmid vector (4,671 basepairs) that encoded a GST tag (700 basepairs), a stop codon was added, and some amino acids from the vector encoding the GST tag were removed in the process.

To confirm that the pulldown approach was able to select proteins that interact with the claudin C-terminal tail, western blot analysis was performed using an antibody that recognizes the tight junction adaptor protein ZO-1, which interacts with the PDZ domain at the C-terminus of the claudin cytoplasmic domain (Monteiro et al., 2013). The predicted size of ZO-1 is 225 kDa. In Experiment 1, a band at ~225 kDa was detected in the HH8 chick embryo extract (Figure 7A-bottom image). However, no bands were detected at 225 kDa in any of the bound fractions for either the GST or Cldn8 C-terminal domain samples. A band at ~130 kDa was observed in the Cldn8 C-terminal domain bound fraction (Figure 7A- bottom image). There were bands at ~225 kDa in one of the unbound GST fractions and in both unbound fractions from the Cldn8 C-terminal domain GST-pulldown (Figure 7A-bottom image).

For the second experiment, a band at ~225 kDa was detected in the bound Cldn8 C-terminal domain fraction (Figure 7B). Faint bands at ~225 kDa were also observed in the unbound fractions from the GST and GST-Cldn8 C-terminal domain pulldowns, and in the HH8 chick embryo extract (Figure 7B). This suggested that ZO-1 was pulled down by GST-Cldn8-Cter fusion protein but not by GST alone. The band at ~130 kDa was also detected in the bound Cldn8 C-terminal domain fraction. Other sized bands in the GST-Cldn8 C-terminal domain bound fraction were also observed in the GST bound fraction, suggesting that they may be non-specific interaction partners. For the third experiment, bands were detected at 225 kDa in the bound Cldn8 C-terminal domain fraction. Faint bands at ~225 kDa were also observed in the unbound fractions from the GST and GST-Cldn8 C-terminal domain pulldowns, and in the HH8 chick embryo extract (Figure 7C).

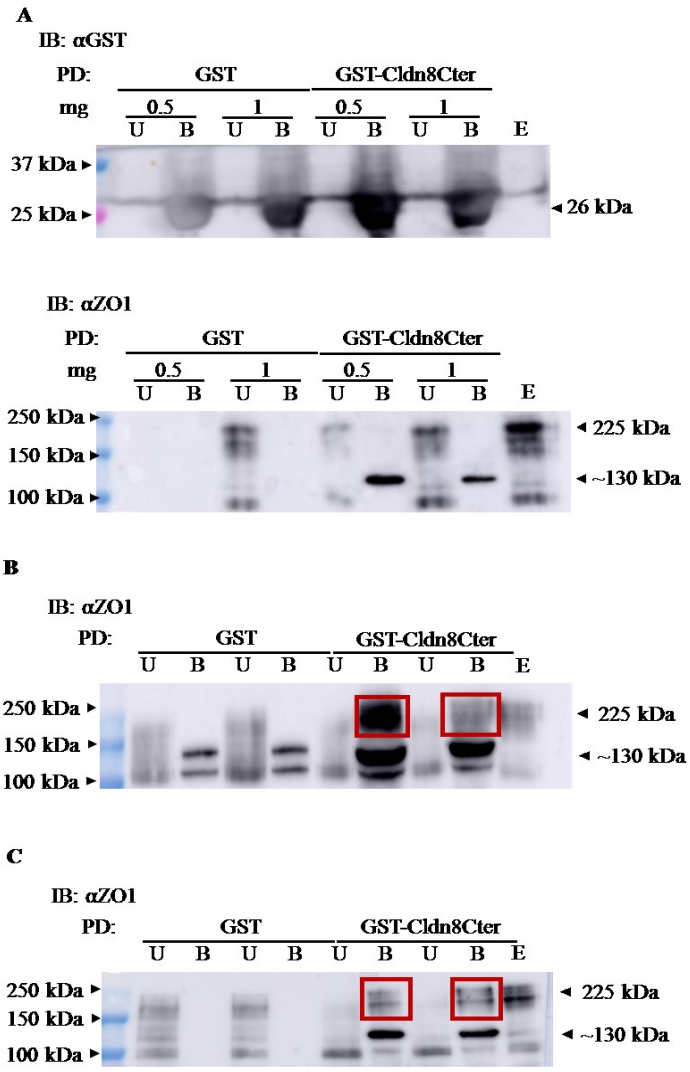

Figure 7: Western Blot Analysis of GST and ZO-1 Localization in Unbound and Bound Fractions from GST-Pulldown Experiments to Identify Cldn8 C-Terminal Domain Interacting Partners

(A) Immunoblot analysis of the unbound protein lysate (U) and proteins bound (B) to GST-agarose beads or GST-Cldn8Cter beads and HH8 chick embryo whole cell extract (E) for expression of GST (upper panel) for Experiment # 1-3 or ZO-1 (lower panel) from Experiment #1. (B) Immunoblot analysis of the unbound protein lysate (U) and proteins bound (B) to GST-agarose beads or GST-Cldn8Cter beads and HH8 chick embryo whole cell extract (E) for expression of ZO-1 from Experiment #2. Bands at 225 kDa are encased by a red box. (C) Immunoblot analysis of the unbound protein lysate (U) and proteins bound (B) to GST-agarose beads or GST-Cldn8Cter beads and HH8 chick embryo whole cell extract (E) for expression of ZO-1 from Experiment #3. Bands at 225 kDa are encased by a red box.

Bands were not detected in any of the GST bound fractions. The band at ~130 kDa was also detected in the bound Cldn8 C-terminal domain fraction. Overall, when bands were detected at 225 kDa in the Cldn8 bound C-terminal domain fractions, the bands were more intense than the bands detected at 225 kDa in unbound GST and unbound Cldn8 C-terminal domain fractions. The band present at ~130 kDa in all Cldn8 C-terminal domain bound fractions had a higher intensity than the bands present at 225 kDa.

3.2 Validation of a GST-Pulldown Approach to Isolate Cldn14 Interaction Partners

An experiment was also done to identify interacting partners of the Cldn14 C-terminal domain, using bacterially-expressed GST control protein or GST-Cldn14 C-terminal domain fusion protein loaded onto glutathione sepharose beads and mixed with either HH8 chick extract or Day 4 chick extract. Day 4 chick extract was used as there is more protein yield per embryo than in HH8 embryos. GST was used as a control to determine the proteins that might interact with the GST domain that is fused to the Cldn14 C-terminal domain. The rationale behind this is that Cldn14 is also expressed during HH8 of neural tube closure, along with Cldn3, -4, and -8. In order to determine if the interacting partners identified were Cldn8 C-terminal domain specific or stage specific during the process of neural tube closure, a GST-pulldown approach was performed, using the C-terminal domain of Cldn14. If the proteins identified by mass spectrometry are stage specific, then these proteins would bind to both the C-terminal domains of Cldn8 and Cldn14 when mixed with HH8 chick extract, as both Cldn8 and Cldn14 are expressed during HH8 of neural tube closure.

For the GST-pulldown conducted using Day 4 chick extract, 250 µg of GST or GST-Cldn14 C-terminal domain fusion protein loaded on 10 µL (GST protein) or 40 µL (GST-Cldn14 C-terminal domain fusion protein) of glutathione sepharose beads were incubated with 4.65 mg of Day 4

whole chick extract. After overnight incubation, unbound protein was removed by washing. For the GST-pulldown conducted using HH8 chick extract, 250 μg of GST or GST-Cldn14 C-terminal domain fusion protein loaded on 10 μL of glutathione sepharose beads were incubated with 3.3 mg of HH8 whole chick extract.

Western blot analysis was conducted using a GST antibody to confirm the presence of GST-fusion protein. The results for the Day 4 experiment are shown in Figure 8A. As expected, a ~26kDa band that corresponds to the GST and a band at approximately 28-32 kDa that corresponds to the GST-Cldn14 C-terminal tail fusion protein was detected in the bound GST and bound Cldn14 C-terminal domain fraction but not in the unbound GST, unbound Cldn14 C-terminal domain, or Day 4 chick extract lanes.

To confirm that the pulldown approach was able to select proteins that interact with the claudin C-terminal tail, western blot analysis was performed using an antibody that recognizes the tight junction adaptor protein ZO-1. For the GST-pulldowns done with Day 4 chick extract, a band at ~225 kDa was detected in the bound Cldn14 C-terminal domain fraction and in the bound GST fraction (Figure 8B). Bands at ~225 kDa were also observed in the unbound fractions from the GST and GST-Cldn14 C-terminal domain pulldowns, and in the Day 4 chick embryo extract (Figure 8B). The band at ~130 kDa that was detected in all bound Cldn8 C-terminal domain fractions was also detected in the bound Cldn14 C-terminal domain fraction. In the unbound fractions from the GST only pulldown, bands are seen at various molecular weights, and not only at 225 kDa. This can be due to the degradation of the protein or other proteins that interact non-specifically with the ZO-1 polyclonal antibody.

For the GST-pulldowns done with HH8 chick extract, a band at ~225 kDa was not detected in the bound Cldn14 C-terminal domain fraction (Figure 8C). Faint bands at ~225 kDa were also observed in the unbound fractions from the GST and GST-Cldn14 C-terminal domain pulldowns (Figure 8C). The band at ~130 kDa that was detected in all bound Cldn8 C-terminal domain fractions was also detected in the bound Cldn14 C-terminal domain fraction. In the unbound fractions from the GST and GST-Cldn14 C-terminal domain pulldowns (Figure 8C), the lanes in the western blot are smeared. This is most likely due to too much protein being loaded onto the western blot.

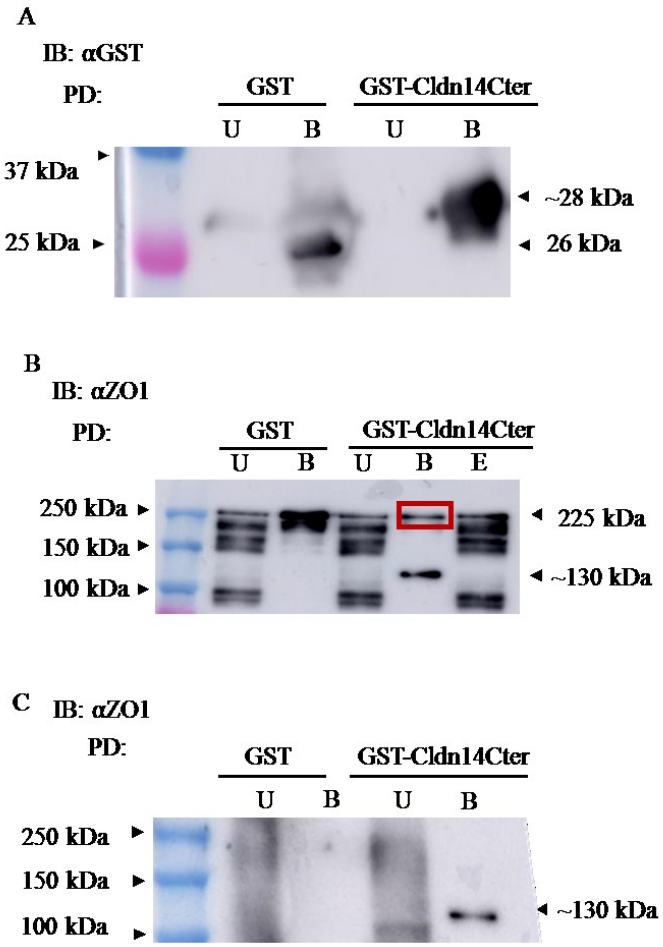

Figure 8: Western Blot Analysis of GST and ZO-1 Localization in Unbound and Bound Fractions from GST-Pulldown Experiments to Identify Cldn14 Interacting Partners
(A) Immunoblot analysis of the unbound protein lysate (U) and proteins bound (B) to GST-agarose beads or GST-Cldn14Cter beads for expression of GST (upper panel) for Experiment # 1-2.(B) Immunoblot analysis of the unbound protein lysate (U) and proteins bound (B) to GST-agarose beads or GST-Cldn14Cter beads and Day 4 chick embryo whole cell extract (E) for expression of ZO-1 from Experiment #1. Band at 225 kDa are encased by a red box.
(C) Immunoblot analysis of the unbound protein lysate (U) and proteins bound (B) to GST-agarose beads or GST-Cldn14Cter beads for HH8 chick embryo whole cell extract (E) for expression of ZO-1 from Experiment #2.

3.3 Mass Spectrometry Data for GST, GST-Cldn8 C-Terminal Domain and GST-Cldn14 C-Terminal Domain GST-Pulldown Experiments

Three biological replicates were sent to mass spectrometry for identification of proteins that interact with the C-terminal domain of Cldn8. Duplicate samples were analyzed for the second and third replicates. For the first biological replicate sent to mass spectrometry, the beads were mixed

with 500 µg whole cell HH8 chick extract, while for the second and third experiment, the beads were mixed with 1 mg whole cell HH8 chick extract. Only a single biological replicate was analyzed for the Cldn14 C-terminal domain pulldowns performed using HH8 and day 4 chick embryonic extracts. The GST-pulldowns to identify the Cldn14 C-terminal domain interacting partners, along with the first and second Cldn8 experiments were done using batch purification. A column purification approach was used during the protein purification process for the third Cldn8 C-terminal tail GST-pulldown experiment. The interacting partners identified by mass spectrometry in the Cldn8 GST-pulldown fraction were analyzed using the Scaffold program, which takes into consideration the number of unique peptides, the number of times each peptide appears, the coverage of the protein per sample, and differentiates proteins by their biological and molecular function (Wilson et al., 2019).

3.3.1 Overview of the Mass Spectrometry Analysis of GST and GST-Cldn8 C-Terminal Domain Pulldowns

The next section will discuss the number of chick and *E. coli* proteins that were identified by mass spectrometry using the GST-pulldown approach performed with the C-terminal domains of Cldn8 and or Cldn14. The rationale for using a GST-pulldown approach was to determine if the proteins identified were specifically interacting with the C-terminal domain of Cldn8, or also with the C-terminal domain of Cldn14, as both are present during HH8 of neural tube closure. The first section will discuss the total number of chick and *E. coli* proteins identified, and the second section will discuss the process used to prioritize candidate interacting partners for further analysis.

The total number of proteins and peptides identified in the three Cldn8 C-terminal domain pulldown replicates are summarized in Table 1. Chick and *E. coli* proteins were identified in all samples. For the first Cldn8 biological replicate, a total of 233 proteins (361 peptides), that

included 127 chick proteins (240 peptides) and 106 *E. coli* proteins (121 peptides) were identified in the GST sample that mass spectrometry identified. For the Cldn8 C-terminal domain sample, a total of 337 proteins (682 peptides) were identified, which is composed of 122 chick proteins (226 peptides) and 215 *E. coli* proteins (456 peptides).

In the second biological replicate, 659 proteins (3,887 peptides) that included 99 chick proteins (398 peptides) and 560 *E. coli* proteins (3,489 peptides) were identified in one of the GST duplicates and 630 proteins (3,489 peptides) that included 105 chick proteins (381 peptides) and 525 *E. coli* proteins (3,108 peptides) were identified in the second GST duplicate (Table 1). Together these samples contained 120 unique proteins, 84 of which were present in both samples (Table 2). For the Cldn8 C-terminal domain pulldowns, 760 proteins (4,867 peptides) that included 134 chick proteins (536 peptides) and 626 *E. coli* proteins (4,331 peptides) were identified in one of the samples and 738 proteins (4,440 peptides) that included 133 chick proteins (503 peptides), and 605 *E. coli* proteins (3,937 peptides) were identified in the second sample (Table 1). When the two GST-pulldown samples for the Cldn8 C-terminal domain samples combined this represented 158 unique proteins of which 109 were present in both Cldn8 C-terminal pulldown samples (Table 2). For further prioritization of candidates, the number of peptides identified for each protein was taken into account. Therefore, the number of proteins with multiple peptides was also noted in Table 2.

There were many more *E. coli* proteins when compared to the number of chick proteins in the second biological replicate in both the GST and Cldn8 C-terminal domain samples. The presence of these proteins may have inhibited potential interactions from occurring with the chick proteins. In an attempt to reduce the number of *E. coli* proteins, column purification was performed for the third biological replicate, anticipating that this might lead to improved washing of the beads and

reduce the background of *E. coli* proteins. In the third biological replicate, 264 proteins (469 peptides) that included 52 chick proteins (94 peptides), and 212 *E. coli* proteins (375 peptides) were identified in the one of the GST duplicates and 172 proteins (191 peptides) that included 43 chick proteins (38 peptides) and 129 *E. coli* proteins (153 peptides) were identified in the second GST duplicate (Table 1). Together these samples contained 65 unique proteins, 30 of which were present in both samples (Table 2).

Cldn8 Replicate	Bait	Total # proteins (# peptides)	# Chick proteins (# peptides)	# *E. coli* proteins (# peptides)
1	GST	233 (361)	127 (240)	106 (121)
	Cldn8 C-terminal domain	337 (682)	122 (226)	215 (456)
2	GST sample #1	659 (3,887)	99 (398)	560 (3,489)
	GST sample #2	630 (3,489)	105 (381)	525 (3,108)
	Cldn8 C-terminal domain sample #1	760 (4,867)	134 (536)	626 (4,331)
	Cldn8 C-terminal domain sample #2	738 (4,440)	133 (503)	605 (3,937)
3	GST sample #1	264 (469)	52 (94)	212 (375)
	GST sample #2	172 (191)	43 (38)	129 (153)
	Cldn8 C-terminal domain sample #1	382 (1,262)	96 (255)	286 (1,007)
	Cldn8 C-terminal domain sample #2	382 (1,402)	100 (318)	282 (1,084)

Table 1: Total Proteins and Peptides Identified in Individual Samples of Cldn8 C-Terminal Domain Biological Replicates

These data describe the total number of proteins and peptides found in each individual Cldn8 C-terminal domain and GST sample. These total proteins are composed of chick proteins and *E. coli* proteins. Biological replicates two and three consist of duplicate samples of both Cldn8 C-terminal domain samples and GST samples. Peptides are in parentheses.

For the Cldn8 C-terminal domain pulldowns, 383 proteins (1,262 peptides) that included 96 chick proteins (255 peptides) and 286 *E. coli* proteins (1,007 peptides) were identified in one of the Cldn8 C-terminal domain duplicates and 382 proteins (1,402 peptides) that included 100 chick proteins (318 peptides) and 282 *E. coli* proteins (1,084 peptides) were identified in the second Cldn8 C-terminal domain duplicate. When these samples were combined this represented 111

unique proteins of which 85 were present in both Cldn8 C-terminal pulldown samples (Table 2). It is difficult to determine if the column purification was the best approach to be taken, as the overall number of proteins for both chick and *E. coli* were lower when compared to the samples from the second biological replicate.

Column purification was performed for the third biological replicate to reduce the number of *E. coli* proteins present. However, there was a reduction in *E. coli* proteins as well as the number of chick proteins. For experiments one and two, in which the batch purification method was used, the ratio of chick to *E. coli* proteins was approximately 1:2 for experiment 1and 1:5 for experiment 2. For experiment three, in which column purification was used, the ratio of chick to *E. coli* proteins was 1:2. Therefore, it is inconclusive to say that one method of purification was better than the other. The presence of so many *E. coli* proteins may have been due to the protein purification process, before the glutathione sepharose beads were mixed with the GST and GST-fusion protein. The salt concentration used in the buffer for pellet resuspension before the glutathione sepharose beads were added was 150 mM NaCl. It is possible that non-specific binding may have been reduced if a higher salt concentration was used. Part of the protein purification process also included sonication and centrifugation. It is possible that after these procedures were performed, not much induced GST or GST-fused C-terminal domain Cldn8 protein was available to bind to the beads, as protein is continuously being lost during the process of protein isolation and purification. For both the batch and column purification methods, common areas were used, such as the centrifuge and the 37°C shaker in which the flasks containing the bacteria were placed Contamination may have occurred as the shaker was in a common space, where other labs were using this shaker

The chick and *E. coli* proteins in table 1 are proteins that had at least one peptide identified. What was also of interest was to look at proteins that had at least two different peptides identified by mass spectrometry (Table 2). The number of peptides reflects the size of the protein and where the tryptic cleavage sites are. For the first biological replicate, the GST sample had 68 proteins with more than one peptide identified, and the Cldn8 C-terminal domain sample had 69 proteins. For the second biological replicate, with the duplicates being pooled together, GST had 90 proteins with more than one peptide identified, and the C-terminal domain sample had 122 proteins. For the third biological replicate, with the duplicates being pooled together, the GST sample has 37 proteins with more than one peptide identified, and the Cldn8 C-terminal domain sample had 80 proteins identified.

Cldn8 Replicate	Bait	# chick proteins (# peptides)	# total individual chick proteins	Number of proteins > 1 peptide	# common b/w duplicates (# peptides)
1	GST	127 (24)	127	68	NA
	Cldn8 C-terminal domain	122 (226)	122	69	NA
2	GST #1	99 (398)	120	90	84 (287)
	GST #2	105 (381)			
	Cldn8 C-terminal domain #1	134 (536)	158	122	109 (335)
	Cldn8 C-terminal domain #2	133 (503)			
3	GST #1	52 (94)	65	37	30 (22)
	GST #2	43 (38)			
	Cldn8 C-terminal domain #1	96 (255)	111	80	85 (208)
	Cldn8 C-terminal domain #2	100 (318)			

Table 2: The Number of Chick Proteins Identified in Individual Cldn8 C-Terminal Domain Samples, and the Total Number of Proteins in Common Between Duplicate Samples
These data describe the individual Cldn8 C-terminal domain and GST samples for all three biological replicates sent to mass spectrometry. Biological replicates two and three contain duplicate samples of Cldn8 C-terminal domain and GST samples. These data show the number of chick proteins and peptides for each sample, and the number of proteins and peptides in common between duplicate samples for biological replicates two and three. The total number of individual chick proteins for duplicate samples was calculated by adding the total number of chick proteins per sample, and then subtracting the number of proteins in common for those samples. This table also shows the number of proteins that had more than one peptide identified by mass spectrometry.

Next, the enrichment of the proteins in the Cldn8 C-terminal pulldown samples was determined by comparison to the GST pulldown samples (Table 3). The rationale behind this was to determine how many proteins identified through mass spectrometry were only interacting with the Cldn8 C-terminal domain, and to look at the fold enrichment of proteins that were identified to interact with both GST and the C-terminal domain of Cldn8. The data provided by this comparison was used to narrow down the potential list of Cldn8 C-terminal domain interacting partners. Data from

duplicates were pooled because it is not possible to distinguish which samples to compare to one another (GST #1 and #2 vs Cldn8 C-terminal domain #1 and #2). Proteins present in the Cldn8 C-terminal domain pulldowns were categorized into three groups: <2-fold enrichment relative to GST, >2-fold enrichment but not unique relative to GST, and unique to Cldn8 C-terminal domain samples (Table 3). For the Cldn8 sample from the first biological replicate, 61 proteins were <2-fold enriched, 21 proteins were >2-fold enriched in Cldn8 C-terminal domain sample vs GST, and 40 proteins were unique to the Cldn8 C-terminal domain sample. For the second Cldn8-C-terminal domain biological replicate, 71 proteins were <2-fold enriched, 33 proteins were >2-fold enriched, and 54 proteins were unique relative to the GST control sample. Finally, for the third Cldn8-C-terminal domain biological replicate, 13 proteins <2-fold enriched, 22 proteins were >2-fold enriched, and 76 proteins were unique to the Cldn8 C-terminal domain sample.

Next the data were analyzed to evaluate the confidence level, or the degree of accuracy predicted by the Scaffold program that a predicted protein based on peptide sequences was indeed that protein. This is based on the unique peptides identified. When the confidence level was set to 95%, a total of 342 chick proteins were identified (Table 3). 176 of these proteins were <2-fold enriched in the Cldn8 C-terminal domain sample when compared to GST, 61 proteins were >2-fold enriched in the Cldn8 C-terminal domain sample vs GST, and 105 proteins were unique to the Cldn8 C-terminal domain sample. When the confidence level was increased to 99%, a total of 226 chick proteins were identified. A complete list of all proteins is presented in the Appendix. 120 of these proteins were <2-fold enriched, 51 proteins were >2-fold enriched, and 55 proteins were unique. 55 of the 226 proteins were present in at least two Cldn8 C-terminal domain samples. Out of these 55, 22 proteins were <2-fold enriched, 13 proteins were >2-fold enriched, and 20 proteins were unique to the Cldn8 C-terminal domain sample. 46 of these proteins were present in

all three biological replicates: 20 proteins were <2-fold enriched, 24 proteins were >2-fold enriched, and 2 proteins were unique to the Cldn8 C-terminal domain sample as compared to the GST samples. These proteins have been further prioritized for analysis as described below.

Cldn8 C-terminal domain bait + chick extract	Total number of chick proteins	0 to 2-fold > GST	>2-fold GST	Unique to Cldn8 C-terminal tail
Cldn8 + HH8 exp1	122	61	21	40
Cldn8 + HH8 exp2	158	71	33	54
Cldn8 + HH8 exp3	111	13	22	76
Total number of unique proteins (95% confidence)	342	176	61	105
Total number of unique proteins (99% confidence)	226	120	51	55
Number of proteins present in at least two replicates	55/226	22	13	20
Number of proteins present in at least three replicates	46/226	20	24	2

Table 3: The Total Number of Chick Proteins in Each Cldn8 C-Terminal Domain Sample Per Biological Replicate, and a Comparison Between Cldn8 C-Terminal Domain and GST Samples per Replicate

These data show the Cldn8 C-terminal domain sample for each biological replicate sent to mass spectrometry, with the Cldn8 C-terminal domain samples being pooled for biological replicates two and three. This table also shows the total number of unique chick proteins with a 95% confidence level based on the Scaffold program, the number of unique proteins with a 99% confidence level, and the number of proteins present in either two or three replicates. This table also categorizes proteins by comparing the proteins present in the Cldn8 C-terminal domain samples vs GST samples, and are categorized as follows: 1) 0-2-fold greater in Cldn8 C-terminal domain vs GST, 2) two times or more greater in Cldn8 C-terminal domain vs GST, and 3) only seen in Cldn8 C-terminal domain samples.

3.3.2 Overview of the Mass Spectrometry Analysis of GST and GST-Cldn14 C-Terminal Domain Pulldowns

This section will describe the total number of proteins and peptides identified in the Cldn14 C-terminal domain samples sent to mass spectrometry, for a total of four samples. The total number

of proteins and peptides identified in all four Cldn14 C-terminal domain pulldown replicates are summarized in Table 4. Two of the four samples that were sent were bound to HH8 chick extract, which consisted of one GST sample and one Cldn14 C-terminal sample. The other two samples were bound to Day 4 chick extract, which consisted of one GST sample and one Cldn14 C-terminal domain sample (Table 4).

For the GST sample bound to HH8 chick extract, a total of 234 proteins (713 peptides), that included 150 chick proteins (573 peptides) and 84 *E. coli* proteins (140 peptides) were identified by mass spectrometry. For the Cldn14 C-terminal domain sample, a total of 525 proteins (2,274 peptides) were identified, which included 242 chick proteins (1,189 peptides) and 283 *E. coli* proteins (1,085 peptides) (Table 4).

For the GST sample bound to Day 4 chick extract, a total of 434 proteins (3,680 peptides), that included 400 chick proteins (3,630 peptides) and 34 *E. coli* proteins (50 peptides) were identified by mass spectrometry. For the Cldn14 C-terminal domain sample, a total of 662 proteins (4,321 peptides) were identified, which included 401 chick proteins (3,310 peptides) and 261 *E. coli* proteins (1,011 peptides) (Table 4).

Chick Extract	Bait	Total # proteins (# peptides)	# Chick proteins (# peptides)	# *E. coli* proteins (# peptides)
HH8	GST	234 (713)	150 (573)	84 (140)
	Cldn14 C-terminal domain	525 (2,274)	242 (1,189)	283 (1,085)
Embryonic Day 4	GST	434 (3,680)	400 (3630)	34 (50)
	Cldn14 C-terminal domain	662 (4,321)	401 (3,310)	261 (1,011)

Table 4: The Total Number of Proteins and Peptides Identified in Cldn14 C-Terminal Domain HH8 and Day 4 Samples

These data describe the total number of proteins and peptides identified in the Cldn14 C-terminal domain samples, either bound to HH8 chick extract or Day 4 chick extract. These proteins and peptides are composed of chick proteins and *E. coli* proteins. Samples are composed of either Cldn14 C-terminal domain or GST samples. Peptides are shown in parentheses.

Next, the enrichment of the proteins in the Cldn14 C-terminal pulldown samples as compared to the GST pulldown samples was evaluated (Table 5). Proteins present in the Cldn14 C-terminal domain pulldowns were categorized into three groups: <2-fold enrichment relative to GST, >2-fold enrichment but not unique relative to GST, and unique to Cldn14 C-terminal domain samples (Table 5). For the Cldn14 sample bound to HH8 chick extract, 94 proteins were <2-fold enriched, 4 proteins were >2-fold enriched in Cldn14 C-terminal domain sample vs GST, and 144 proteins were unique to the Cldn14 C-terminal domain sample, for a total of 242 proteins. For the Cldn14 sample bound to Day 4 chick extract, 314 proteins were <2-fold enriched, 26 proteins were >2-fold enriched, and 61 proteins were unique relative to the GST control sample, for a total of 400 proteins (Table 5). Out of the 242 chick proteins identified in the GST-pulldown using HH8 chick extract in the Cldn14 sample, 144 of them were only seen in Cldn14 sample, accounting for roughly 60% of the proteins. For the GST-pulldowns using Day 4 chick extract, 314 out of the 401 proteins were <2-fold enriched in Cldn14 vs GST samples, accounting for roughly 78% of the proteins.

Then, the number of chick proteins present in both Cldn14 C-terminal domain samples was determined in order to identify the Cldn14 C-terminal domain putative interacting partners present during HH8 and Day 4 chick extract (Table 5). 209 chick proteins were present in both Cldn14 C-terminal domain samples. 148 of these proteins were <2-fold enriched relative to GST, 23 proteins were >2-fold enriched but not unique relative to GST, and 38 proteins were only unique to Cldn14 C-terminal domain samples.

Cldn14 C-terminal domain bait + chick extract	Total number of chick proteins	0 to 2-fold > GST	>2-fold GST	Unique to Cldn14 C-terminal tail
Cldn14 + HH8	242	94	4	144
Cldn14 + Day 4	401	314	26	61
Present in both Cldn14 pull-downs	209	148	23	38

Table 5: The Total Number of Chick Proteins Identified in Cldn14 C-Terminal Domain Samples and A Comparison of Cldn14 C-Terminal Domain Samples Vs GST
These data describe the total number of chick proteins in each individual Cldn14 C-terminal domain or GST sample, which are bound to either HH8 or Day 4 chick extract. The number of proteins present in both GST-pulldowns to identify Cldn14 interacting partners are shown. This table also categorizes proteins by comparing the proteins present in the Cldn14 C-terminal domain samples vs GST samples, and are categorized as follows: 1) 0-2-fold greater in Cldn814 C-terminal domain vs GST, 2) two times or moregreater in Cldn14 C-terminal domain vs GST, and 3) only seen in Cldn14 C-terminal domain samples.

3.3.3 Validating the Efficiency of the GST-Pulldowns by Characterization of Claudin and ZO-1 Peptides Present in Cldn8 and Cldn14 C-Terminal Domain GST-Pulldowns

Given that GST-Cldn8 C-terminal domain and GST-Cldn14 C-terminal domain fusion proteins were used as bait and present in the pulldown sample sent for mass spectrometry analysis, it was expected that peptides for GST, Cldn8 and Cldn14 would be present. For the first Cldn8 C-terminal domain experiment, Cldn8 was identified seven times. In the second experiment, Cldn8 was identified 132 times in the first sample, and 177 times in the second sample. In the third experiment, Cldn8 was identified 189 times in the first sample, and 191 times in the second sample

(Table 5). In the first two Cldn8 experiments, only one peptide of the C-terminal domain of Cldn8 was identified, while three and two peptides were seen in the Cldn8 C-terminal domain samples one and two of the last experiment, respectively. This suggests that the first Cldn8 biological replicate sent to mass spectrometry was insufficient to identify Cldn8 interacting partners, as Cldn8 was seen only seven times. This is what led to additional GST-pulldowns being conducted, and Cldn8 was seen over 130 times in the remaining biological replicates. However, the first biological replicate was kept for further analysis, to determine if proteins present in the second and third biological replicates were also present in the first. Cldn14 was only seen 37 times in the Day 4 sample and 43 times in the HH8 sample.

As described above, the presence of ZO-1 was used to validate the GST-pulldowns. ZO-1 was not detected in any of the GST control samples in the Cldn8 experiments. Importantly, it was detected in three out of the five Cldn8 samples: one peptide in one sample and six peptides in the second sample from the second biological replicate and 3 peptides in one sample from the third replicate. ZO-1 was not detected in the first Cldn8 biological replicate, and this coincides with the western blot analysis, where a band at 225 kDa was not detected in the bound Cldn8 C-terminal domain fraction. For the Cldn14 pulldowns, ZO-1 was only seen in the Cldn14 C-terminal domain GST-pulldown performed with the Day 4 embryonic extract. However, it was observed equivalently in both the GST and the Cldn14 samples: 39 times in the GST sample and 32 times in the Cldn14 C-terminal domain sample. This coincides with the observation that a band at 225 kDa for ZO-1 was detected in both the GST and Cldn14 bound fraction samples by western blot analysis. ZO-1 was not detected in the Cldn14 GST-pulldown using HH8 chick extract, and that also coincides with a band at 225 kDa not being detected by western blot analysis in the Cldn14 bound fraction. Although ZO-1 was present in both GST and Cldn14 samples from the Day 4 GST-

pulldown, the number of times ZO-1 was detected in Cldn8 samples was lower when compared to Cldn14 samples. However, this may have been due to the amount of *E. coli* proteins present, which was significantly more in Cldn8 experiments versus Cldn14 experiments.

3.4 Prioritizing Cldn8 Interacting Partners for Further Analysis

In order to determine which of the 226 putative Cldn8 interaction partners should be prioritized for further analysis, different approaches were taken to prioritize these potential partners. The first criteria that was used to narrow the potential interacting partners was to look at all the proteins present in Cldn8 C-terminal domain vs GST samples. As described above the 226 proteins were separated into three categories: 1) proteins only present in Cldn8, 2) proteins present >2-fold in Cldn8 vs GST, and 3) proteins present <2-fold in Cldn8 vs GST (Table 6). 55 proteins were only seen in Cldn8, 51 were at least two times greater in Cldn8 vs GST, and 120 were less than two times greater in Cldn8 when compared to GST. The second criteria used was to select proteins present in more than one experiment. The rationale for this was to determine if these proteins only showed up in one experiment, or if they were pulled-down in at least two experiments. Those identified in multiple pull-down experiments have an increased likelihood that these are indeed interacting with the Cldn8 C-terminal domain. 24 out of the 55 proteins unique to the Cldn8 pulldown were present in more than one experiment, 38 out of the 51 proteins that were >2-fold enriched in Cldn8 vs GST were present in more than one experiment, and 48 out of the 120 proteins less than two times greater in Cldn8 vs GST were present in more than one experiment. Next, a Fisher's exact test ($p < 0.05$) within the context of the Scaffold program was conducted for the proteins present in more than one experiment. 6 of the 24 proteins that were unique to Cldn8 samples, 13 of the 38 proteins >2-fold enriched in Cldn8, and 13 of the 48 proteins that <2-fold enriched in Cldn8 vs GST passed the significance test.

Next, the list of proteins was compared to proteins that were identified as potential interactors with the C-terminal domain of Cldn4 by a BioID proximity ligation assay (Fredriksson et al., 2015). Cldn4 and Cldn8 have been shown to co-localize in tight junctions and therefore proteins that are in close proximity to Cldn4 may be Cldn8 interaction partners (Hou et al., 2010). Ten out of the 226 proteins identified by mass spectrometry were identified as potential Cldn4 interaction partners (Table 6). One out of the seven proteins unique to the Cldn8 samples that passed the significance test was identified in the Cldn4 BioID assay, while five out of the 24 proteins present in more than one experiment were also known to interact with Cldn4. One out of the 13 proteins that was >2-fold enriched and passed the significance test was also known to interact with Cldn4. For the proteins less than two times greater in Cldn8 vs GST, three out of the 120 proteins were known to interact with Cldn4.

Based on these criteria, 40 proteins were prioritized for further analysis (Table 6). These include six proteins that were significant in the "only in Cldn8" category; 13 proteins that were significant in the ">2-fold enriched in Cldn8 vs GST" category; 13 proteins that were significant in the "<2-fold enriched in Cldn8 vs GST" category; five proteins in the "unique to Cldn8" category that were known to interact with Cldn4; and three proteins in the "<2-fold enriched in Cldn8 vs GST" category that were known to interact with Cldn4. These proteins, along with their function, are listed in Table 7.

1st Criteria		2nd Criteria		
Proteins in Cldn8 vs GST		**> 1 exp**	**Significance**	**Interact with Cldn4**
Only in Cldn8	55	24/55	6/24	1/6 5/24
≤ 2X greater in Cldn8 vs GST	51	38/51	13/38	1/13
> 2X greater in Cldn8 vs GST	120	48/120	13/48	3/120

Table 6: The Criteria Used to Prioritize Cldn8 Interacting Partners
This table shows the criteria that were used to choose the interacting partners for further analysis. The first criteria used to select interacting partners was to look at proteins that were only in Cldn8, were two times greater in the Cldn8 samples versus the control samples, or less than two times greater in Cldn8 versus GST. Multiple secondary criteria were then used. Proteins that were only present in more than one experiment were looked at, and then proteins that were present in more than one experiment and passed a significance test. The last criteria used was to look at proteins already known to interact with Cldn4.

	Protein	ID	Function	Enrichment in Cldn8 C-Terminal vs GST
Only in Cldn8	Afadin	MLLT4	Afadin adherens junction formation factor	INF
	Caspase-3	CASP3	Apoptosis-related cysteine peptidase	INF
	CFR-associated protein p70	N/A	Fatty acid beta-oxidation	INF
	Growth factor receptor-bound protein 2	GRB2	Adapter protein that provides a critical link between cell surface growth factor receptors and the Ras signaling pathway; Belongs to the GRB2/sem-5/DRK family	INF
	Protein transport protein Sec23A	SEC23A	Protein transport protein homolog COPII coat complex component	INF
	S-adenosylmethionine synthase	MAT1A	Catalyzes the formation of S-adenosylmethionine from methionine and ATP	INF
	SEC24 homolog C, COPII coat complex component	SEC24C	COPII coat complex component; SEC24 family member C	INF
	Serine/threonine-protein phosphatase	PPP2CA	Catalytic subunit, alpha isozyme (PPP2CA), mRNA	INF
	Serine/threonine-protein phosphatase 2A 55 kDa regulatory subunit B	PPP2R2A	Serine/threonine-protein phosphatase 2A 55 kDa regulatory subunit B alpha isoform	INF
	Tight Junction Protein 1	TJP1	Adapter protein that interacts with the PDZ domain of claudins; Belongs to the MAGUK family	INF
	Tight Junction Protein 2	TJP2	Adapter protein that interacts with other ZO proteins	INF

	Protein	ID	Function	Enrichment in Cldn8 C-Terminal vs GST
At least 2X greater in Cldn8	Elongation factor 2	EEF2	Catalyzes the GTP-dependent ribosomal translocation step during translation elongation.	4.6
	Elongation factor Tu, mitochondrial	TUFM	Translational elongation	2.6
	Glyceraldehyde-3-phosphate dehydrogenase	GAPDH	Has both glyceraldehyde-3-phosphate dehydrogenase and nitrosylase activities, thereby playing a role in glycolysis and nuclear functions, respectively. Modulates the organization and assembly of the cytoskeleton.	2.3
	Lysozyme	LYZ	Lysozymes have primarily a bacteriolytic function; those in tissues and body fluids are associated with the monocyte- macrophage system and enhance the activity of immunoagents.	2.4
	Peroxiredoxin-1	PRDX1	Thiol-specific peroxidase that catalyzes the reduction of hydrogen peroxide and organic hydroperoxides to water and alcohols, respectively.	5.2
	Pyruvate kinase	PKM	Plays a key role in glycolysis; Belongs to the pyruvate kinase family	6.7
	Tubulin beta chain	TUBB	Tubulin, beta class I; Major component of the cytoskeleton.	2.4
	Tubulin beta-2 chain	TBB2	Tubulin; Major component of the cytoskeleton.	2.0

	Protein	ID	Function	Enrichment in Cldn8 C-Terminal vs GST
At least 2X greater in Cldn8	Tubulin beta-7 chain	N/A	Tubulin; Major component of the cytoskeleton.	2.0
	Tudor-interacting repair regulator protein	NUDT16L1	Key regulator of TP53BP1 required to stabilize TP53BP1 and regulate its recruitment to chromatin	13
	Vitellogenin-1	VTG1	Precursor of the egg-yolk proteins that are sources of nutrients during early development of oviparous organisms	2.3
	Vitellogenin-2	VTG2	Precursor of the egg-yolk proteins that are sources of nutrients during early development of oviparous organisms	2.2
	Vitellogenin-3	VTG3	Precursor of the egg-yolk proteins that are sources of nutrients during early development of oviparous organisms	2.3

	Protein	ID	Function	Enrichment in Cldn8 C-Terminal vs GST
Less than 2X greater in Cldn8	20-hydroxysteroid dehydrogenase	CBR1	Carbonyl reductase 1 (CBR1), mRNA; Belongs to the short-chain dehydrogenases/reductases (SDR) family	0.4
	Actin, cytoplasmic 2	ACTG1	Highly conserved proteins that are involved in various types of cell motility and are ubiquitously expressed in all eukaryotic cells	1.0
	Complement C1q binding protein	N/A	Is mitochondrial, yields the first component of the serum complement system.	1.2
	Glutathione peroxidase	GPX4	Glutathione peroxidase activity	0.4
	Glutathione S-transferase	N/A	Glutathione transferase activity	0.3
	Glutathione S-transferase	N/A	Glutathione transferase activity	0.4
	Glutathione S-transferase 2	GSTM2	Glutathione transferase activity	0.3
	Glutathione S-transferase class-alpha	N/A	Glutathione transferase activity	0.7
	Heat shock cognate 71 kDa protein	HSPA8	Molecular chaperone implicated in folding and transport of newly synthesized polypeptides, activation of proteolysis of misfolded proteins and the formation and dissociation of protein complexes.	1.0
	LanC-like protein 1	LANCL1	Glutathione binding	0.3
	Leucine-rich repeat transmembrane protein FLRT1	FLRT1	Extracellular matrix organization	1.5

	Protein	ID	Function	Enrichment in Cldn8 C-Terminal vs GST
Less than 2X greater in Cldn	Leucine-rich repeat transmembrane protein FLRT3	FLRT3	Modulates the structure and function of the apical ectodermal ridge (AER) that controls embryonic limb development. Functions in cell-cell adhesion, cell migration and axon guidance.	1.1
	Nucleosome-remodeling factor subunit BPTF	N/A	Histone-binding component of NURF (nucleosome-remodeling factor), a complex which catalyzes ATP-dependent nucleosome sliding and facilitates transcription of chromatin	0.5
Interact w/Cldn4	Stress-70 protein, mitochondrial	HSPA9	Chaperone protein which plays an important role in mitochondrial iron-sulfur cluster (ISC) biogenesis.	0.4
	Transforming acidic coiled-coil-containing protein 1	TACC1	Cell population proliferation, microtubule cytoskeleton organization	0.4
	Tubulin alpha chain	TUBA8A	Tubulin; Major component of the cytoskeleton	1.2

Table 7: The 40 Proteins Chosen for Further Analysis That Were Identified by Mass Spectrometry in Cldn8 C-Terminal Domain Samples
The top 40 interacting partners (column 1), their ID (column 2), their function in the cell (column 3), and the enrichment when comparing Cldn8 C-terminal domain samples vs GST in HH8 samples (column 4).

The next approach used as means of comparison was to see if these 40 proteins were only present in the Cldn8 dataset or also present in the Cldn14 dataset. Only six of the 40 putative Cldn8 interacting partners that were prioritized for further analysis were not present in the Cldn14 data set. These included: SEC24C, SEC23A, GRB2, MAT1A, TACC1, and FLRT3. The other Cldn8 putative interacting partners were present in either the Day 4 or HH8 Cldn14 samples and were sometimes present in the GST control sample done in parallel (Table 8).

	Protein	ID	Is it in the Cldn14 C-Terminal Domain Mass Spectrometry Data?	Enrichment in Cldn14 C-Terminal vs GST
Only in Cldn8	Afadin	MLLT4	Y- in both D4 GST and Cldn14	0.3 in Day 4
	Caspase-3	CASP3	Y- in both D4 and HH8	INF in HH8 INF in Day 4
	CFR-associated protein p70	N/A	Y- in D4 GST	0.0
	Growth factor receptor-bound protein 2	GRB2	N	Only in Cldn8 samples
	Protein transport protein Sec23A	SEC23A	N	Only in Cldn8 samples
	S-adenosylmethionine synthase	MAT1A	N	Only in Cldn8 samples
	SEC24 homolog C, COPII coat complex component	SEC24C	N	Only in Cldn8 samples
	Serine/threonine-protein phosphatase	PPP2CA	Y- in HH8	INF
	Serine/threonine-protein phosphatase 2A 55 kDa regulatory subunit B	PPP2R2A	Y- in both D4 and HH8	INF 5.3 in Day 4
	Tight Junction Protein 1	TJP1	Y- in both D4 GST and Cldn14	0.8 in Day 4
	Tight Junction Protein 2	TJP2	Y- in both D4 GST and Cldn14	0.7 in Day 4
Interact w/Cldn4	Stress-70 protein, mitochondrial	HSPA9	Y- in all samples	0.5 in HH8 0.3 in Day 4
	Transforming acidic coiled-coil-containing protein 1	TACC1	N	Only in Cldn8 samples
	Tubulin alpha chain	TUBA8A	Y- in all samples	0.9 in HH8 1.0 in Day 4

	Protein	ID	Is it in the Cldn14 C-Terminal Domain Mass Spectrometry Data?	Enrichment in Cldn14 C-Terminal vs GST
At least 2X greater in Cldn8	Elongation factor 2	EEF2	Y- in all samples	0.6 in HH8 3.8 in Day 4
	Elongation factor Tu, mitochondrial	TUFM	Y- except HH8 GST	INF in HH8 1.0 in Day 4
	Glyceraldehyde-3-phosphate dehydrogenase	GAPDH	Y- in all samples	1.2 in HH8 1.2 in Day 4
	Lysozyme	LYZ	Y- all samples	1.2 in HH8 0.7 in Day 4
	Peroxiredoxin-1	PRDX1	Y- in both D4 and HH8 GST and Cldn14	0.9 in HH8 2.7 in Day 4
	Pyruvate kinase	PKM	Y- in both D4 and HH8	INF in HH8 INF
	Tubulin beta chain	TUBB	Y- in both D4 GST and Cldn and HH8 Cldn14	INF in HH8 1.2 in Day 4
	Tubulin beta-2 chain	TBB2	Y- in both D4 and 8 GST and Cldn14	INF in HH8 1.2 in Day 4
	Tubulin beta-7 chain	N/A	Y- in both D4 and 8 GST and Cldn14	1.0 in HH8 1.1 in Day 4
	Tudor-interacting repair regulator protein	NUDT16L1	Y- in Day 4 GST and Cldn14	2.9 in Day 4
	Vitellogenin-1	VTG1	Y- in both D4 and HH8	0.7 in HH8 INF in Day 4
	Vitellogenin-2	VTG2	Y- in both D4 and HH8	0.6 in HH8 2.9 in Day 4
	Vitellogenin-3	VTG3	Y- in both D4 and HH8	INF in HH8 INF in Day 4
Less than 2X greater in Cldn8	20-hydroxysteroid dehydrogenase	CBR1	Y- except D4 GST	1.3 in HH8 INF in Day 4
	Actin, cytoplasmic 2	ACTG1	Y- in all samples	0.6 in HH8 1.0 in Day 4
	Complement C1q binding protein	N/A	Y- D4 and HH8 Cldn14	INF in HH8 INF in Day 4
	Glutathione peroxidase	GPX4	Y- D4 GST	0.0 in Day 4
	Glutathione S-transferase	N/A	Y- in all samples	0.7 in HH8 1.2 in Day 4
	Glutathione S-transferase	N/A	Y- in all samples	0.8 in HH8 1.7 in Day 4
	Glutathione S-transferase 2	GSTM2	Y- in all samples	0.6 in HH8 2.6 in Day 4

	Protein	ID	Is it in the Cldn14 C-Terminal Domain Mass Spectrometry Data?	Enrichment in Cldn14 C-Terminal vs GST
<2X greater in Cldn8	Glutathione S-transferase class-alpha	N/A	Y- in all samples	0.5 in HH8 1.8 in Day 4
	Heat shock cognate 71 kDa protein	HSPA8	Y- in all samples	0.2 in HH8 0.8 in Day 4
	LanC-like protein 1	LANCL1	Y- except D4 GST	1.5 in HH8 INF in Day 4
	Leucine-rich repeat transmembrane protein FLRT1	FLRT1	Y- in D4 Cldn14 and HH8 GST	0.0 in HH8 1.0 in Day 4
	Leucine-rich repeat transmembrane protein FLRT3	FLRT3	N	Only in Cldn8 samples
	Nucleosome-remodeling factor subunit BPTF	N/A	Y- in all samples	0.4 in HH8 0.2 in Day 4

Table 8: Do the Cldn8 Interacting Partners Also Interact with Cldn14?
The top 40 interacting partners (column 1), their ID (column 2), whether these proteins were identified by mass spectrometry in the Cldn14 C-terminal domain samples (column 3), and the enrichment when comparing Cldn14 C-terminal domain samples vs GST in HH8 and Day 4 samples (column 4).

3.5 The Top 10 Cldn8 Proteins Identified for Further Functional Analysis

The 40 proteins were then prioritized by the following criteria: (i) proteins previously shown to interact with other claudin family members, (ii) proteins previously shown to be associated with NTDs or the processes of convergent extension and apical constriction, and (iii) proteins located in the cytosol, as that is where the C-terminal domain of claudins are located. Proteins were removed if they were known to be components of chick embryos, such as vitellogenin and tubulin, as they were seen in Cldn8 and GST samples. Lysozyme and GST were also removed from the list, as lysozyme was used as part of the protein purification process, and glutathione sepharose beads were used for the pulldown assay. After removal of these proteins, 29 proteins remained, and 10 were chosen from the remaining proteins based on the above prioritization. These 10 proteins were: ZO-1, SEC24C, SEC23A, MAT1A, Afadin, Caspase-3, PPP2R2A, PPP2CA, CFR-

p70, and MAPK1 (Table 9). When looking at the Cldn8 data, all ten interacting partners were only present in Cldn8 samples and not in any GST samples. ZO-1, Caspase-3 and Afadin also interact with Cldn4 (Fredriksson et al., 2015) (Table 9). Seven out of the ten proteins also passed the significance test, except for Caspase-3, Afadin, and Serine/threonine-protein phosphatase subunit C (PPP2CA) (Table 9).

ZO-1 is involved in tight junction assembly and is known to interact with claudins. However, the role it plays in neural tube closure is unclear (Itoh et al., 1999). ZO-1 was seen in both the Cldn14 Day 4 samples and in Cldn8 samples (Table 8). Caspase-3 is a protease that is involved in apoptosis and has been associated with claudins and NTDs (Harris et al., 2007; Massa et al., 2009; Weil et al., 1997). Caspase-3 was seen in both the Cldn14 Day 4 and HH8 samples, and in Cldn8 samples (Table 8). Afadin is an adherens junction formation factor and has been associated with claudins and NTDs (Sawyer et al., 2011; Tabaries et al., 2019). Afadin was seen in the Cldn14 and GST Day 4 samples and was also seen in Cldn8 samples (Table 8). SEC24C and SEC23A are part of the COPII-coat mediated protein transport vesicle system, and both transport cargo proteins (Barlowe et al., 1994; Lee et al., 2004). SEC24C has been associated with claudins (Yin et al., 2017), while SEC23A has been associated with claudins and NTDs (Yin et al., 2017; Zhu et al., 2015). Both SEC24C and SEC23A were only seen in Cldn8 samples (Table 8). S-adenosylmethionine synthase (MAT1A) is involved in the folic acid pathway and has been associated with NTDs (Afman et al., 2005; Afman et al., 2003). MAT1A was seen in all the Cldn8 samples (Table 8). PPP2R2A and PPP2CA are both subunits of the serine/threonine-protein phosphatase PP2a (Sontag, 2001). PPP2R2A has been associated with claudins and NTDs (O'Shaughnessy et al., 2009; Thompson et al., 2018), while PPP2CA has been associated with NTDs (Campanale et al., 2017). PPP2R2A was seen in both the Cldn14 Day 4 and HH8 samples,

and in Cldn8 samples. PPP2CA was seen only once in the Cldn14 HH8 sample and was seen in three Cldn8 samples (Table 8). CFR-associated protein p70 is a fibroblast growth factor and has been associated with NTDs (Antoine et al., 2009). It was only seen in Cldn8 samples. MAPK1 was seen twice in the Cldn14 Day 4 samples and in two of the Cldn8 samples (Table 8). Mitogen activated protein kinase 1 (MAPK1) is a kinase in the ERK1/ERK2 pathway and has been associated with claudins and NTDs (Fyffe-Maricich et al., 2011; Imamura et al., 2010; Kim et al., 2016). Some of these proteins will be discussed in further detail on how they may potentially interact with the C-terminal domain of Cldn8, and how these interactions may possibly regulate processes during neural tube closure.

	Protein	ID	Only in Cldn8	Significant	Cldn4 BioID	Interact w/ cldns	NTDs	Function
1	ZO-1	TJP1				Yes	No	Tight junction assembly
2	Caspase-3	CASP3				Yes	Yes	Apoptosis pathway
3	Afadin, adherens junction	MLLT4				Yes	Yes	Adherens junction formation
4	SEC24 homolog C	SEC24C				Yes	N/A	Protein transport
5	Protein transport Sec23A	SEC23A				Yes	Yes	Protein transport
6	S-adenosylmethionine synthase	MAT1A				N/A	Yes	Folic acid pathway
7	Serine/threonine-protein phosphatase 2A regulatory subunit B	PPP2R2A				Yes	Yes	Phosphatase
8	CFR-associated protein p70	N/A				N/A	Yes	Fibroblast growth factor
9	Mitogen-activated protein kinase 1	MAPK1				Yes	Yes	Kinase, ERK1/2 pathway
10	Serine/threonine-protein phosphatase subunit C	PPP2CA				N/A	Yes	Phosphatase

Table 9: The Top 10 Cldn8 Interacting Partners for Further Analysis
This table represents the top 10 interacting partners chosen based on multiple criteria. These top ten are grouped based on the following: 1) If they are present only in Cldn8 samples, significant, and known to interact with Cldn4; 2) If they are only in Cldn8 samples and are significant, and 3) If they are only in Cldn8 samples. This table also shows if these proteins have been known to interact with other claudins, if they've been associated with NTDs, and states the function of the proteins.

CHAPTER 4: Discussion

My thesis research identified putative interaction partners that bind to the C-terminal domain of Cldn8 by using a GST-pulldown method. Some of the proteins identified have been associated with NTDs, while others have been previously shown to interact with other claudins. For this discussion, I have focused on the interacting partners that I would prioritize for further study. I will discuss how some of these proteins are involved in pathways and processes that regulate neural tube closure and when mutated cause a NTD. I will also discuss how some of the proteins that were identified in this study are shown to be important for the formation of tight junctions.

I conducted three experiments for my Cldn8 GST-pulldowns, and three biological replicates were sent to mass spectrometry for identification of proteins. The first replicate was composed of one sample of GST and one sample of GST-Cldn8 beads, while the second and third biological replicates consisted of duplicate samples of GST and GST-Cldn8 beads. The first experiment did not work as well as the other two experiments as determined by the absence of ZO-1 in the Cldn8 pulldown samples. ZO-1 was used as a positive control as it is known to interact with the C-terminal domain of claudins. ZO-1 was present in the subsequent two GST-Cldn8 C-terminal domain pulldown experiments. The absence of a band at 225 kDa (the predicted molecular weight of ZO-1) in the western blot analysis correlates to the absence of ZO-1 in the mass spectrometry results. A total of 226 unique chick proteins were identified when all the mass spectrometry data were pooled.

When validating the GST-pulldowns for both Cldn8 and Cldn14 experiments by western blot analysis using the ZO-1 antibody, a ~130 kDa band was present in the bound lanes (GST beads or GST-Cldn8 beads) for the Cldn samples that was not present in the GST control lane, the unbound fraction, or the chick embryo protein extract lane. Very few of the peptides identified by mass

spectrometry corresponded to proteins that were ~130 kDa, and that were only present in my Cldn samples. Peptides corresponding to ZO-2, which has a molecular weight of 150 kDa and binds to ZO-1 and occludin (Gumbiner et al., 1991), were identified in some of the Cldn8 samples. The band at ~130 kDa was present even when the 225 kDa band corresponding to ZO-1 was not detected. This band was present in all the western blot analyses and was present even when ZO-1 was not detected in the mass spectrometry data. Although I cannot conclude what this band was it is possible that this band is ZO-3. As stated in the Introduction, ZO-1 does interact with ZO-3 and ZO-3 has a molecular weight of 130 kDa (Balda et al., 1993; Haskins et al., 1998). When aligning the protein sequences by BLAST, there is 44% similarity between the entire sequences of ZO-1 and ZO-3. The first PDZ domain of zonula occluden proteins bind to the C-terminal domain of claudins. When aligning the first PDZ domain of both ZO-1 and ZO-3 against each other, there was found to be a 52% similarity. When looking up the immunogen information for the anti-ZO-1 antibody used for western blot analysis, the data sheet shows that it is a synthetic peptide in the middle region of ZO-1. The peptide is found between amino acid positions 400-1200. When this region was aligned to that of ZO-3, there was a 53% similarity found between the regions. It is possible that the antibody did interact with a region of ZO-3, specifically the first PDZ domain. Although ZO-3 was not detected in the mass spectrometry data, the band present at 130 kDa in all western blots pertaining to the C-terminal domain of Cldn8 and 14 may correspond to ZO-3.

There were also many more proteins present in the Cldn14 data versus the Cldn8 data. This could be because more chick extract protein was used for the Cldn14 experiments (3.3 mg of HH8 chick extract and 4.65 mg of Day 4 chick extract), whereas 500 µg or 1 mg of HH8 chick extract was used for the Cldn8 experiments. The Cldn14 samples also included HH8 and Day 4 samples. Day 4 chick extract has more tissue and potentially has more protein-protein interactions occurring

during that stage of development versus HH8, which can also be another reason as to why more proteins were detected when compared to Cldn8 HH8 data (mass spectrometry data is in Appendix C). Out of the 40 Cldn8 interacting partners chosen to further study, 34 of these proteins were also identified as Cldn14 putative interacting partners. The six proteins that were only identified in the Cldn8 data were: SEC24C, SEC23A, GRB2, MAT1A, TACC1, and FLRT3. SEC24C, SEC23A, GRB2, and MAT1A were only seen in Cldn8 samples, while TACC1 and FLRT3 were seen in both Cldn8 and GST samples.

A limiting factor with this experiment is that although we can determine the protein-protein interactions, we cannot see where they are binding to in the Cldn8 C-terminal domain. Do these proteins interact with specific residues at the C-terminal domain, or do they interact with the PDZ-binding motif? This is why it is crucial to identify the proteins that interact with the Cldn8 variants, and also to perform co-immunoprecipitations.

4.1 Interactions that Occur Between ZO-1 and Cldn8 Are Important for TJ Assembly, Linking the TJ to the Actin Cytoskeleton and Formation of the TJ Cytoplasmic Plaque

ZO-1 was one of the proteins that was identified by mass spectrometry in the Cldn8 GST-pulldown fraction and was also part of the top 10 protein list. It is important to note that when the YV residues, which are part of the PDZ-binding motif of claudins, were removed from the Cldn8 C-terminal domain and this variant was overexpressed in chick embryos, over 90% of embryos had normal neural tube closure, while embryos overexpressing variants with mutated residues at positions S198 and S216 showed a NTD phenotype (Baumholtz, 2018). This suggests that the direct interactions between the PDZ-binding motif, located on the C-terminal domain of Cldn8, and ZO-1, which binds to this domain, may not play a role in neural tube closure or for signaling

morphogenetic events such as cell shaping, signifying the importance of considering other interaction partners for this analysis. This does not dispute the fact that interactions with proteins such as ZO-1 are not important. The Cldn8 variants generated also co-localized with ZO-1 to the tight junction, suggesting its importance to bringing claudins to the tight junction (Baumholtz, 2018). It is possible that variants in the Cldn8 C-terminal domain can indirectly disable interactions that occur at the PDZ-binding motif, thus inhibiting interaction with proteins such as ZO-1. It has been hypothesized that core planar cell polarity (PCP) proteins and scaffolding proteins such as ZO-1 interact with each other, and indirectly interact with claudins (Chen et al., 2016).

Although this thesis focuses on direct interactions with the Cldn8 C-terminal domain, this data suggests that ZO-1 is needed for claudins to localize to the tight junction and that its proximity to and interactions with PCP proteins may indirectly link Cldn8 to proteins in the PCP pathway, potentially regulating events such as cell shaping, and processes such as convergent extension, which are crucial during neural tube closure(Van Itallie, 2013).

4.2 COPII-Mediated Vesicle Transport Proteins Sec23A and Sec24C Are Known to Interact with Claudins and Sec23A Has Been Associated with NTDs

My data identified two proteins that are part of the COPII-mediated vesicle transport pathway, Sec23A and Sec24C, as candidate interaction partners for the Cldn8 C-terminal domain. Both of these proteins are known to interact with YV residues in the C-terminal domain of Cldn1, and mice deficient in Sec23A showed cranial NTDs and also exhibited neural tube openings in the midbrain (Zhu et al., 2015). Neither of these proteins were identified as Cldn14 putative interacting partners. The COPII complex is made of highly conserved proteins that are responsible for creating small membrane vesicles that originate from the endoplasmic reticulum (ER) (Barlowe et al., 1994; Lee et al., 2004). This pathway aids in transporting membrane and luminal cargo proteins from the ER

to the Golgi and other membrane compartments in the cell (Jensen et al., 2011). In cells, Sec23 and Sec24 are found in tight heterodimers, which form the inner COPII coat (Barlowe et al., 1994). Gene-duplication events have created multiple paralogs: two Sec23 paralogs, Sec23A and Sec23B; and four Sec24 paralogs, Sec24A, Sec24B, Sec24C and Sec24D. Sec24 is the primary subunit responsible for binding to membrane cargo proteins at the ER and concentrating them into the forming vesicle (Miller et al., 2002)

4.2.1 The Non-Canonical and Canonical Wnt/PCP Pathways, and the Regulation of Convergent Extension during Neural Tube Closure

Although Sec24C has not been associated with NTDs, one of its paralogs, Sec24B does cause NTDs when mutated (Merte et al., 2010). Sec24B is a cargo-sorting protein in the COPII complex and is responsible for the sorting and trafficking of *Vangl2*, a core protein in the PCP pathway (Wendeler et al., 2007). Mouse mutants in the PCP pathway have convergent extension defects that result in craniorachischisis, a severe NTD (Merte et al., 2010). Mutations in *Sec24b* contribute to NTDs such as spina bifida (Merte et al., 2010). In C-CPE treated chick embryos, *Vangl2* shows reduced localization when Cldn3, -4, and -8 are removed from the neural (Cldn4 and -8) and non-neural (Cldn3 and -4) ectoderm (Baumholtz et al., 2018), suggesting claudins somehow interact with *Vangl2* (unknown whether they are direct or indirect interactions) and possibly by directly interacting with ZO-1. If the C-terminal domain of Cldn8 is mutated, *Vangl2* may no longer be able to interact with Cldn8, thus causing defects in convergent extension, leading to NTDs. This can be because Sec24C can no longer bind to the C-terminal domain of Cldn8, and Sec24B can no longer indirectly interact with Cldn8, unable to get cargo proteins (such as *Vangl2*) to the apical membrane.

The canonical-β-catenin dependent Wnt signaling pathway is important in the process of neural tube closure, and defects in this pathway lead to NTDs (Copp et al., 2003; Ybot-Gonzalez et al., 2007; Zhao et al., 2014). Subunits of Serine/threonine-protein phosphatase 2A (PP2A), a phosphatase, was identified by mass spectrometry in the Cldn8 GST-pulldown fraction. PP2A is made up of catalytic (PPP2C), structural (PPP2R21) and regulatory (b-type) subunits. Two different subunits were identified by mass spectrometry in the Cldn8 GST-pulldown fraction, PPP2R2A and PPP2CA. PP2A has been shown to dephosphorylate cytoplasmic phospho-β-catenin (Su et al., 2008) and co-localize with it at the plasma membrane (Thompson & Williams, 2018). It has been shown that PPP2R2A binds directly to cytoplasmic β-catenin in HEK293T and SV480 epithelial cells. Knockdown of PPP2CA in cells results in hyperphosphorylation of β-catenin (Su et al., 2008) while knocking down PPP2R2A results in the phosphorylation of β-catenin and decreased Wnt signaling (Zhang et al., 2009). Overexpression of PPP2R2A enhances Wnt signaling. As the canonical-β-catenin dependent Wnt signaling pathway is important during neural tube closure, and knocking down PPP2R2A results in decreased Wnt signaling, the interactions between PP2A and Cldn8 can potentially play a role in the canonical Wnt pathway, and when the C-terminal domain is mutated, can inhibit these interactions from occurring.

4.3 The Association of Folic Acid and NTDs

Folate has been shown to be crucial in the involvement of neural tube closure. The folic acid pathway is required for neural tube closure, and mutations in this pathway or reduced dietary folate result in a NTD phenotype (Kibar et al., 2007; Pangilinan et al., 2012). MAT1A, also known as S-adenosylmethionine synthase, is involved in the transfer of adenosyl moiety of ATP to methionine to form S-adenosylmethionine and tripolyphosphate and plays a role in the folic acid pathway. It is one of the interacting partners identified by mass spectrometry in the Cldn8 GST-pulldown

fraction. As the folic acid pathway is involved in the process of neural tube closure, it is possible that MAT1A interacts with Cldn8 during stages of neurulation, and potentially plays a process in neural plate shaping and bending of the neural folds. It would be interesting to see if MAT1A also interacts with Cldn3 or -4, as these claudins are present during these stages in neurulation.

When there is a low amount of folate, there is reduced remethylation of homocysteine (Hcy) to methionine, meaning there is a rise in Hcy levels. These increased levels of Hcy concentrations has been reported in mothers who have children with NTDs (Afman et al., 2005). In order to test the hypothesis that methylation is important for neural tube closure, chick embryos were treated with Hcy, and a delay in neural tube closure was observed (Afman et al., 2003). It was determined that the rise in Hcy levels is because of inhibition of transmethylation due to elevation of S-adenosylhomocysteine (AdoHcy) and a reduction of S-adenosylmethionine (AdoMet) (Afman et al., 2005). Similar results were seen when MAT was inhibited. When MAT was inhibited in mouse embryos, there was a decrease in the AdoMet/AdoHcy ratio, and the resulting phenotype was cranial defects (Dunlevy et al., 2006). This data suggests that a mutation in the folic acid pathway can lead to inhibition of MAT1A, and this can possibly disable interactions to occur with the Cldn8 C-terminal domain, causing a NTD phenotype. It can also suggest that environmental factors, such as reduced folate in mothers can lead to these interactions not properly occurring.

4.4 Apoptosis May Be Necessary During Stages of Neurulation

Caspases are a family of cysteine proteases involved in programmed cell death, which is a crucial factor during embryonic development (Massa et al., 2009). Caspase-3 cleaves protein substrates within the apoptotic cell and was one of the interacting partners identified by mass spectrometry in the Cldn8 GST-pulldown fraction. Apoptosis is an important process for neural tube closure (Weil et al., 1997).

A study in mice determined the role of apoptosis during neural tube closure. This study found that apoptosis is linked to three events during neural tube closure: 1) bending and fusion of the neural folds, 2) epithelial remodeling after fusion, and 3) emigration of neural crest cells (Massa et al., 2009). This study concluded that apoptosis may be required during closure at the midbrain and hindbrain. It has been shown that Caspase-3 null mice have cranial NTDs, and these mice have a lack of apoptosis (Harris & Juriloff, 2007).

Excessive amounts of apoptosis also lead to neural tube defects such as spina bifida in mice embryos (Wei et al., 2012). Apoptosis may be stage specific. During neural plate induction (around HH4), not much apoptosis seems to be occurring at the neural plate, while later stages have more apoptosis occurring. Cells undergoing apoptosis are concentrated at the neural and non-neural border. In a study looking at how the inhibition of caspase affects neural tube closure, chick embryos were cultured in the presence of cell-permeable peptide caspase inhibitors (Weil et al., 1997). In embryos treated with these inhibitors, the neural tube remained open. In some of the embryos treated with these inhibitors, the neural folds were able to appose each other, but were not able to fuse. This suggests that apoptosis may be required during later stages of neurulation.

It is possible that Cldn8 directly interacts with Caspase-3 during neurulation, especially at HH8 where the bending of the neural plate is occurring. These interactions enable apoptosis to occur at the appropriate staging, allowing the neural folds to fuse properly. Cldn8 variants generated in the C-terminal domain of Cldn8 can affect the binding of Caspase-3, leading to excessive amounts of apoptosis or lack of apoptosis, both of which are associated with NTDs. This, in turn, can affect neural tube closure during later stages of neurulation, where the neural folds can bend and elevate, eventually apposing each other, but cannot fuse properly.

4.5 Kinases and Phosphatases that Regulate Tight Junction Formation and the Phosphorylation Events that Mediate These Processes

Protein phosphorylation is a post-translational modification that occurs at the C-terminal domain of claudins (Tanaka et al., 2005; Van Itallie et al., 2018). The putative Cldn8 interaction partners that are involved in phosphorylation are the Mitogen-activated protein kinase-1 (MAPK1) and Serine/threonine-protein phosphatase 2A (PP2A). MAPK1 is a member of the mitogen-activated protein kinase family (Upadhya et al., 2013), and is itself activated by phosphorylation. RAS, a small G protein, leads to the activation of the MAPK kinase MEK, and MEK phosphorylates and activates MAPK (Sebolt-Leopold et al., 2004). This pathway regulates different processes such as cell proliferation and differentiation (Yoon et al., 2006). PP2A is a phosphatase that regulates signal transduction pathways (Sontag, 2001). It also is involved in cell-cell adhesion, which is important for apicobasal polarity. Both subunits identified in the bound Cldn8 fraction (PPP2R2A and PPP2CA) were also identified as putative Cldn14 interacting partners, suggesting that it dephosphorylates multiple Cldns, and is not only specific to Cldn8.

Different kinase pathways have been associated with the CLDN family, including MAPK pathway and Akt (Lu et al., 2011). Both Protein Kinase B (Akt/PKB) and atypical αPKC play a role in tight junction biogenesis and cell polarity, and have been shown to bind to PP2A. αPKC activity is involved in the phosphorylation of occludin and ZO-1 (Stuart et al., 1995). The phosphorylation predictor program NetPhos 3.1, predicts that both MAPK and Akt can phosphorylate Cldn8 at positions S198 and S216. It has been shown that when there is an increase in Akt signaling, there is epidermal barrier acquisition (O'Shaughnessy et al., 2009), and when PP2A and Akt signaling are inhibited, there are defects in epithelial barrier acquisition. Interactions between Cldn8, MAPK, and Akt are likely due to MAPK and Akt phosphorylating and

dephosphorylating Cldn8. Consequently, this could affect interactions with other proteins that are related to cell shape changes. It has also been shown that MAPK and Akt are not phosphorylated in Cldn8 knockdown cells (Ashikari et al., 2017), suggesting Cldn8 modulates these phosphorylation pathways. This data can also suggest that if the C-terminal domain of Cldn8 is mutated at a specific residue, such as S198 and S216 that this can disable interactions to occur with MAPK and Akt. If these interactions do not occur, and Cldn8 cannot be phosphorylated or dephosphorylated, then this can affect the process of neural tube closure.

Protein Kinase C (PKC) participates in regulating tight junction proteins such as Cldn1, occludin, and ZO-1 (Stuart & Nigam, 1995). αPKC-mediated phosphorylation is important for Ca^{2+} tight junction assembly (Stuart & Nigam, 1995; Suzuki et al., 2001). PP2A may directly regulate the αPKC/Par-3 complex, which is part of the Par complex and is important for the formation of tight junctions (Campanale et al., 2017). Afadin, an adherens junction formation factor identified by mass spectrometry in the Cldn8 GST-pulldown fraction, is also associated with αPKC and when there is a loss of afadin, the localization of both Par-3 and αPKC change (Sawyer et al., 2011). It has been shown that BMP interacts with apicobasal polarity proteins during MHP formation, a cell shaping event in neural tube closure (Eom et al., 2011). BMP overexpression disables the MHP to form and does not allow the neural tube to properly close. There is low BMP activity at the ventral midline and at the MHP. BMP interacts with the Par complex, which consists of Par3, Par6, and αPKC, and this complex localizes at apical junctions. These interactions are crucial for apical constriction and for the formation of the MHP. Since PP2A interacts with this complex, and the loss of afadin changes the localization of this complex, it is possible that the interactions between Cldn8 and these two proteins are necessary to regulate cell shape events during later stages of neurulation which enable the neural plate to bend and elevate.

It has been shown that for the neural tube to properly close, there needs to be proper proliferation, migration, and differentiation of neural stem cells (Turner et al., 2013; Zhang et al., 2015). MAPK1/MAPK3 double knockout mice have an increase in apoptotic cells and have a decrease in neural progenitor cell proliferation (Fyffe-Maricich et al., 2011; Imamura et al., 2010). When the MAPK pathway was inhibited in mice with PD325901, there was a reduction in phosphorylation of MAPK1 and MAPK3, along with decreased expression of Cldn1 and -4 at the tight junction while no effect was seen in Cldn3 expression (Kim & Breton, 2016). This is of interest, as Cldn4 is also present in the neural ectoderm with Cldn8 during HH8 of neurulation. MAPK1 was identified as a putative interacting partner of wild-type Cldn8. If the C-terminal domain of Cldn8 is mutated at positions S198 and S216, identified as putative serine phosphorylation sites, phosphorylation that normally occurs for MAPK1 may not occur, and NTDs can form.

4.6 Limitations of Using a GST-Pulldown Approach to Identify Cldn8 C-Terminal Domain Interacting Partners

A limitation to this project was that many *E. coli* proteins were present in the mass spectrometry results when compared to the number of chick proteins present. This was especially noticeable in the Cldn8 C-terminal domain samples, which led me to doing column purification for the third experiment instead of the batch purification that was performed for the first two sets of pulldown experiments. The presence of so many *E. coli* proteins may have taken up depth on the mass spectrometer, thus not enabling potential interacting partners from being present in the dataset or reducing the number of times a certain peptide was seen. The presence of *E. coli* proteins also could have prevented certain proteins from binding to the beads. The presence of many *E. coli* proteins may have reduced the number of times ZO-1 was detected. A similar amount of chick and

E. coli proteins were present in Cldn14 C-terminal domain Day 4 and HH8 samples, yet many more *E. coli* proteins than chick proteins were present in the Cldn8 C-terminal domain samples. This may have been due to the protein purification process.

4.7 A Proposed Model of Interactions that Occur at the C-Terminal Domain of Cldn-8

In my thesis project, I identified multiple proteins that may interact with the C-terminal domain of Cldn8 at HH8 of chick neurulation. These proteins are involved in various functions, such as regulating cell-adhesion, tight junction formation, programmed cell death, and in sorting and transporting cargo proteins. Some proteins are associated with pathways that have been shown to participate in neural tube closure, such as the folic acid pathway, PCP pathway, and the ERK1/ERK2 pathway. Several of the proteins identified in this study are known to affect convergent extension and cell shaping events, including apical constriction, which we have previously shown to be affected by Cldn8 depletion. For example, localization of Vangl2, a component of the non-canonical Wnt-PCP signaling pathway, is reduced in Cldn8-depleted neural ectoderm (Baumholtz et al., 2017). In my study, Sec24C, a paralog of Sec24B that is known to interact with Vangl2 and play a role in regulating convergent extension (Merte et al., 2010; Wendeler et al., 2007), was identified as a candidate interaction partner of Cldn8. As of now, there is no evidence to show that Sec24C is associated with NTDs but mutations in Sec24B that inhibit its binding to *Vangl2* are associated with NTDs (Merte et al., 2010). Another candidate whose interactions with Cldn8 might be linked to neural tube closure is Caspase-3, which is involved in the apoptosis pathway. In chick embryos treated with caspase inhibitors, the neural folds are unable to fuse (Weil et al., 1997), suggesting that Caspase-3 might play a role in the cell shaping events required for neural tube closure.

The data from the mass spectrometry analysis suggests that there is a large network of interactions that are occurring at the cytoplasmic domain of tight junctions and that these interactions involve proteins with many different functions. Figure 9 shows a hypothetical model of how the C-terminal domain of Cldn8 could interact with the candidate proteins discussed. The C-terminal two amino acids (YV) of most classical claudins form the PDZ-binding domain that is known to interact with the first PDZ domain of ZO-1 (Itoh et al., 1999) (Figure 9). Sec23A and Sec24C, which form a complex and are part of the COPII-mediated vesicle transport system, have also been shown to bind to the YV region of Claudin-1 (Zhu et al., 2015) (Figure 9). MAPK1 is a kinase that has been predicted by the post-translational modification prediction software NetPhos 3.1 to phosphorylate the C-terminal domain of Cldn8, specifically at positions S198 and S216 (Figure 9). It is not clear if phosphorylation of S198 or S216 would affect the binding of candidate interaction partners MAT1A, which is part of the folic acid pathway, or Caspase-3, which is part of the apoptosis pathway. The GST-fusion protein used for the pulldown experiments was prepared in *E. coli* and therefore would not be phosphorylated.

I propose that when the wildtype Cldn8 is expressed that these protein-protein interactions occur at the C-terminal domain. However, if positions S198 and S216 are mutated, these interactions may not occur. Thus, this could also affect interactions that occur at the YV residues, and the ability of the YV residues to interact with ZO-1 and potentially the COPII-mediated vesicle system, specifically with Sec23A and Sec24C. This can inhibit the tight junction from linking to the actin cytoskeleton. These interactions may no longer occur because of a difference in protein folding or even the protein shape, hindering only one or both ZO-1 and the Sec proteins from properly binding to the YV residues, thus inhibiting the neural tube from closing properly. I do not believe that ZO-1 and the COPII-mediated vesicle system are competing for interactions with the

YV residues. ZO-1 interacts with all the C-terminal domains of claudins, while the interactions with the COPII-mediated vesicle with all known claudins is still unknown. Based on the mass spectrometry analysis, this complex does not interact with the C-terminal domain of Cldn14. A change in the protein conformation of the C-terminal domain of Cldn8 may inhibit these proteins interactions.

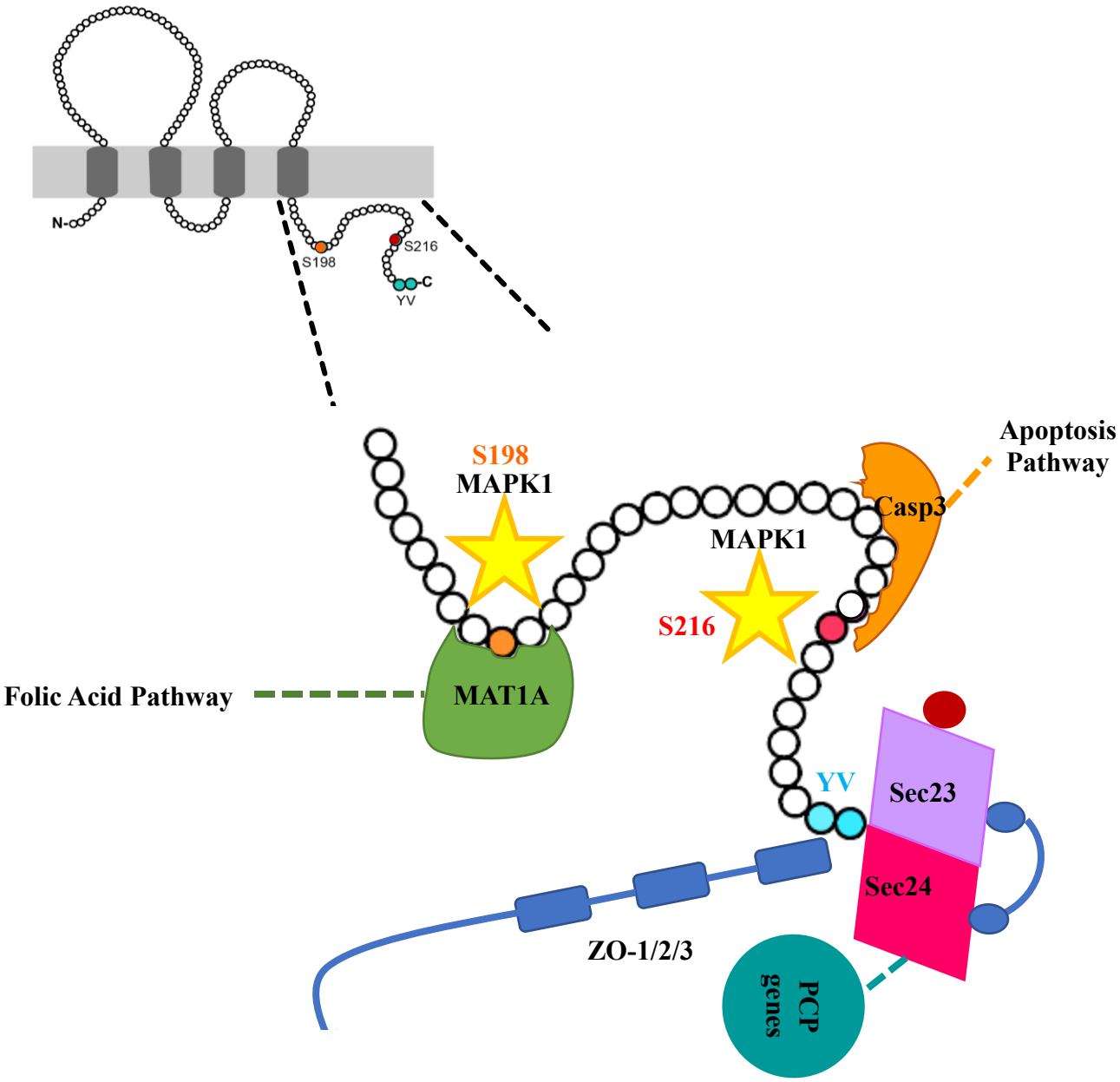

Figure 9: Proposed Model of Cldn8 C-Terminal Domain Interactions
This diagram shows a proposed model for protein-protein interactions between the wild-type Cldn8 C-terminal domain and some of the proteins that were identified by mass spectrometry analysis of the GST-Cldn8 pulldown sample. The ZO proteins are depicted by the three linked blue rectangles. Sec23A and Sec24C are part of the COPII-mediated vesicle transport system and these proteins are depicted by the pink and purple quadrilaterals. The PCP genes have also been hypothesized to be in proximity to ZO-1, and *Vangl2*, a core PCP protein is represented by the teal circle, with the dotted line representing interaction with Sec24B. The kinase MAPK1 is represented by the yellow star, MAT1A is depicted by a green circle, and Caspase-3 is depicted by an orange shape, with the dotted lines showing the association of a protein to its function or pathway. Candidate interaction proteins are not to scale.

CHAPTER 5: Conclusions and Future Directions

5.1 Conclusions

The purpose of this thesis project was to identify putative interacting partners of the Cldn8 C-terminal domain. This was achieved by using a GST-pulldown methodology, and then using mass spectrometry to identify these partners. The GST-pulldown approach was used as it looks at direct interactions between bait and prey. I believe that the methodology used was the most reasonable for this thesis project. However, as stated previously, there were limitations in terms of the amount of *E. coli* proteins present. These proteins may have inhibited crucial interacting partners from being identified by the mass spectrometer.

Although a future direction for this project, it would have been beneficial to also perform GST-pulldowns with the Cldn8 variants generated previously in our lab (S198A, S216A, S216I and ΔYV), as it would have been a great means of comparison between the wild-type and variant Cldn8. While the chick is a great and effective model for studying neural tube closure, the protein dataset in chick is not as established as other animal models, such as the mouse. It would have been beneficial to determine the Cldn8 C-terminal domain interacting partners in more established animal models, in order to have full coverage of possible interacting partners.

At this moment, we have not yet proven that direct interactions occur with the proteins identified by mass spectrometry and the Cldn8 C-terminal domain, and if the interactions are associated with neural tube closure. Some of these proteins have been associated with NTDs when interacting with other proteins, but until now, there has not been any evidence of these proteins interacting with claudins and during the process of neural tube closure. These interactions may be crucial for getting Cldn8 to the tight junction, for barrier properties and cell adhesion, or even for regulating events such as phosphorylation once at the tight junctions, but we can only speculate

the role of these interactions with wild-type Cldn8 during neural tube closure. It is possible that mutating the Cldn8 C-terminal domain may inhibit interactions that normally occur with the wild-type Cldn8. Inhibiting protein function in processes such as apoptosis (Caspase-3) phosphorylation (MAPK pathway, or inhibiting PP2A from binding to different kinases) may cause a NTD phenotype.

5.2 Future Directions

The next steps of this project will be to validate the top 10 interacting partners of Cldn8 by performing co-expression and co-localization analyses. The first type of co-expression experiment to be done will be whole mount *in-situ* hybridization. This is a relatively simple and inexpensive method of determining if the mRNA of the interacting partners are co-expressed with Cldn8 in the neural ectoderm at HH8 of neurulation. If the interacting partners are expressed in the neural ectoderm at this stage, then immunofluorescence will be performed to determine if the interacting partners co-localize with Cldn8 at tight junctions in the neural ectoderm at HH8. HH8 of neurulation is a beneficial stage to look at during neurulation as the neural folds are elevating but part of the neural plate is still flat.

Protein-protein interaction experiments will then be conducted, such as co-immunoprecipitation. Ideally, the Cldn8 antibody would be used to do a co-immunoprecipitation. However, the epitope of the antibody is located on the C-terminal domain of Cldn8 and could potentially inhibit protein-protein interactions. Another possibility would be to use antibodies for the interacting partners and use those to do a co-immunoprecipitation. However, if *in vivo* co-immunoprecipitation cannot be performed, two alternatives can be done: The first will be to electroporate the tagged interacting partners into chick embryos and then do a co-

immunoprecipitation *in vivo*. The other alternative method would be to an *in vitro* experiment by transfecting HEK293 cells and tag wild-type Cldn8 and the interacting partners.

Additionally, it will be beneficial to look at protein-protein interactions with the Cldn8 C-terminal domain variants and determine if the partners identified in the wild-type samples interact with these variants. Do mutations at these residues affect the interactions that occur at the PDZ-binding domain with proteins such as ZO-1? Will mutating the C-terminal domain of Cldn8 potentially inhibit crucial events during neural tube closure to occur properly, thus causing NTDs? It will also be crucial to determine why the variants cause a NTD phenotype.

The big question that our lab would like to answer is if the protein-protein interactions that occur at the Cldn8 C-terminal domain are required for recruiting claudins to the tight junction, or if they are important once claudins are at the tight junction. Our lab has shown that Cldn8 variants do localize to tight junctions (Baumholtz et al., 2018), so it may be possible that the protein-protein interactions are important once at the tight junction. If we mutate the C-terminal domain at specific residues (such as putative serine phosphorylation sites), will this inhibit or affect the interactions with these proteins? When S198 was mutated to S198A, defects were seen. This may be because phosphorylation could no longer occur at S198A, and the proper interactions did not occur. Mutating S216 to S216A did not cause a NTD phenotype. However, mutating S216 to S216I caused NTDs and convergent extension defects. Isoleucine is a larger amino acid than serine and is also hydrophobic. This may have changed the protein conformation or protein folding, and the proper interactions that normally occur may no longer occur. Do the Cldn8 variants disable certain protein interactions from occurring, and does this increase susceptibility to NTDs?

Overall, the data from this thesis project is the first step to examine protein-protein interactions that occur with Cldn8 during neural tube closure. Further validation studies of the candidate partners identified can help us determine and pinpoint the role of Cldn8 during neural tube closure, and the proteins that may potentially regulate the processes that regulate cell shaping events or may be part of pathways that, if mutated, can contribute to NTDs.

CHAPTER 6: References

Afman, L. A., Blom, H. J., Drittij, M. J., Brouns, M. R., & van Straaten, H. W. (2005). Inhibition of transmethylation disturbs neurulation in chick embryos. *Brain Res Dev Brain Res, 158*(1-2), 59-65. Retrieved from https://www.ncbi.nlm.nih.gov/pubmed/15996755. doi:10.1016/j.devbrainres.2005.06.002

Afman, L. A., Blom, H. J., Van der Put, N. M., & Van Straaten, H. W. (2003). Homocysteine interference in neurulation: a chick embryo model. *Birth Defects Res A Clin Mol Teratol, 67*(6), 421-428. Retrieved from https://www.ncbi.nlm.nih.gov/pubmed/12962286. doi:10.1002/bdra.10040

Antoine, M., Kohl, R., Tag, C. G., Gressner, A. M., Hellerbrand, C., & Kiefer, P. (2009). Secreted cysteine-rich FGF receptor derives from posttranslational processing by furin-like prohormone convertases. *Biochem Biophys Res Commun, 382*(2), 359-364. Retrieved from https://www.ncbi.nlm.nih.gov/pubmed/19285038. doi:10.1016/j.bbrc.2009.03.026

Ashikari, D., Takayama, K. I., Obinata, D., Takahashi, S., & Inoue, S. (2017). CLDN8, an androgen-regulated gene, promotes prostate cancer cell proliferation and migration. *Cancer Sci, 108*(7), 1386-1393. Retrieved from https://www.ncbi.nlm.nih.gov/pubmed/28474805. doi:10.1111/cas.13269

Au, K. S., Ashley-Koch, A., & Northrup, H. (2010). Epidemiologic and genetic aspects of spina bifida and other neural tube defects. *Dev Disabil Res Rev, 16*(1), 6-15. Retrieved from https://www.ncbi.nlm.nih.gov/pubmed/20419766. doi:10.1002/ddrr.93

Balda, M. S., Gonzalez-Mariscal, L., Matter, K., Cereijido, M., & Anderson, J. M. (1993). Assembly of the tight junction: the role of diacylglycerol. *J Cell Biol, 123*(2), 293-302. Retrieved from https://www.ncbi.nlm.nih.gov/pubmed/8408213. doi:10.1083/jcb.123.2.293

Balda, M. S., Whitney, J. A., Flores, C., Gonzalez, S., Cereijido, M., & Matter, K. (1996). Functional dissociation of paracellular permeability and transepithelial electrical resistance and disruption of the apical-basolateral intramembrane diffusion barrier by expression of a mutant tight junction membrane protein. *J Cell Biol, 134*(4), 1031-1049. Retrieved from https://www.ncbi.nlm.nih.gov/pubmed/8769425. doi:10.1083/jcb.134.4.1031

Barlowe, C., Orci, L., Yeung, T., Hosobuchi, M., Hamamoto, S., Salama, N., Rexach, M. F., Ravazzola, M., Amherdt, M., & Schekman, R. (1994). COPII: a membrane coat formed by Sec proteins that drive vesicle budding from the endoplasmic reticulum. *Cell, 77*(6), 895-907. Retrieved from https://www.ncbi.nlm.nih.gov/pubmed/8004676.

Baumholtz, A. I., Simard, A., Nikolopoulou, E., Oosenbrug, M., Collins, M. M., Piontek, A., Krause, G., Piontek, J., Greene, N. D. E., & Ryan, A. K. (2017). Claudins are essential for cell shape changes and convergent extension movements during neural tube closure. *Dev Biol, 428*(1), 25-38. Retrieved from https://www.ncbi.nlm.nih.gov/pubmed/28545845. doi:10.1016/j.ydbio.2017.05.013

Baumholtz, A (2018): Characterization of Claudin-dependent morphogenetic events during neural tube closure and the impact of CLDN variants. Dissertation. McGill University, Canada.

Bazzoni, G., Martinez-Estrada, O. M., Orsenigo, F., Cordenonsi, M., Citi, S., & Dejana, E. (2000). Interaction of junctional adhesion molecule with the tight junction components ZO-1, cingulin, and occludin. *J Biol Chem, 275*(27), 20520-20526. Retrieved from https://www.ncbi.nlm.nih.gov/pubmed/10877843. doi:10.1074/jbc.M905251199

Bell, R., Glinianaia, S. V., Tennant, P. W., Bilous, R. W., & Rankin, J. (2012). Peri-conception hyperglycaemia and nephropathy are associated with risk of congenital anomaly in women with pre-existing diabetes: a population-based cohort study. *Diabetologia*. Retrieved from https://www.ncbi.nlm.nih.gov/pubmed/22314812. doi:10.1007/s00125-012-2455-y

Blencowe, H., Cousens, S., Modell, B., & Lawn, J. (2010). Folic acid to reduce neonatal mortality from neural tube disorders. *Int J Epidemiol, 39 Suppl 1*, i110-121. Retrieved from https://www.ncbi.nlm.nih.gov/pubmed/20348114. doi:10.1093/ije/dyq028

Botto, L. D., Moore, C. A., Khoury, M. J., & Erickson, J. D. (1999). Neural-tube defects. *N Engl J Med, 341*(20), 1509-1519. Retrieved from https://www.ncbi.nlm.nih.gov/pubmed/10559453. doi:10.1056/NEJM199911113412006

Campanale, J. P., Sun, T. Y., & Montell, D. J. (2017). Development and dynamics of cell polarity at a glance. *J Cell Sci, 130*(7), 1201-1207. Retrieved from https://www.ncbi.nlm.nih.gov/pubmed/28365593. doi:10.1242/jcs.188599

Cecconi, F., Alvarez-Bolado, G., Meyer, B. I., Roth, K. A., & Gruss, P. (1998). Apaf1 (CED-4 homolog) regulates programmed cell death in mammalian development. *Cell, 94*(6), 727-737. Retrieved from https://www.ncbi.nlm.nih.gov/pubmed/9753320.

Chen, H., Mruk, D. D., Lee, W. M., & Cheng, C. Y. (2016). Planar Cell Polarity (PCP) Protein Vangl2 Regulates Ectoplasmic Specialization Dynamics via Its Effects on Actin Microfilaments in the Testes of Male Rats. *Endocrinology, 157*(5), 2140-2159. Retrieved from https://www.ncbi.nlm.nih.gov/pubmed/26990065. doi:10.1210/en.2015-1987

Chen, X., An, Y., Gao, Y., Guo, L., Rui, L., Xie, H., Sun, M., Lam Hung, S., Sheng, X., Zou, J., Bao, Y., Guan, H., Niu, B., Li, Z., Finnell, R. H., Gusella, J. F., Wu, B. L., & Zhang, T. (2017). Rare Deleterious PARD3 Variants in the aPKC-Binding Region are Implicated in the Pathogenesis of Human Cranial Neural Tube Defects Via Disrupting Apical Tight Junction Formation. *Hum Mutat, 38*(4), 378-389. Retrieved from https://www.ncbi.nlm.nih.gov/pubmed/27925688. doi:10.1002/humu.23153

Colas, J. F., & Schoenwolf, G. C. (2001). Towards a cellular and molecular understanding of neurulation. *Dev Dyn, 221*(2), 117-145. Retrieved from https://www.ncbi.nlm.nih.gov/pubmed/11376482. doi:10.1002/dvdy.1144

Collins, M. M., Baumholtz, A. I., & Ryan, A. K. (2013). Claudin family members exhibit unique temporal and spatial expression boundaries in the chick embryo. *Tissue Barriers, 1*(3), e24517. Retrieved from https://www.ncbi.nlm.nih.gov/pubmed/24665397. doi:10.4161/tisb.24517

Copp, A. J., & Greene, N. D. (2013). Neural tube defects--disorders of neurulation and related embryonic processes. *Wiley Interdiscip Rev Dev Biol, 2*(2), 213-227. Retrieved from https://www.ncbi.nlm.nih.gov/pubmed/24009034. doi:10.1002/wdev.71

Copp, A. J., Greene, N. D., & Murdoch, J. N. (2003). The genetic basis of mammalian neurulation. *Nat Rev Genet, 4*(10), 784-793. Retrieved from https://www.ncbi.nlm.nih.gov/pubmed/13679871. doi:10.1038/nrg1181

Correa, A., Gilboa, S. M., Botto, L. D., Moore, C. A., Hobbs, C. A., Cleves, M. A., Riehle-Colarusso, T. J., Waller, D. K., Reece, E. A., & National Birth Defects Prevention, S. (2012). Lack of periconceptional vitamins or supplements that contain folic acid and diabetes mellitus-associated birth defects. *Am J Obstet Gynecol, 206*(3), 218 e211-213. Retrieved from https://www.ncbi.nlm.nih.gov/pubmed/22284962. doi:10.1016/j.ajog.2011.12.018

Curtin, J. A., Quint, E., Tsipouri, V., Arkell, R. M., Cattanach, B., Copp, A. J., Henderson, D. J., Spurr, N., Stanier, P., Fisher, E. M., Nolan, P. M., Steel, K. P., Brown, S. D. M., Gray, I. C., & Murdoch, J. N. (2003). Mutation of Celsr1 Disrupts Planar Polarity of Inner Ear Hair Cells and Causes Severe Neural Tube Defects in the Mouse. *Current Biology, 13*(13), 1129-1133. doi:10.1016/s0960-9822(03)00374-9

D'Souza, T., Agarwal, R., & Morin, P. J. (2005). Phosphorylation of claudin-3 at threonine 192 by cAMP-dependent protein kinase regulates tight junction barrier function in ovarian cancer cells. *J Biol Chem, 280*(28), 26233-26240. Retrieved from https://www.ncbi.nlm.nih.gov/pubmed/15905176. doi:10.1074/jbc.M502003200

Davidson, L. A., & Keller, R. E. (1999). Neural tube closure in Xenopus laevis involves medial migration, directed protrusive activity, cell intercalation and convergent extension. *Development, 126*(20), 4547-4556. Retrieved from https://www.ncbi.nlm.nih.gov/pubmed/10498689.

De Marco, P., Merello, E., Cama, A., Kibar, Z., & Capra, V. (2011). Human neural tube defects: genetic causes and prevention. *Biofactors, 37*(4), 261-268. Retrieved from https://www.ncbi.nlm.nih.gov/pubmed/21674647. doi:10.1002/biof.170

De Marco, P., Merello, E., Consales, A., Piatelli, G., Cama, A., Kibar, Z., & Capra, V. (2013). Genetic analysis of disheveled 2 and disheveled 3 in human neural tube defects. *J Mol Neurosci, 49*(3), 582-588. Retrieved from https://www.ncbi.nlm.nih.gov/pubmed/22892949. doi:10.1007/s12031-012-9871-9

De Marco, P., Merello, E., Rossi, A., Piatelli, G., Cama, A., Kibar, Z., & Capra, V. (2012). FZD6 is a novel gene for human neural tube defects. *Hum Mutat, 33*(2), 384-390. Retrieved from https://www.ncbi.nlm.nih.gov/pubmed/22045688. doi:10.1002/humu.21643

Devenport, D. (2016). Tissue morphodynamics: Translating planar polarity cues into polarized cell behaviors. *Semin Cell Dev Biol, 55*, 99-110. Retrieved from https://www.ncbi.nlm.nih.gov/pubmed/26994528. doi:10.1016/j.semcdb.2016.03.012

Dunlevy, L. P., Burren, K. A., Mills, K., Chitty, L. S., Copp, A. J., & Greene, N. D. (2006). Integrity of the methylation cycle is essential for mammalian neural tube closure. *Birth Defects Res A Clin Mol Teratol, 76*(7), 544-552. Retrieved from https://www.ncbi.nlm.nih.gov/pubmed/16933307. doi:10.1002/bdra.20286

Ebnet, K., Aurrand-Lions, M., Kuhn, A., Kiefer, F., Butz, S., Zander, K., Meyer zu Brickwedde, M. K., Suzuki, A., Imhof, B. A., & Vestweber, D. (2003). The junctional adhesion molecule (JAM) family members JAM-2 and JAM-3 associate with the cell polarity protein PAR-3: a possible role for JAMs in endothelial cell polarity. *J Cell Sci, 116*(Pt 19), 3879-3891. Retrieved from https://www.ncbi.nlm.nih.gov/pubmed/12953056. doi:10.1242/jcs.00704

Ebnet, K., Suzuki, A., Ohno, S., & Vestweber, D. (2004). Junctional adhesion molecules (JAMs): more molecules with dual functions? *J Cell Sci, 117*(Pt 1), 19-29. Retrieved from https://www.ncbi.nlm.nih.gov/pubmed/14657270. doi:10.1242/jcs.00930

Eom, D. S., Amarnath, S., Fogel, J. L., & Agarwala, S. (2011). Bone morphogenetic proteins regulate neural tube closure by interacting with the apicobasal polarity pathway. *Development, 138*(15), 3179-3188. Retrieved from https://www.ncbi.nlm.nih.gov/pubmed/21750029. doi:10.1242/dev.058602

Escuin, S., Vernay, B., Savery, D., Gurniak, C. B., Witke, W., Greene, N. D., & Copp, A. J. (2015). Rho-kinase-dependent actin turnover and actomyosin disassembly are necessary for mouse

spinal neural tube closure. *J Cell Sci, 128*(14), 2468-2481. Retrieved from https://www.ncbi.nlm.nih.gov/pubmed/26040287. doi:10.1242/jcs.164574

Fanning, A. S., Jameson, B. J., Jesaitis, L. A., & Anderson, J. M. (1998). The tight junction protein ZO-1 establishes a link between the transmembrane protein occludin and the actin cytoskeleton. *J Biol Chem, 273*(45), 29745-29753. Retrieved from https://www.ncbi.nlm.nih.gov/pubmed/9792688. doi:10.1074/jbc.273.45.29745

Farquhar, M. G., & Palade, G. E. (1963). Junctional complexes in various epithelia. *J Cell Biol, 17*, 375-412. Retrieved from https://www.ncbi.nlm.nih.gov/pubmed/13944428. doi:10.1083/jcb.17.2.375

Fredriksson, K., Van Itallie, C. M., Aponte, A., Gucek, M., Tietgens, A. J., & Anderson, J. M. (2015). Proteomic analysis of proteins surrounding occludin and claudin-4 reveals their proximity to signaling and trafficking networks. *PLoS One, 10*(3), e0117074. Retrieved from https://www.ncbi.nlm.nih.gov/pubmed/25789658. doi:10.1371/journal.pone.0117074

Fujibe, M., Chiba, H., Kojima, T., Soma, T., Wada, T., Yamashita, T., & Sawada, N. (2004). Thr203 of claudin-1, a putative phosphorylation site for MAP kinase, is required to promote the barrier function of tight junctions. *Exp Cell Res, 295*(1), 36-47. Retrieved from https://www.ncbi.nlm.nih.gov/pubmed/15051488. doi:10.1016/j.yexcr.2003.12.014

Fujita, H., Hamazaki, Y., Noda, Y., Oshima, M., & Minato, N. (2012). Claudin-4 deficiency results in urothelial hyperplasia and lethal hydronephrosis. *PLoS One, 7*(12), e52272. Retrieved from https://www.ncbi.nlm.nih.gov/pubmed/23284964. doi:10.1371/journal.pone.0052272

Fujita, K., Katahira, J., Horiguchi, Y., Sonoda, N., Furuse, M., & Tsukita, S. (2000). Clostridium perfringens enterotoxin binds to the second extracellular loop of claudin-3, a tight junction integral membrane protein. *FEBS Lett, 476*(3), 258-261. Retrieved from https://www.ncbi.nlm.nih.gov/pubmed/10913624.

Furuse, M., Fujita, K., Hiiragi, T., Fujimoto, K., & Tsukita, S. (1998). Claudin-1 and -2: Novel Integral Membrane Proteins Localizing at Tight Junctions with No Sequence Similarity to Occludin. *The Journal of Cell Biology, 141*(7), 1539-1550. Retrieved from http://jcb.rupress.org/content/jcb/141/7/1539.full.pdf. doi:10.1083/jcb.141.7.1539

Furuse, M., Hirase, T., Itoh, M., Nagafuchi, A., Yonemura, S., Tsukita, S., & Tsukita, S. (1993). Occludin: a novel integral membrane protein localizing at tight junctions. *J Cell Biol, 123*(6 Pt 2), 1777-1788. Retrieved from https://www.ncbi.nlm.nih.gov/pubmed/8276896. doi:10.1083/jcb.123.6.1777

Furuse, M., Itoh, M., Hirase, T., Nagafuchi, A., Yonemura, S., Tsukita, S., & Tsukita, S. (1994). Direct association of occludin with ZO-1 and its possible involvement in the localization of occludin at tight junctions. *J Cell Biol, 127*(6 Pt 1), 1617-1626. Retrieved from https://www.ncbi.nlm.nih.gov/pubmed/7798316. doi:10.1083/jcb.127.6.1617

Fyffe-Maricich, S. L., Karlo, J. C., Landreth, G. E., & Miller, R. H. (2011). The ERK2 mitogen-activated protein kinase regulates the timing of oligodendrocyte differentiation. *J Neurosci, 31*(3), 843-850. Retrieved from https://www.ncbi.nlm.nih.gov/pubmed/21248107. doi:10.1523/JNEUROSCI.3239-10.2011

Gong, Y., Wang, J., Yang, J., Gonzales, E., Perez, R., & Hou, J. (2015). KLHL3 regulates paracellular chloride transport in the kidney by ubiquitination of claudin-8. *Proc Natl Acad Sci U S A, 112*(14), 4340-4345. Retrieved from https://www.ncbi.nlm.nih.gov/pubmed/25831548. doi:10.1073/pnas.1421441112

Greene, N. D., & Copp, A. J. (2014). Neural tube defects. *Annu Rev Neurosci, 37*, 221-242. Retrieved from https://www.ncbi.nlm.nih.gov/pubmed/25032496. doi:10.1146/annurev-neuro-062012-170354

Guillemot, L., Paschoud, S., Pulimeno, P., Foglia, A., & Citi, S. (2008). The cytoplasmic plaque of tight junctions: a scaffolding and signalling center. *Biochim Biophys Acta, 1778*(3), 601-613. Retrieved from https://www.ncbi.nlm.nih.gov/pubmed/18339298. doi:10.1016/j.bbamem.2007.09.032

Gumbiner, B., Lowenkopf, T., & Apatira, D. (1991). Identification of a 160-kDa polypeptide that binds to the tight junction protein ZO-1. *Proc Natl Acad Sci U S A, 88*(8), 3460-3464. Retrieved from https://www.ncbi.nlm.nih.gov/pubmed/2014265. doi:10.1073/pnas.88.8.3460

Gupta, I. R., & Ryan, A. K. (2010). Claudins: unlocking the code to tight junction function during embryogenesis and in disease. *Clin Genet, 77*(4), 314-325. Retrieved from https://www.ncbi.nlm.nih.gov/pubmed/20447145. doi:10.1111/j.1399-0004.2010.01397.x

Haigo, S. L., Hildebrand, J. D., Harland, R. M., & Wallingford, J. B. (2003). Shroom induces apical constriction and is required for hingepoint formation during neural tube closure. *Curr Biol, 13*(24), 2125-2137. Retrieved from https://www.ncbi.nlm.nih.gov/pubmed/14680628.

Hamazaki, Y., Itoh, M., Sasaki, H., Furuse, M., & Tsukita, S. (2002). Multi-PDZ domain protein 1 (MUPP1) is concentrated at tight junctions through its possible interaction with claudin-1 and junctional adhesion molecule. *J Biol Chem, 277*(1), 455-461. Retrieved from https://www.ncbi.nlm.nih.gov/pubmed/11689568. doi:10.1074/jbc.M109005200

Hamburger, V., & Hamilton, H. L. (1951). A series of normal stages in the development of the chick embryo. *J Morphol, 88*(1), 49-92. Retrieved from https://www.ncbi.nlm.nih.gov/pubmed/24539719.

Haorah, J., Heilman, D., Knipe, B., Chrastil, J., Leibhart, J., Ghorpade, A., Miller, D. W., & Persidsky, Y. (2005). Ethanol-Induced Activation of Myosin Light Chain Kinase Leads to Dysfunction of Tight Junctions and Blood-Brain Barrier Compromise. *Alcoholism: Clinical & Experimental Research, 29*(6), 999-1009. doi:10.1097/01.Alc.0000166944.79914.0a

Harris, M. J., & Juriloff, D. M. (2007). Mouse mutants with neural tube closure defects and their role in understanding human neural tube defects. *Birth Defects Res A Clin Mol Teratol, 79*(3), 187-210. Retrieved from https://www.ncbi.nlm.nih.gov/pubmed/17177317. doi:10.1002/bdra.20333

Harris, M. J., & Juriloff, D. M. (2010). An update to the list of mouse mutants with neural tube closure defects and advances toward a complete genetic perspective of neural tube closure. *Birth Defects Res A Clin Mol Teratol, 88*(8), 653-669. Retrieved from https://www.ncbi.nlm.nih.gov/pubmed/20740593. doi:10.1002/bdra.20676

Haskins, J., Gu, L., Wittchen, E. S., Hibbard, J., & Stevenson, B. R. (1998). ZO-3, a novel member of the MAGUK protein family found at the tight junction, interacts with ZO-1 and occludin. *J Cell Biol, 141*(1), 199-208. Retrieved from https://www.ncbi.nlm.nih.gov/pubmed/9531559. doi:10.1083/jcb.141.1.199

Hawley, S. H., Wunnenberg-Stapleton, K., Hashimoto, C., Laurent, M. N., Watabe, T., Blumberg, B. W., & Cho, K. W. (1995). Disruption of BMP signals in embryonic Xenopus ectoderm leads to direct neural induction. *Genes Dev, 9*(23), 2923-2935. Retrieved from https://www.ncbi.nlm.nih.gov/pubmed/7498789.

Hildebrand, J. D. (2005). Shroom regulates epithelial cell shape via the apical positioning of an actomyosin network. *J Cell Sci, 118*(Pt 22), 5191-5203. Retrieved from https://www.ncbi.nlm.nih.gov/pubmed/16249236. doi:10.1242/jcs.02626

Hou, J., Renigunta, A., Yang, J., & Waldegger, S. (2010). Claudin-4 forms paracellular chloride channel in the kidney and requires claudin-8 for tight junction localization. *Proc Natl Acad Sci U S A, 107*(42), 18010-18015. Retrieved from https://www.ncbi.nlm.nih.gov/pubmed/20921420. doi:10.1073/pnas.1009399107

Hung, T. J., & Kemphues, K. J. (1999). PAR-6 is a conserved PDZ domain-containing protein that colocalizes with PAR-3 in Caenorhabditis elegans embryos. *Development, 126*(1), 127-135. Retrieved from https://www.ncbi.nlm.nih.gov/pubmed/9834192.

Hurd, T. W., Gao, L., Roh, M. H., Macara, I. G., & Margolis, B. (2003). Direct interaction of two polarity complexes implicated in epithelial tight junction assembly. *Nat Cell Biol, 5*(2), 137-142. Retrieved from https://www.ncbi.nlm.nih.gov/pubmed/12545177. doi:10.1038/ncb923

Imamura, O., Pages, G., Pouyssegur, J., Endo, S., & Takishima, K. (2010). ERK1 and ERK2 are required for radial glial maintenance and cortical lamination. *Genes Cells, 15*(10), 1072-1088. Retrieved from https://www.ncbi.nlm.nih.gov/pubmed/20825492. doi:10.1111/j.1365-2443.2010.01444.x

Itoh, M., Furuse, M., Morita, K., Kubota, K., Saitou, M., & Tsukita, S. (1999). Direct binding of three tight junction-associated MAGUKs, ZO-1, ZO-2, and ZO-3, with the COOH termini of claudins. *J Cell Biol, 147*(6), 1351-1363. Retrieved from https://www.ncbi.nlm.nih.gov/pubmed/10601346. doi:10.1083/jcb.147.6.1351

Itoh, M., Sasaki, H., Furuse, M., Ozaki, H., Kita, T., & Tsukita, S. (2001). Junctional adhesion molecule (JAM) binds to PAR-3: a possible mechanism for the recruitment of PAR-3 to tight junctions. *J Cell Biol, 154*(3), 491-497. Retrieved from https://www.ncbi.nlm.nih.gov/pubmed/11489913. doi:10.1083/jcb.200103047

Jeansonne, B., Lu, Q., Goodenough, D. A., & Chen, Y. H. (2003). Claudin-8 interacts with multi-PDZ domain protein 1 (MUPP1) and reduces paracellular conductance in epithelial cells. *Cell Mol Biol (Noisy-le-grand), 49*(1), 13-21. Retrieved from https://www.ncbi.nlm.nih.gov/pubmed/12839333.

Jensen, D., & Schekman, R. (2011). COPII-mediated vesicle formation at a glance. *J Cell Sci, 124*(Pt 1), 1-4. Retrieved from https://www.ncbi.nlm.nih.gov/pubmed/21172817. doi:10.1242/jcs.069773

Katahira, J., Sugiyama, H., Inoue, N., Horiguchi, Y., Matsuda, M., & Sugimoto, N. (1997). Clostridium perfringens enterotoxin utilizes two structurally related membrane proteins as functional receptors in vivo. *J Biol Chem, 272*(42), 26652-26658. Retrieved from https://www.ncbi.nlm.nih.gov/pubmed/9334247. doi:10.1074/jbc.272.42.26652

Katsuno, T., Umeda, K., Matsui, T., Hata, M., Tamura, A., Itoh, M., Takeuchi, K., Fujimori, T., Nabeshima, Y., Noda, T., Tsukita, S., & Tsukita, S. (2008). Deficiency of zonula occludens-1 causes embryonic lethal phenotype associated with defected yolk sac angiogenesis and apoptosis of embryonic cells. *Mol Biol Cell, 19*(6), 2465-2475. Retrieved from https://www.ncbi.nlm.nih.gov/pubmed/18353970. doi:10.1091/mbc.E07-12-1215

Kemphues, K. J., Priess, J. R., Morton, D. G., & Cheng, N. S. (1988). Identification of genes required for cytoplasmic localization in early C. elegans embryos. *Cell, 52*(3), 311-320. Retrieved from https://www.ncbi.nlm.nih.gov/pubmed/3345562.

Kibar, Z., Bosoi, C. M., Kooistra, M., Salem, S., Finnell, R. H., De Marco, P., Merello, E., Bassuk, A. G., Capra, V., & Gros, P. (2009). Novel mutations in VANGL1 in neural tube defects. *Hum Mutat, 30*(7), E706-715. Retrieved from https://www.ncbi.nlm.nih.gov/pubmed/19319979. doi:10.1002/humu.21026

Kibar, Z., Capra, V., & Gros, P. (2007). Toward understanding the genetic basis of neural tube defects. *Clin Genet, 71*(4), 295-310. Retrieved from https://www.ncbi.nlm.nih.gov/pubmed/17470131. doi:10.1111/j.1399-0004.2007.00793.x

Kibar, Z., Vogan, K. J., Groulx, N., Justice, M. J., Underhill, D. A., & Gros, P. (2001). Ltap, a mammalian homolog of Drosophila Strabismus/Van Gogh, is altered in the mouse neural tube mutant Loop-tail. *Nat Genet, 28*(3), 251-255. Retrieved from https://www.ncbi.nlm.nih.gov/pubmed/11431695. doi:10.1038/90081

Kim, B., & Breton, S. (2016). The MAPK/ERK-Signaling Pathway Regulates the Expression and Distribution of Tight Junction Proteins in the Mouse Proximal Epididymis. *Biol Reprod, 94*(1), 22. Retrieved from https://www.ncbi.nlm.nih.gov/pubmed/26658708. doi:10.1095/biolreprod.115.134965

Kinoshita, N., Sasai, N., Misaki, K., & Yonemura, S. (2008). Apical accumulation of Rho in the neural plate is important for neural plate cell shape change and neural tube formation. *Mol Biol Cell, 19*(5), 2289-2299. Retrieved from https://www.ncbi.nlm.nih.gov/pubmed/18337466. doi:10.1091/mbc.E07-12-1286

Kobayashi, J., Inai, T., & Shibata, Y. (2002). Formation of tight junction strands by expression of claudin-1 mutants in their ZO-1 binding site in MDCK cells. *Histochem Cell Biol, 117*(1), 29-39. Retrieved from https://www.ncbi.nlm.nih.gov/pubmed/11819095. doi:10.1007/s00418-001-0359-x

Laukoetter, M. G., Nava, P., Lee, W. Y., Severson, E. A., Capaldo, C. T., Babbin, B. A., Williams, I. R., Koval, M., Peatman, E., Campbell, J. A., Dermody, T. S., Nusrat, A., & Parkos, C. A. (2007). JAM-A regulates permeability and inflammation in the intestine in vivo. *J Exp Med, 204*(13), 3067-3076. Retrieved from https://www.ncbi.nlm.nih.gov/pubmed/18039951. doi:10.1084/jem.20071416

Lee, C., Scherr, H. M., & Wallingford, J. B. (2007). Shroom family proteins regulate gamma-tubulin distribution and microtubule architecture during epithelial cell shape change. *Development, 134*(7), 1431-1441. Retrieved from https://www.ncbi.nlm.nih.gov/pubmed/17329357. doi:10.1242/dev.02828

Lee, M. C., Miller, E. A., Goldberg, J., Orci, L., & Schekman, R. (2004). Bi-directional protein transport between the ER and Golgi. *Annu Rev Cell Dev Biol, 20*, 87-123. Retrieved from https://www.ncbi.nlm.nih.gov/pubmed/15473836. doi:10.1146/annurev.cellbio.20.010403.105307

Lu, Z., Ding, L., Hong, H., Hoggard, J., Lu, Q., & Chen, Y. H. (2011). Claudin-7 inhibits human lung cancer cell migration and invasion through ERK/MAPK signaling pathway. *Exp Cell Res, 317*(13), 1935-1946. Retrieved from https://www.ncbi.nlm.nih.gov/pubmed/21641901. doi:10.1016/j.yexcr.2011.05.019

Martin-Padura, I., Lostaglio, S., Schneemann, M., Williams, L., Romano, M., Fruscella, P., Panzeri, C., Stoppacciaro, A., Ruco, L., Villa, A., Simmons, D., & Dejana, E. (1998). Junctional adhesion molecule, a novel member of the immunoglobulin superfamily that distributes at intercellular junctions and modulates monocyte transmigration. *J Cell Biol, 142*(1), 117-127. Retrieved from https://www.ncbi.nlm.nih.gov/pubmed/9660867. doi:10.1083/jcb.142.1.117

Massa, V., Savery, D., Ybot-Gonzalez, P., Ferraro, E., Rongvaux, A., Cecconi, F., Flavell, R., Greene, N. D., & Copp, A. J. (2009). Apoptosis is not required for mammalian neural tube closure. *Proc Natl Acad Sci U S A, 106*(20), 8233-8238. Retrieved from https://www.ncbi.nlm.nih.gov/pubmed/19420217. doi:10.1073/pnas.0900333106

Merte, J., Jensen, D., Wright, K., Sarsfield, S., Wang, Y., Schekman, R., & Ginty, D. D. (2010). Sec24b selectively sorts Vangl2 to regulate planar cell polarity during neural tube closure. *Nat Cell Biol, 12*(1), 41-46; sup pp 41-48. Retrieved from https://www.ncbi.nlm.nih.gov/pubmed/19966784. doi:10.1038/ncb2002

Miller, E., Antonny, B., Hamamoto, S., & Schekman, R. (2002). Cargo selection into COPII vesicles is driven by the Sec24p subunit. *EMBO J, 21*(22), 6105-6113. Retrieved from https://www.ncbi.nlm.nih.gov/pubmed/12426382.

Monteiro, A. C., Sumagin, R., Rankin, C. R., Leoni, G., Mina, M. J., Reiter, D. M., Stehle, T., Dermody, T. S., Schaefer, S. A., Hall, R. A., Nusrat, A., & Parkos, C. A. (2013). JAM-A associates with ZO-2, afadin, and PDZ-GEF1 to activate Rap2c and regulate epithelial barrier function. *Mol Biol Cell, 24*(18), 2849-2860. Retrieved from https://www.ncbi.nlm.nih.gov/pubmed/23885123. doi:10.1091/mbc.E13-06-0298

Moury, J. D., & Schoenwolf, G. C. (1995). Cooperative model of epithelial shaping and bending during avian neurulation: autonomous movements of the neural plate, autonomous movements of the epidermis, and interactions in the neural plate/epidermis transition zone. *Dev Dyn, 204*(3), 323-337. Retrieved from https://www.ncbi.nlm.nih.gov/pubmed/8573723. doi:10.1002/aja.1002040310

Muller, D., Kausalya, P. J., Claverie-Martin, F., Meij, I. C., Eggert, P., Garcia-Nieto, V., & Hunziker, W. (2003). A novel claudin 16 mutation associated with childhood hypercalciuria abolishes binding to ZO-1 and results in lysosomal mistargeting. *Am J Hum Genet, 73*(6), 1293-1301. Retrieved from https://www.ncbi.nlm.nih.gov/pubmed/14628289. doi:10.1086/380418

Murdoch, J. N., Damrau, C., Paudyal, A., Bogani, D., Wells, S., Greene, N. D., Stanier, P., & Copp, A. J. (2014). Genetic interactions between planar cell polarity genes cause diverse neural tube defects in mice. *Dis Model Mech, 7*(10), 1153-1163. Retrieved from https://www.ncbi.nlm.nih.gov/pubmed/25128525. doi:10.1242/dmm.016758

Nikolopoulou, E., Galea, G. L., Rolo, A., Greene, N. D., & Copp, A. J. (2017). Neural tube closure: cellular, molecular and biomechanical mechanisms. *Development, 144*(4), 552-566. Retrieved from https://www.ncbi.nlm.nih.gov/pubmed/28196803. doi:10.1242/dev.145904

Nishi, H., Hashimoto, K., & Panchenko, A. R. (2011). Phosphorylation in protein-protein binding: effect on stability and function. *Structure, 19*(12), 1807-1815. Retrieved from https://www.ncbi.nlm.nih.gov/pubmed/22153503. doi:10.1016/j.str.2011.09.021

Nishimura, T., Honda, H., & Takeichi, M. (2012). Planar cell polarity links axes of spatial dynamics in neural-tube closure. *Cell, 149*(5), 1084-1097. Retrieved from https://www.ncbi.nlm.nih.gov/pubmed/22632972. doi:10.1016/j.cell.2012.04.021

Nitta, T., Hata, M., Gotoh, S., Seo, Y., Sasaki, H., Hashimoto, N., Furuse, M., & Tsukita, S. (2003). Size-selective loosening of the blood-brain barrier in claudin-5-deficient mice. *J Cell Biol, 161*(3), 653-660. Retrieved from https://www.ncbi.nlm.nih.gov/pubmed/12743111. doi:10.1083/jcb.200302070

O'Shaughnessy, R. F., Welti, J. C., Sully, K., & Byrne, C. (2009). Akt-dependent Pp2a activity is required for epidermal barrier formation during late embryonic development.

Development, 136(20), 3423-3431. Retrieved from https://www.ncbi.nlm.nih.gov/pubmed/19762425. doi:10.1242/dev.037010

Pai, Y. J., Abdullah, N. L., Mohd-Zin, S. W., Mohammed, R. S., Rolo, A., Greene, N. D., Abdul-Aziz, N. M., & Copp, A. J. (2012). Epithelial fusion during neural tube morphogenesis. *Birth Defects Res A Clin Mol Teratol, 94*(10), 817-823. Retrieved from https://www.ncbi.nlm.nih.gov/pubmed/22945349. doi:10.1002/bdra.23072

Pangilinan, F., Molloy, A. M., Mills, J. L., Troendle, J. F., Parle-McDermott, A., Signore, C., O'Leary, V. B., Chines, P., Seay, J. M., Geiler-Samerotte, K., Mitchell, A., VanderMeer, J. E., Krebs, K. M., Sanchez, A., Cornman-Homonoff, J., Stone, N., Conley, M., Kirke, P. N., Shane, B., Scott, J. M., & Brody, L. C. (2012). Evaluation of common genetic variants in 82 candidate genes as risk factors for neural tube defects. *BMC Med Genet, 13*, 62. Retrieved from https://www.ncbi.nlm.nih.gov/pubmed/22856873. doi:10.1186/1471-2350-13-62

Patten, I., & Placzek, M. (2002). Opponent activities of Shh and BMP signaling during floor plate induction in vivo. *Curr Biol, 12*(1), 47-52. Retrieved from https://www.ncbi.nlm.nih.gov/pubmed/11790302.

Persidsky, Y., Heilman, D., Haorah, J., Zelivyanskaya, M., Persidsky, R., Weber, G. A., Shimokawa, H., Kaibuchi, K., & Ikezu, T. (2006). Rho-mediated regulation of tight junctions during monocyte migration across the blood-brain barrier in HIV-1 encephalitis (HIVE). *Blood, 107*(12), 4770-4780. Retrieved from https://www.ncbi.nlm.nih.gov/pubmed/16478881. doi:10.1182/blood-2005-11-4721

Piontek, J., Winkler, L., Wolburg, H., Müller, S. L., Zuleger, N., Piehl, C., Wiesner, B., Krause, G., & Blasig, I. E. (2008). Formation of tight junction: determinants of homophilic interaction between classic claudins. *The FASEB Journal, 22*(1), 146-158. Retrieved from https://www.fasebj.org/doi/abs/10.1096/fj.07-8319com. doi:10.1096/fj.07-8319com

Qiu, R. G., Abo, A., & Steven Martin, G. (2000). A human homolog of the C. elegans polarity determinant Par-6 links Rac and Cdc42 to PKCzeta signaling and cell transformation. *Curr Biol, 10*(12), 697-707. Retrieved from https://www.ncbi.nlm.nih.gov/pubmed/10873802.

Robinson, A., Escuin, S., Doudney, K., Vekemans, M., Stevenson, R. E., Greene, N. D., Copp, A. J., & Stanier, P. (2012). Mutations in the planar cell polarity genes CELSR1 and SCRIB are associated with the severe neural tube defect craniorachischisis. *Hum Mutat, 33*(2), 440-447. Retrieved from https://www.ncbi.nlm.nih.gov/pubmed/22095531. doi:10.1002/humu.21662

Rodriguez-Gallardo, L., Climent, V., Garcia-Martinez, V., Schoenwolf, G. C., & Alvarez, I. S. (1997). Targeted over-expression of FGF in chick embryos induces formation of ectopic neural cells. *Int J Dev Biol, 41*(5), 715-723. Retrieved from https://www.ncbi.nlm.nih.gov/pubmed/9415491.

Rogers, C. D., Ferzli, G. S., & Casey, E. S. (2011). The response of early neural genes to FGF signaling or inhibition of BMP indicate the absence of a conserved neural induction module. *BMC Dev Biol, 11*, 74. Retrieved from https://www.ncbi.nlm.nih.gov/pubmed/22172147. doi:10.1186/1471-213X-11-74

Rossa, J., Ploeger, C., Vorreiter, F., Saleh, T., Protze, J., Gunzel, D., Wolburg, H., Krause, G., & Piontek, J. (2014). Claudin-3 and claudin-5 protein folding and assembly into the tight junction are controlled by non-conserved residues in the transmembrane 3 (TM3) and extracellular loop 2 (ECL2) segments. *J Biol Chem, 289*(11), 7641-7653. Retrieved from https://www.ncbi.nlm.nih.gov/pubmed/24478310. doi:10.1074/jbc.M113.531012

Ruffer, C., & Gerke, V. (2004). The C-terminal cytoplasmic tail of claudins 1 and 5 but not its PDZ-binding motif is required for apical localization at epithelial and endothelial tight junctions. *Eur J Cell Biol, 83*(4), 135-144. Retrieved from https://www.ncbi.nlm.nih.gov/pubmed/15260435. doi:10.1078/0171-9335-00366

Sawyer, J. K., Choi, W., Jung, K. C., He, L., Harris, N. J., & Peifer, M. (2011). A contractile actomyosin network linked to adherens junctions by Canoe/afadin helps drive convergent extension. *Mol Biol Cell, 22*(14), 2491-2508. Retrieved from https://www.ncbi.nlm.nih.gov/pubmed/21613546. doi:10.1091/mbc.E11-05-0411

Schoenwolf, G. C. (1979). Observations on closure of the neuropores in the chick embryo. *Am J Anat, 155*(4), 445-465. Retrieved from https://www.ncbi.nlm.nih.gov/pubmed/484511. doi:10.1002/aja.1001550404

Schoenwolf, G. C. (1988). Microsurgical analyses of avian neurulation: separation of medial and lateral tissues. *J Comp Neurol, 276*(4), 498-507. Retrieved from https://www.ncbi.nlm.nih.gov/pubmed/3198787. doi:10.1002/cne.902760404

Schoenwolf, G. C., & Alvarez, I. S. (1989). Roles of neuroepithelial cell rearrangement and division in shaping of the avian neural plate. *Development, 106*(3), 427-439. Retrieved from https://www.ncbi.nlm.nih.gov/pubmed/2598817.

Schoenwolf, G. C., & Franks, M. V. (1984). Quantitative analyses of changes in cell shapes during bending of the avian neural plate. *Dev Biol, 105*(2), 257-272. Retrieved from https://www.ncbi.nlm.nih.gov/pubmed/6479439.

Schoenwolf, G. C., & Powers, M. L. (1987). Shaping of the chick neuroepithelium during primary and secondary neurulation: role of cell elongation. *Anat Rec, 218*(2), 182-195. Retrieved from https://www.ncbi.nlm.nih.gov/pubmed/3619086. doi:10.1002/ar.1092180214

Shrestha, A., & McClane, B. A. (2013). Human claudin-8 and -14 are receptors capable of conveying the cytotoxic effects of Clostridium perfringens enterotoxin. *MBio, 4*(1). Retrieved from https://www.ncbi.nlm.nih.gov/pubmed/23322640. doi:10.1128/mBio.00594-12

Smith, J. L., Schoenwolf, G. C., & Quan, J. (1994). Quantitative analyses of neuroepithelial cell shapes during bending of the mouse neural plate. *J Comp Neurol, 342*(1), 144-151. Retrieved from https://www.ncbi.nlm.nih.gov/pubmed/8207124. doi:10.1002/cne.903420113

Sontag, E. (2001). Protein phosphatase 2A: the Trojan Horse of cellular signaling. *Cell Signal, 13*(1), 7-16. Retrieved from https://www.ncbi.nlm.nih.gov/pubmed/11257442.

Stern, C. D. (2005). Neural induction: old problem, new findings, yet more questions. *Development, 132*(9), 2007-2021. Retrieved from https://www.ncbi.nlm.nih.gov/pubmed/15829523. doi:10.1242/dev.01794

Stevenson, B. R., Siliciano, J. D., Mooseker, M. S., & Goodenough, D. A. (1986). Identification of ZO-1: a high molecular weight polypeptide associated with the tight junction (zonula occludens) in a variety of epithelia. *J Cell Biol, 103*(3), 755-766. Retrieved from https://www.ncbi.nlm.nih.gov/pubmed/3528172. doi:10.1083/jcb.103.3.755

Streit, A., Berliner, A. J., Papanayotou, C., Sirulnik, A., & Stern, C. D. (2000). Initiation of neural induction by FGF signalling before gastrulation. *Nature, 406*(6791), 74-78. Retrieved from https://www.ncbi.nlm.nih.gov/pubmed/10894544. doi:10.1038/35017617

Stuart, R. O., & Nigam, S. K. (1995). Regulated assembly of tight junctions by protein kinase C. *Proc Natl Acad Sci U S A, 92*(13), 6072-6076. Retrieved from https://www.ncbi.nlm.nih.gov/pubmed/7597083. doi:10.1073/pnas.92.13.6072

Su, Y., Fu, C., Ishikawa, S., Stella, A., Kojima, M., Shitoh, K., Schreiber, E. M., Day, B. W., & Liu, B. (2008). APC is essential for targeting phosphorylated beta-catenin to the SCFbeta-TrCP ubiquitin ligase. *Mol Cell, 32*(5), 652-661. Retrieved from https://www.ncbi.nlm.nih.gov/pubmed/19061640. doi:10.1016/j.molcel.2008.10.023

Suzuki, H., Nishizawa, T., Tani, K., Yamazaki, Y., Tamura, A., Ishitani, R., Dohmae, N., Tsukita, S., Nureki, O., & Fujiyoshi, Y. (2014). Crystal structure of a claudin provides insight into the architecture of tight junctions. *Science, 344*(6181), 304-307. Retrieved from https://www.ncbi.nlm.nih.gov/pubmed/24744376. doi:10.1126/science.1248571

Suzuki, T., Grand, E., Bowman, C., Merchant, J. L., Todisco, A., Wang, L., & Del Valle, J. (2001). TNF-alpha and interleukin 1 activate gastrin gene expression via MAPK- and PKC-dependent mechanisms. *Am J Physiol Gastrointest Liver Physiol, 281*(6), G1405-1412. Retrieved from https://www.ncbi.nlm.nih.gov/pubmed/11705745. doi:10.1152/ajpgi.2001.281.6.G1405

Tabaries, S., McNulty, A., Ouellet, V., Annis, M. G., Dessureault, M., Vinette, M., Hachem, Y., Lavoie, B., Omeroglu, A., Simon, H. G., Walsh, L. A., Kimbung, S., Hedenfalk, I., & Siegel, P. M. (2019). Afadin cooperates with Claudin-2 to promote breast cancer metastasis. *Genes Dev, 33*(3-4), 180-193. Retrieved from https://www.ncbi.nlm.nih.gov/pubmed/30692208. doi:10.1101/gad.319194.118

Tanaka, M., Kamata, R., & Sakai, R. (2005). EphA2 phosphorylates the cytoplasmic tail of Claudin-4 and mediates paracellular permeability. *J Biol Chem, 280*(51), 42375-42382. Retrieved from https://www.ncbi.nlm.nih.gov/pubmed/16236711. doi:10.1074/jbc.M503786200

Tepass, U., Theres, C., & Knust, E. (1990). crumbs encodes an EGF-like protein expressed on apical membranes of Drosophila epithelial cells and required for organization of epithelia. *Cell, 61*(5), 787-799. Retrieved from https://www.ncbi.nlm.nih.gov/pubmed/2344615.

Thompson, J. J., & Williams, C. S. (2018). Protein Phosphatase 2A in the Regulation of Wnt Signaling, Stem Cells, and Cancer. *Genes (Basel), 9*(3). Retrieved from https://www.ncbi.nlm.nih.gov/pubmed/29495399. doi:10.3390/genes9030121

Turner, C. G., Klein, J. D., Wang, J., Thakor, D., Benedict, D., Ahmed, A., Teng, Y. D., & Fauza, D. O. (2013). The amniotic fluid as a source of neural stem cells in the setting of experimental neural tube defects. *Stem Cells Dev, 22*(4), 548-553. Retrieved from https://www.ncbi.nlm.nih.gov/pubmed/22957979. doi:10.1089/scd.2012.0215

Ullmer, C., Schmuck, K., Figge, A., & Lubbert, H. (1998). Cloning and characterization of MUPP1, a novel PDZ domain protein. *FEBS Lett, 424*(1-2), 63-68. Retrieved from https://www.ncbi.nlm.nih.gov/pubmed/9537516.

Umeda, K., Ikenouchi, J., Katahira-Tayama, S., Furuse, K., Sasaki, H., Nakayama, M., Matsui, T., Tsukita, S., Furuse, M., & Tsukita, S. (2006). ZO-1 and ZO-2 independently determine where claudins are polymerized in tight-junction strand formation. *Cell, 126*(4), 741-754. Retrieved from https://www.ncbi.nlm.nih.gov/pubmed/16923393. doi:10.1016/j.cell.2006.06.043

UniProt, C. (2019). UniProt: a worldwide hub of protein knowledge. *Nucleic Acids Res, 47*(D1), D506-D515. Retrieved from https://www.ncbi.nlm.nih.gov/pubmed/30395287. doi:10.1093/nar/gky1049

Upadhya, D., Ogata, M., & Reneker, L. W. (2013). MAPK1 is required for establishing the pattern of cell proliferation and for cell survival during lens development. *Development, 140*(7),

1573-1582. Retrieved from https://www.ncbi.nlm.nih.gov/pubmed/23482492. doi:10.1242/dev.081042

Utepbergenov, D. I., Fanning, A. S., & Anderson, J. M. (2006). Dimerization of the scaffolding protein ZO-1 through the second PDZ domain. *J Biol Chem, 281*(34), 24671-24677. Retrieved from https://www.ncbi.nlm.nih.gov/pubmed/16790439. doi:10.1074/jbc.M512820200

Van Itallie, C. M., & Anderson, J. M. (2013). Claudin interactions in and out of the tight junction. *Tissue Barriers, 1*(3), e25247. Retrieved from https://www.ncbi.nlm.nih.gov/pubmed/24665401. doi:10.4161/tisb.25247

Van Itallie, C. M., & Anderson, J. M. (2018). Phosphorylation of tight junction transmembrane proteins: Many sites, much to do. *Tissue Barriers, 6*(1), e1382671. Retrieved from https://www.ncbi.nlm.nih.gov/pubmed/29083946. doi:10.1080/21688370.2017.1382671

Van Itallie, C. M., Colegio, O. R., & Anderson, J. M. (2004). The cytoplasmic tails of claudins can influence tight junction barrier properties through effects on protein stability. *J Membr Biol, 199*(1), 29-38. Retrieved from https://www.ncbi.nlm.nih.gov/pubmed/15366421.

Van Itallie, C. M., Gambling, T. M., Carson, J. L., & Anderson, J. M. (2005). Palmitoylation of claudins is required for efficient tight-junction localization. *J Cell Sci, 118*(Pt 7), 1427-1436. Retrieved from https://www.ncbi.nlm.nih.gov/pubmed/15769849. doi:10.1242/jcs.01735

Wallingford, J. B. (2002). Neural tube closure requires Dishevelled-dependent convergent extension of the midline. *Development, 129*(24), 5815-5825. doi:10.1242/dev.00123

Wang, J., Hamblet, N. S., Mark, S., Dickinson, M. E., Brinkman, B. C., Segil, N., Fraser, S. E., Chen, P., Wallingford, J. B., & Wynshaw-Boris, A. (2006). Dishevelled genes mediate a conserved mammalian PCP pathway to regulate convergent extension during neurulation. *Development, 133*(9), 1767-1778. Retrieved from https://www.ncbi.nlm.nih.gov/pubmed/16571627. doi:10.1242/dev.02347

Wang, Y., Guo, N., & Nathans, J. (2006). The role of Frizzled3 and Frizzled6 in neural tube closure and in the planar polarity of inner-ear sensory hair cells. *J Neurosci, 26*(8), 2147-2156. Retrieved from https://www.ncbi.nlm.nih.gov/pubmed/16495441. doi:10.1523/JNEUROSCI.4698-05.2005

Wei, X., Li, H., Miao, J., Zhou, F., Liu, B., Wu, D., Li, S., Wang, L., Fan, Y., Wang, W., & Yuan, Z. (2012). Disturbed apoptosis and cell proliferation in developing neuroepithelium of lumbo-sacral neural tubes in retinoic acid-induced spina bifida aperta in rat. *Int J Dev Neurosci, 30*(5), 375-381. Retrieved from https://www.ncbi.nlm.nih.gov/pubmed/22504176. doi:10.1016/j.ijdevneu.2012.03.340

Weil, M., Jacobson, M. D., & Raff, M. C. (1997). Is programmed cell death required for neural tube closure? *Curr Biol, 7*(4), 281-284. Retrieved from https://www.ncbi.nlm.nih.gov/pubmed/9094312.

Wendeler, M. W., Paccaud, J. P., & Hauri, H. P. (2007). Role of Sec24 isoforms in selective export of membrane proteins from the endoplasmic reticulum. *EMBO Rep, 8*(3), 258-264. Retrieved from https://www.ncbi.nlm.nih.gov/pubmed/17255961. doi:10.1038/sj.embor.7400893

Wieckowski, E. U., Wnek, A. P., & McClane, B. A. (1994). Evidence that an approximately 50-kDa mammalian plasma membrane protein with receptor-like properties mediates the amphiphilicity of specifically bound Clostridium perfringens enterotoxin. *J Biol Chem, 269*(14), 10838-10848. Retrieved from https://www.ncbi.nlm.nih.gov/pubmed/8144671.

Willott, E., Balda, M. S., Fanning, A. S., Jameson, B., Van Itallie, C., & Anderson, J. M. (1993). The tight junction protein ZO-1 is homologous to the Drosophila discs-large tumor suppressor protein of septate junctions. *Proc Natl Acad Sci U S A, 90*(16), 7834-7838. Retrieved from https://www.ncbi.nlm.nih.gov/pubmed/8395056. doi:10.1073/pnas.90.16.7834

Wilson, R. S., Rauniyar, N., Sakaue, F., Lam, T. T., Williams, K. R., & Nairn, A. C. (2019). Development of Targeted Mass Spectrometry-Based Approaches for Quantitation of Proteins Enriched in the Postsynaptic Density (PSD). *Proteomes, 7*(2). Retrieved from https://www.ncbi.nlm.nih.gov/pubmed/30986977. doi:10.3390/proteomes7020012

Winkler, L., Gehring, C., Wenzel, A., Muller, S. L., Piehl, C., Krause, G., Blasig, I. E., & Piontek, J. (2009). Molecular determinants of the interaction between Clostridium perfringens enterotoxin fragments and claudin-3. *J Biol Chem, 284*(28), 18863-18872. Retrieved from https://www.ncbi.nlm.nih.gov/pubmed/19429681. doi:10.1074/jbc.M109.008623

Wittchen, E. S., Haskins, J., & Stevenson, B. R. (1999). Protein interactions at the tight junction. Actin has multiple binding partners, and ZO-1 forms independent complexes with ZO-2 and ZO-3. *J Biol Chem, 274*(49), 35179-35185. Retrieved from https://www.ncbi.nlm.nih.gov/pubmed/10575001. doi:10.1074/jbc.274.49.35179

Xu, J., Kausalya, P. J., Phua, D. C., Ali, S. M., Hossain, Z., & Hunziker, W. (2008). Early embryonic lethality of mice lacking ZO-2, but Not ZO-3, reveals critical and nonredundant roles for individual zonula occludens proteins in mammalian development. *Mol Cell Biol, 28*(5), 1669-1678. Retrieved from https://www.ncbi.nlm.nih.gov/pubmed/18172007. doi:10.1128/MCB.00891-07

Ybot-Gonzalez, P., Gaston-Massuet, C., Girdler, G., Klingensmith, J., Arkell, R., Greene, N. D., & Copp, A. J. (2007). Neural plate morphogenesis during mouse neurulation is regulated by antagonism of Bmp signalling. *Development, 134*(17), 3203-3211. Retrieved from https://www.ncbi.nlm.nih.gov/pubmed/17693602. doi:10.1242/dev.008177

Yin, P., Li, Y., & Zhang, L. (2017). Sec24C-Dependent Transport of Claudin-1 Regulates Hepatitis C Virus Entry. *J Virol, 91*(18). Retrieved from https://www.ncbi.nlm.nih.gov/pubmed/28679754. doi:10.1128/JVI.00629-17

Yu, A. S., McCarthy, K. M., Francis, S. A., McCormack, J. M., Lai, J., Rogers, R. A., Lynch, R. D., & Schneeberger, E. E. (2005). Knockdown of occludin expression leads to diverse phenotypic alterations in epithelial cells. *Am J Physiol Cell Physiol, 288*(6), C1231-1241. Retrieved from https://www.ncbi.nlm.nih.gov/pubmed/15689410. doi:10.1152/ajpcell.00581.2004

Zaganjor, I., Sekkarie, A., Tsang, B. L., Williams, J., Razzaghi, H., Mulinare, J., Sniezek, J. E., Cannon, M. J., & Rosenthal, J. (2016). Describing the Prevalence of Neural Tube Defects Worldwide: A Systematic Literature Review. *PLoS One, 11*(4), e0151586. Retrieved from https://www.ncbi.nlm.nih.gov/pubmed/27064786. doi:10.1371/journal.pone.0151586

Zhang, T., Leng, Z., Liu, W., Wang, X., Yan, X., & Yu, L. (2015). Suppressed expression of mitogen-activated protein kinases in hyperthermia induced defective neural tube. *Neurosci Lett, 594*, 6-11. Retrieved from https://www.ncbi.nlm.nih.gov/pubmed/25818329. doi:10.1016/j.neulet.2015.03.046

Zhang, W., Yang, J., Liu, Y., Chen, X., Yu, T., Jia, J., & Liu, C. (2009). PR55 alpha, a regulatory subunit of PP2A, specifically regulates PP2A-mediated beta-catenin dephosphorylation. *J Biol Chem, 284*(34), 22649-22656. Retrieved from https://www.ncbi.nlm.nih.gov/pubmed/19556239. doi:10.1074/jbc.M109.013698

Zhao, T., Gan, Q., Stokes, A., Lassiter, R. N., Wang, Y., Chan, J., Han, J. X., Pleasure, D. E., Epstein, J. A., & Zhou, C. J. (2014). beta-catenin regulates Pax3 and Cdx2 for caudal neural tube closure and elongation. *Development, 141*(1), 148-157. Retrieved from https://www.ncbi.nlm.nih.gov/pubmed/24284205. doi:10.1242/dev.101550

Zhu, M., Tao, J., Vasievich, M. P., Wei, W., Zhu, G., Khoriaty, R. N., & Zhang, B. (2015). Neural tube opening and abnormal extraembryonic membrane development in SEC23A deficient mice. *Sci Rep, 5*, 15471. Retrieved from https://www.ncbi.nlm.nih.gov/pubmed/26494538. doi:10.1038/srep15471

Appendix A: Permission to Reprint

August 14, 2019

COPYRIGHT RELEASE

I, Amanda Baumholtz, am the owner and copyright holder of the figures described below from my doctoral thesis entitled "Characterization of Claudin-dependent morphogenetic events during neural tube closure and the impact of CLDN variants":

Figure 1.3. Schematic of components of the tight junction polarity complex

Figure 1.6. Phases of neural tube closure in the chick embryo

Figure 4.6C. S198 and S216, but not the PDZ-binding domain, are critical residues for Cldn8 function

I hereby grant Amanda Vaccarella permission to reuse the above-described figures in her dissertation / thesis.

Sincerely,

Amanda Baumholtz, PhD

JOHN WILEY AND SONS LICENSE TERMS AND CONDITIONS

Aug 15, 2019

This Agreement between Amanda Vaccarella ("You") and John Wiley and Sons ("John Wiley and Sons") consists of your license details and the terms and conditions provided by John Wiley and Sons and Copyright Clearance Center.

License Number	4646801413395
License date	Aug 12, 2019
Licensed Content Publisher	John Wiley and Sons
Licensed Content Publication	Clinical Genetics
Licensed Content Title	Claudins: unlocking the code to tight junction function during embryogenesis and in disease
Licensed Content Author	AK Ryan, IR Gupta
Licensed Content Date	Mar 16, 2010
Licensed Content Volume	77
Licensed Content Issue	4
Licensed Content Pages	12
Type of use	Dissertation/Thesis
Requestor type	University/Academic
Format	Electronic
Portion	Figure/table
Number of figures/tables	2
Original Wiley figure/table number(s)	Figure 1 and Figure 2
Will you be translating?	No
Title of your thesis / dissertation	Identification of Claudin-8 Interaction Partners during Neural Tube Closure
Expected completion date	Aug 2019
Expected size (number of pages)	120

Publisher Tax ID	EU826007151
Total	0.00 USD
Terms and Conditions	

TERMS AND CONDITIONS

This copyrighted material is owned by or exclusively licensed to John Wiley & Sons, Inc. or one of its group companies (each a"Wiley Company") or handled on behalf of a society with which a Wiley Company has exclusive publishing rights in relation to a particular work (collectively "WILEY"). By clicking "accept" in connection with completing this licensing transaction, you agree that the following terms and conditions apply to this transaction (along with the billing and payment terms and conditions established by the Copyright Clearance Center Inc., ("CCC's Billing and Payment terms and conditions"), at the time that you opened your RightsLink account (these are available at any time at http://myaccount.copyright.com).

Appendix B: Mass Spectrometry Data for Cldn8 C-Terminal Domain HH8 Samples

					GST					Cldn8 C-Terminal Domain				
#	Identified Proteins (227/946)	Accession Number	Alternate ID	MW kDa	E1	E2 #1	E2 #2	E3 #1	E3 #2	E1	E2 #1	E2 #2	E3 #1	E3 #2
1	Tubulin alpha chain	F1NMP5_CHICK	TUBA8A	50	102	34	17	12	15	103	18	16	51	37
2	Claudin	E1BS22_CHICK	CLDN8	25	0	0	0	0	8	7	132	177	189	191
3	Rho guanine nucleotide exchange factor 17	E1C588_CHICK	ARHGEF17	196	24	0	0	0	0	14	0	0	0	0
4	Vitellogenin-2	F1NFL6_CHICK	VTG2	205	17	6	4	57	49	22	79	79	46	60
5	Bromodomain PHD finger transcription factor	A0A1D5PE97_CHICK		325	15	12	20	52	55	2	2	1	2	2
6	Ubiquitin specific peptidase 42	E1C4I0_CHICK	USP42	139	4	0	0	0	0	1	1	0	0	0
7	Transforming acidic coiled-coil containing protein 1	A0A1D5PZD9_CHICK		91	13	0	0	0	1	5	0	0	1	0
8	Tubulin beta-7 chain	TBB7_CHICK		50	8	10	0	39	30	7	74	58	19	20
9	CgABP260	Q90WF0_CHICK		280	28	0	0	0	0	19	0	0	0	0
10	Glyceraldehyde-3-phosphate dehydrogenase	F1NH87_CHICK (+1)	GAPDH	36	4	3	0	30	29	9	38	57	25	22
11	Apolipoprotein B	F1NV02_CHICK	APOB	523 kDa	6	7	6	36	26	3	50	44	14	20
12	Tubulin alpha chain	A0A1D5NW27_CHICK	TUBA1C	50	5	8	0	28	24	7	36	37	20	21
13	Lysozyme	B8YK79_CHICK (+1)	LYZ	16	3	3	0	26	23	4	44	53	14	16
14	Vitellogenin-1	A0A1D5NUW2_CHICK (+1)	VTG1	211	2	5	2	21	19	5	33	31	24	18
15	Glutathione S-transferase	A0A1D5PDF1_CHICK		25	16	18	6	25	33	20	12	15	7	10
16	Actin, cytoplasmic 2	A0A1D5P630_CHICK (+3)	ACTG1	42	4	2	0	41	31	7	39	21	6	7
17	Myosin-11	A0A1D5P1M0_CHICK (+4)	MYH11	225	1	0	0	0	0	2	0	0	3	1
18	Sulfatase 2	E1BZH8_CHICK	SULF2	100	13	0	0	0	0	12	0	0	0	0

					GST					Cldn8 C-Terminal Domain				
#	Identified Proteins (227/946)	Accession Number	Alternate ID	MW kDa	E1	E2 #1	E2 #2	E3 #1	E3 #2	E1	E2 #1	E2 #2	E3 #1	E3 #2
19	Elongation factor 1-alpha 1	EF1A_CHICK (+1)	EEF1A	50	5	5	0	22	16	11	17	25	16	16
20	Elongation factor 2	A0A1D5PS29_CHICK	EEF2	95	5	3	5	5	5	8	17	17	30	33
21	Stress-70 protein, mitochondrial	GRP75_CHICK	HSPA9	73	23	6	2	20	23	4	8	8	2	7
22	Myosin-9	MYH9_CHICK	MYH9	227	0	0	0	19	19	0	41	10	0	0
23	Obscurin, cytoskeletal calmodulin and titin-interacting RhoGEF	A0A1D5P9K1_CHICK		969	0	0	0	0	0	1	0	0	0	0
24	Heat shock cognate 71 kDa protein	A0A1D5PFJ6_CHICK	HSPA8	71	11	5	0	16	16	4	11	13	7	11
25	Plasminogen	F1NWX6_CHICK	PLG	91	12	0	0	0	0	20	0	0	0	1
26	Glutathione S-transferase 2	GSTM2_CHICK	GSTM2	26	11	13	5	10	13	8	4	3	0	2
27	Elongation factor Tu, mitochondrial (Fragment)	EFTU_CHICK	TUFM	38	1	1	4	9	4	4	14	14	9	9
28	Apovitellenin-1	APOV1_CHICK		12	6	5	4	3	5	7	2	5	7	6
29	Ovalbumin	OVAL_CHICK	SERPINB 14	43	2	0	0	0	0	0	0	0	0	0
30	Nucleoside diphosphate kinase	NDK_CHICK		17	1	1	0	6	6	1	3	9	7	8
31	Fascin	A0A1D5NV23_CHICK (+2)		53	0	0	0	14	7	0	16	4	2	3
32	20-hydroxysteroid dehydrogenase	F1N8Y3_CHICK (+1)	CBR1	30	8	2	0	5	14	7	2	4	0	0
33	ADP/ATP translocase 3	Q5ZLG7_CHICK	SLC25A6	33	0	2	0	10	8	0	10	9	2	3
34	DEAD-box helicase 3,X-linked	Q5F491_CHICK	DDX3X	72	2	3	3	1	2	4	3	5	7	12
35	Nebulin (Fragment)	Q9DEH4_CHICK		277	1	0	0	0	0	3	0	0	0	0
36	Destrin	DEST_CHICK (+1)	DSTN	19	5	0	0	3	3	7	5	4	3	5
37	Peroxiredoxin-1	PRDX1_CHICK	PRDX1	22	5	0	0	0	1	4	3	5	10	9
38	Eukaryotic initiation factor 4A-II	A0A1D5PR64_CHICK		28	1	0	0	7	3	2	8	9	1	2
39	Nucleophosmin SV=1	A0A1L1RJ18_CHICK (+1)	NPM1	31	0	2	0	8	5	0	10	7	0	1

					GST					Cldn8 C-Terminal Domain				
#	Identified Proteins (227/946)	Accession Number	Alternate ID	MW kDa	E1	E2 #1	E2 #2	E3 #1	E3 #2	E1	E2 #1	E2 #2	E3 #1	E3 #2
40	Glutathione S-transferase class-alpha (Fragment)	Q9W6J3_CHICK		21	4	5	0	3	3	3	3	2	1	2
41	Eukaryotic initiation factor 4A-II	A0A1L1RUX2_CHICK	EIF4A2	45	2	1	0	6	5	5	7	3	2	2
42	Tubulin alpha chain	A0A1D5P198_CHICK	TUBA1C	50	7	11	0	28	23	7	38	37	24	25
43	Cyclin-dependent kinase 1	F1NBD7_CHICK	CDK1	35	0	0	0	6	6	0	9	11	2	0
44	Leucine-rich repeat transmembrane protein FLRT3	FLRT3_CHICK	FLRT3	73	9	0	0	1	0	1	0	0	4	6
45	Glutathione S-transferase	GSTA2_CHICK		25	1	0	0	5	9	2	2	5	0	1
46	Pyruvate kinase	F1NW43_CHICK	PKM	58	2	0	0	0	1	4	3	2	5	6
47	Thioredoxin reductase 3	A0A1D5NVZ3_CHICK (+1)	TXNRD3	66	5	0	0	1	5	6	2	3	0	0
48	14-3-3 protein theta	1433T_CHICK	YWHAQ	28	1	0	1	2	3	2	4	6	1	0
49	SEC24 homolog C, COPII coat complex component	E1BUD8_CHICK		119	0	0	0	0	0	0	0	5	4	13
50	39S ribosomal protein L44	E1C5L8_CHICK	MRPL44	36	4	0	0	1	1	0	0	2	0	0
51	Type II alpha-keratin IIC	A0A146F047_CHICK (+2)	KRT6A	57	6	0	0	1	2	3	4	3	0	0
52	Sorbin and SH3 domain-containing protein 1	E1C009_CHICK		65	1	0	0	1	2	0	1	1	0	0
53	Fanconi anemia group M protein	FANCM_CHICK	FANCM	224	3	0	0	0	0	3	0	0	0	0
54	Peroxisomal biogenesis factor 5 like	A0A1D5PYF9_CHICK	PEX5L	68	3	0	0	0	0	0	0	0	0	0
55	DIS3-like exonuclease 2	E1C372_CHICK	dis3l2	92	1	0	0	0	0	1	0	0	0	0
56	Vitellogenin-2	VIT2_CHICK	VTG2	205	18	0	0	56	50	23	78	82	45	59
57	leucine-rich repeat transmembrane neuronal protein 2 (not complete)	E1C5R1_CHICK	FLRT1	58	3	0	0	1	0	1	0	1	2	2
58	Kinesin family member 14	E1BW44_CHICK	KIF14	183	0	0	0	1	0	0	0	0	0	0

					GST					Cldn8 C-Terminal Domain				
#	Identified Proteins (227/946)	Accession Number	Alternate ID	MW kDa	E1	E2 #1	E2 #2	E3 #1	E3 #2	E1	E2 #1	E2 #2	E3 #1	E3 #2
59	Calcium voltage-gated channel auxiliary subunit alpha2delta 3	F1NX89_CHICK	CACNA2D3	124	1	0	0	1	1	1	1	1	2	2
60	Glutathione peroxidase	Q8QG67_CHICK	GPX4	19	3	1	0	4	4	2	0	2	0	1
61	Tubulin beta chain	F1NYB1_CHICK	TUBB	50	0	0	0	32	25	0	59	50	12	15
62	Serine/threonine-protein phosphatase 2A 55 kDa regulatory subunit B	A0A1D5PED5_CHICK (+2)	PPP2R2A	52	0	0	0	0	0	2	0	2	6	4
63	ATP-dependent RNA helicase DDX1	DDX1_CHICK (+1)	DDX1	82	0	0	0	0	0	0	3	2	0	0
64	Peroxiredoxin-6	F1NBV0_CHICK	PRDX6	25	3	0	0	1	3	1	3	0	0	0
65	Hsc70-interacting protein	A0A1L1RVN1_CHICK (+2)	ST13	30	1	0	0	1	0	2	1	0	0	0
66	Calponin	E1BSX2_CHICK	ALG14	37	3	1	0	1	2	1	1	2	1	1
67	Complement C1q binding protein	F1NJF0_CHICK (+1)		24	0	2	2	1	1	0	3	2	1	1
68	Eukaryotic translation initiation factor 5A	A0A1D5PL54_CHICK (+2)		18	1	1	0	0	0	2	3	1	2	2
69	Tudor-interacting repair regulator protein	A0A1L1RIX9_CHICK (+1)	NUDT16L1	34	0	0	0	0	1	1	3	3	2	4
70	Type II alpha-keratin IIA	A0A1L1RIW5_CHICK (+1)	KRT5	61	4	1	0	1	2	0	4	3	0	0
71	Vitellogenin-3	A0A1D5PA29_CHICK (+1)		37	0	0	0	0	1	0	5	3	2	2
72	LanC-like protein 1	A0A1D5PYA4_CHICK (+1)	LANCL1	45	1	0	0	4	5	2	1	0	0	0
73	Dynein heavy chain 5, axonema	F1NHE5_CHICK		533	1	0	0	0	0	0	0	0	0	0
74	Tight junction protein 1	A0A1D5NWX9_CHICK (+1)	TJP1	198	0	0	0	0	0	0	1	6	0	3
75	Ryanodine receptor 2	F1NLZ9_CHICK	RYR2	563	1	0	0	0	0	0	0	0	0	0
76	ADP/ATP translocase 3	A0A1D5NZH4_CHICK (+1)		196	0	0	0	0	1	1	0	0	0	0
77	Pyruvate carboxylase	Q8JHF6_CHICK	PYC	127	0	0	1	0	0	0	0	0	4	3

					GST					Cldn8 C-Terminal Domain				
#	Identified Proteins (227/946)	Accession Number	Alternate ID	MW kDa	E1	E2 #1	E2 #2	E3 #1	E3 #2	E1	E2 #1	E2 #2	E3 #1	E3 #2
78	Meiotic double-stranded break formation protein 4	A0A1D5NY65_CHICK		39	1	0	0	0	0	2	0	0	0	0
79	Cell division protein kinase 11	A0A1D5NZU4_CHICK (+1)	CDC2L1	91	0	0	1	0	0	0	0	0	0	0
80	Thrombospondin type 1 domain containing 7B	F1NAE3_CHICK	THSD7B	141	1	0	0	1	1	1	1	1	0	0
81	78 kDa glucose-regulated protein	GRP78_CHICK	HSPA5	72	8	0	0	5	5	0	3	5	0	0
82	Flap endonuclease 1	FEN1_CHICK	FEN1	43	0	0	0	1	2	0	5	4	0	0
83	Family with sequence similarity 193 member B	A0A1D5P4I8_CHICK		84	2	0	0	3	4	0	0	0	0	0
84	Thioredoxin	THIO_CHICK	TXN	12	2	1	0	2	1	0	2	2	1	1
85	T-complex protein 1 subunit delta	Q9I8D6_CHICK	tcp-1	58	0	0	0	0	1	0	5	5	0	0
86	ATP synthase subunit alpha	A0A1D5PJG9_CHICK	ATP5A1 W	60	2	0	0	1	2	1	0	1	1	1
87	Keratin 12	F1NDN6_CHICK		54	2	0	0	1	1	2	2	3	0	0
88	Protein disulfide isomerase family A member 6	F1NK96_CHICK	PDIA6	49	0	0	1	0	0	1	0	2	3	3
89	Acidic leucine-rich nuclear phosphoprotein 32 family member B	A0A1L1RVX5_CHICK (+2)	ANP32B	30	0	0	0	2	1	0	5	3	0	0
90	Nucleolin	A0A1D5NZ30_CHICK (+1)	NCL	75	0	0	0	3	1	0	5	2	0	0
91	PDZ domain containing 8	R4GJL4_CHICK	PDZD8	128	0	0	0	0	0	2	0	0	0	0
92	Polyubiquitin-B	A0A1D5NVA7_CHICK (+7)	UBB	11	1	0	0	1	1	1	2	2	1	1
93	14-3-3 protein zeta	1433Z_CHICK	YWHAZ	28	1	2	1	2	0	1	3	4	0	0
94	Solute carrier family 25 member 3	A0A1D5PS40_CHICK (+1)	SLC25A3	40	0	0	0	1	1	0	4	2	1	0
95	Ig lambda chain C region	R9PXM5_CHICK (+1)	IGLL1	24	0	0	0	1	2	0	1	3	0	0
96	Histone H4 type VIII	H48_CHICK (+1)	H4-VIII	11	0	0	0	3	1	0	3	2	0	0
97	Isocitrate dehydrogenase [NADP]	Q5ZL82_CHICK	RCJMB04 _7e11	50	0	0	0	0	1	0	1	4	0	0

					GST					Cldn8 C-Terminal Domain				
#	Identified Proteins (227/946)	Accession Number	Alternate ID	MW kDa	E1	E2 #1	E2 #2	E3 #1	E3 #2	E1	E2 #1	E2 #2	E3 #1	E3 #2
98	Nonmuscle myosin heavy chain	Q02015_CHICK (+3)	MYH10	231	0	0	0	4	3	0	12	0	0	0
99	Protein transport protein Sec23A	SC23A_CHICK	SEC23A	86	0	0	0	0	0	0	0	5	1	3
100	5-aminoimidazole ribonucleotide/carboxylase-5-aminoimidazole-4-N-succinocarboxamide ribonucleotide synthetase	A7UEA7_CHICK (+2)	AS	47	0	0	0	0	0	0	0	0	7	2
101	Liprin-alpha-1	A0A1D5NW82_CHICK (+5)	PPFIA1	138	0	1	1	0	0	0	0	0	0	0
102	Karyopherin subunit beta 1	A0A1D5P1W7_CHICK		120	1	0	3	0	0	0	0	0	0	0
103	glutaredoxin-3 (blasted	F1NNP6_CHICK	GLRX3	37	2	0	0	1	0	1	2	1	1	1
104	Tubulin alpha chain	A0A1D5PAR5_CHICK (+1)	TUBA3E	50	0	0	0	19	16	0	22	24	0	0
105	60S acidic ribosomal protein P0	A0A1D5PK69_CHICK (+2)	RPLP0	29	0	0	0	3	1	0	1	3	0	0
106	Poly(rC) binding protein 2	A0A1D5P893_CHICK (+1)	LOC426023	35	1	0	0	0	1	1	0	2	1	1
107	S-adenosylmethionine synthase	E1C735_CHICK	MAT1A	44	0	0	0	0	0	1	1	2	1	2
108	Tubulin beta-2 chain	TBB2_CHICK		50	5	0	0	27	22	0	52	41	0	13
109	Caspase-3	O93417_CHICK	CASP3	32	0	0	0	0	0	0	2	0	0	1
110	Casein kinase II subunit alpha	CSK21_CHICK	CSNK2A1	45	0	0	0	2	2	0	2	1	0	0
111	acetyl-CoA acetyltransferase, mitochondrial (blasted)	E1C0Q5_CHICK	ACAT1	44	1	0	0	0	0	1	2	0	0	1
112	Cytochrome c oxidase subunit NDUFA4	A0A1L1RIQ5_CHICK (+1)	NDUFA4	12	0	0	0	2	2	0	2	1	0	0
113	Acyl-CoA synthetase long chain family member 1	Q5F420_CHICK	ACSL1	79	0	0	0	1	1	0	0	3	1	0

					GST					Cldn8 C-Terminal Domain				
#	Identified Proteins (227/946)	Accession Number	Alternate ID	MW kDa	E1	E2 #1	E2 #2	E3 #1	E3 #2	E1	E2 #1	E2 #2	E3 #1	E3 #2
114	Aconitate hydratase, mitochondrial	A0A1D5NWW1_CHICK (+2)	ACO2	87	1	0	0	0	2	2	0	0	0	0
115	Glutathione S-transferase	A0A1D5NZK9_CHICK	LOC100859645	19	5	2	0	0	0	3	0	0	0	0
116	Cytochrome b-c1 complex subunit Rieske, mitochondrial	A0A1L1RWY0_CHICK	UQCRFS1	24	2	0	0	0	0	4	0	0	1	0
117	Afadin, adherens junction formation factor	A0A1D5PJR8_CHICK	MLLT4	210	0	0	0	0	0	0	0	0	1	4
118	Type I alpha-keratin 15	Q6PVZ2_CHICK		48	2	0	0	0	0	0	1	0	0	0
119	Tight Junction Protein 2	A0A1D5P943_CHICK (+3)	TJP2	153	0	0	0	0	0	0	0	3	0	3
120	60S ribosomal protein L23 (blasted)	A0A1D5PDZ9_CHICK (+1)	RPL23	10	0	0	0	1	1	1	1	1	1	1
121	Ribosomal protein S16	R4GGJ0_CHICK	RPS16	16	0	0	0	2	0	0	1	1	1	1
122	ATP synthase subunit g, mitochondrial (blasted)	F1NIL3_CHICK	ATP5L	12	0	0	0	1	1	0	3	0	1	1
123	CFR-associated protein p70	O57660_CHICK		83	0	0	0	0	0	0	2	3	1	1
124	Glutathione reductase	A0A1D5P338_CHICK (+1)	GSR	50	1	0	0	0	0	0	3	2	0	1
125	ATP-citrate synthase	A0A1D5PSE5_CHICK (+2)	ACLY	121	0	0	0	0	0	0	1	2	1	1
126	Histone H2B	A0A1D5PC92_CHICK (+4)	HIST1H2B5L	14	0	0	0	1	1	0	0	4	0	1
127	Serum albumin	ALBU_CHICK	ALB	70	1	1	0	0	0	2	0	0	0	0
128	Hemoglobin subunit beta	A0A1D5PPV0_CHICK (+3)		17	2	0	0	0	0	2	1	0	0	0
129	Centrosomal protein	F1N9A0_CHICK	CEP126	129	0	0	0	0	0	1	0	0	0	0
130	Utrophin	A0A1D5P9A8_CHICK (+3)	UTRN	399	0	0	0	0	0	1	0	0	0	0
131	Hypothetical protein CIB84_008831	A0A1L1RSL1_CHICK		14	1	0	0	1	1	1	1	1	0	0

					GST					Cldn8 C-Terminal Domain				
#	Identified Proteins (227/946)	Accession Number	Alternate ID	MW kDa	E1	E2 #1	E2 #2	E3 #1	E3 #2	E1	E2 #1	E2 #2	E3 #1	E3 #2
132	ATP synthase subunit f, mitochondrial (blasted)	A0A1D5P1J7_CHICK (+1)	ATP5J2	10	0	0	0	1	1	1	1	1	1	0
133	Heterogeneous nuclear ribonucleoprotein H1-like protein (blasted)	A0A1D5NY02_CHICK (+4)	HNRNPH1	54	0	0	0	0	0	0	1	1	1	1
134	S-adenosylmethionine synthase	A0A1L1RNS1_CHICK		21	0	0	0	0	0	0	1	1	1	2
135	Ribosomal protein S25	A0A1L1RR89_CHICK (+2)	RPS25	9	0	0	0	1	1	0	2	2	0	0
136	T-complex protein 1 subunit gamma	A0A1D5P2D9_CHICK	CCT3	61	0	0	0	1	0	0	0	2	1	0
137	4-trimethylaminobutyraldehyde dehydrogenase	F1NMN7_CHICK	ALDH9A1	64	0	0	0	0	0	0	1	1	1	2
138	Ribonucleoside-diphosphate reductase	E1C4Q0_CHICK (+1)	RRM1	90	0	0	0	0	0	0	0	1	1	3
139	Serine/threonine-protein phosphatase	Q5ZM47_CHICK	PPP2CA	36	0	0	0	0	0	0	0	2	1	2
140	40S ribosomal protein S3	F1NPA9_CHICK	RPS3	27	0	0	0	2	1	0	0	1	0	0
141	Plastin-3	A0A1D5PE96_CHICK (+1)	PLS3	71	0	0	0	0	0	2	0	0	1	1
142	Keratin, type II cytoskeletal 6B-like	A0A1L1RKR4_CHICK (+1)	KRT75L4	65	3	0	0	0	1	0	2	0	0	0
143	Formin-like protein 2	A0A1D5PCY9_CHICK (+2)	FMNL2	124	0	0	0	0	0	1	0	0	0	0
144	Keratin, type I cytoskeletal 19	A0A1D5NW11_CHICK (+2)	KRT19	46	3	0	0	0	0	0	2	0	0	0
145	Heat shock protein 10	F1NGP9_CHICK (+1)	HSPE1	11	2	0	0	0	0	1	0	0	0	0
146	Polyadenylate-binding protein	E1C903_CHICK	PABPC4	70	2	0	0	0	0	1	0	0	0	0
147	CAD protein	E1BTX8_CHICK		223	0	0	0	0	0	0	0	1	0	5
148	Alcohol dehydrogenase [NADP(+)]	A0A1L1RPK9_CHICK (+3)	AKR1A1	37	0	0	0	0	0	2	0	0	0	0

					GST					Cldn8 C-Terminal Domain				
#	Identified Proteins (227/946)	Accession Number	Alternate ID	MW kDa	E1	E2 #1	E2 #2	E3 #1	E3 #2	E1	E2 #1	E2 #2	E3 #1	E3 #2
149	Importin subunit alpha	F6RHH1_CHICK (+1)	KPNA4	56	0	1	2	0	0	0	0	0	1	1
150	40S ribosomal protein S8 (Fragment)	Q6EE57_CHICK		22	0	0	0	1	0	1	1	2	0	0
151	Ribosomal protein S19	A0A1D5PDV6_CHICK	RPS19	15	0	0	0	1	1	0	2	1	0	0
152	Heat shock cognate protein HSP 90-beta	A0A1D5PHC5_CHICK (+2)	HSP90AB1	80	2	0	0	1	1	0	1	0	0	0
153	Arf-GAP with SH3 domain, ANK repeat and PH domain-containing protein 2	A0A1D5P5F3_CHICK (+1)	ASAP2	109	1	0	0	0	1	0	1	1	0	0
154	14-3-3 protein epsilon	1433E_CHICK (+1)	YWHAE	29	0	0	0	3	0	0	3	3	0	0
155	RuvB-like helicase	F1N8Z4_CHICK	RUVBL1	50	0	0	0	0	0	0	1	2	0	2
156	Nucleophosmin/nucleoplasmin 3	A0A1D5PLH4_CHICK	NPM3	16	0	0	0	1	0	0	3	1	0	0
157	Peptidyl-prolyl cis-trans isomerase	D0EKR3_CHICK	PPIA	18	0	0	0	0	0	3	1	1	0	0
158	Ribosomal protein S15a	A0A1L1RU99_CHICK (+1)	RPS15A	11	0	0	0	0	3	0	1	1	0	0
159	60 kDa heat shock protein, mitochondrial	CH60_CHICK	HSPD1	61	0	0	0	0	2	0	0	1	0	0
160	D-beta-hydroxybutyrate dehydrogenase, mitochondrial	A0A1L1RJK2_CHICK (+2)	BDH1	38	0	0	0	0	0	0	0	0	0	1
161	protein transport protein Sec24A (blasted)	E1BSA7_CHICK	SEC24A	120	0	0	0	0	0	0	0	0	1	3
162	ATP synthase subunit beta	A0A1D5PU77_CHICK (+3)	ATP5B	57	1	0	0	0	0	2	0	0	0	0
163	Zinc finger protein 106	E1BRP5_CHICK	ZNF106	207	1	0	0	0	0	0	0	0	0	0
164	Tubulin-specific chaperone D	A0A1D5NTW7_CHICK (+2)	TBCD	114	0	0	0	0	0	1	0	0	0	0
165	Laminin subunit alpha-3	F1NQ51_CHICK		192	1	0	0	0	0	0	0	0	0	0

					GST					Cldn8 C-Terminal Domain				
#	Identified Proteins (227/946)	Accession Number	Alternate ID	MW kDa	E1	E2 #1	E2 #2	E3 #1	E3 #2	E1	E2 #1	E2 #2	E3 #1	E3 #2
166	Spatacsin	A0A1D5PRP5_CHICK (+1)	SPG11	269	0	0	0	0	0	1	0	0	0	0
167	Stathmin-2	STMN2_CHICK	STMN2	21	4	0	0	0	0	0	0	0	0	0
168	Neuronal pentraxin-1	F1NHL5_CHICK	NPTX1	50	0	0	4	0	0	0	0	0	0	0
169	SHC-transforming protein 1	A0A1D5NYP8_CHICK (+1)	SHC1	68	0	1	1	0	0	0	0	0	1	1
170	40S ribosomal protein S23	F1NDC2_CHICK	RPS23	16	0	0	0	1	1	1	0	1	0	0
171	Tubulin beta chain	G1K338_CHICK	TUBB2B	50	0	0	0	0	22	0	41	38	0	0
172	Growth factor receptor-bound protein 2	A3R0S3_CHICK	GRB2	25	0	0	0	0	0	1	0	1	0	0
173	ubiquitin-conjugating enzyme E2 L3 (blasted)	A0A1D5NX21_CHICK (+2)	UBE2L3	18	0	0	0	0	0	0	2	1	0	0
174	Carbonic anhydrase 2	A0A1D5P3R2_CHICK (+1)	CA2	31	1	0	0	0	0	2	0	0	0	0
175	F-box protein 22	Q5ZLD9_CHICK	FBXO22	43	0	0	0	0	0	0	0	0	1	1
176	Desmin	E1BZ05_CHICK	DES	53	3	0	0	0	0	1	0	0	0	0
177	Filamin	Q90WF1_CHICK		273	0	0	0	0	0	0	2	0	0	1
178	60S ribosomal protein L4	A0A1D5NUQ4_CHICK (+7)	RPL4	47	0	0	0	2	0	0	1	0	0	0
179	Ubiquinol-cytochrome c reductase core protein 2	A0A1D5PEW4_CHICK (+2)	UQCRC2	49	0	0	0	0	0	0	0	3	1	0
180	splicing factor, arginine/serine-rich 6 (blasted)	A0A1D5P892_CHICK (+2)	SRSF6	40	0	0	0	0	0	0	2	0	0	0
181	Keratin, type II cytoskeletal cochleal	K2CO_CHICK		54	4	0	0	0	2	0	5	0	0	0
182	Hypothetical protein RCJMB04_19e2	A0A1D5NZK3_CHICK		304	0	0	0	0	0	1	0	0	0	0

					GST					Cldn8 C-Terminal Domain				
#	Identified Proteins (227/946)	Accession Number	Alternate ID	MW kDa	E1	E2 #1	E2 #2	E3 #1	E3 #2	E1	E2 #1	E2 #2	E3 #1	E3 #2
183	E3 SUMO-protein ligase PIAS2	A0A1D5P523_CHICK (+1)	PIAS2	68	0	0	1	0	0	0	0	0	0	0
184	keratin, type I cytoskeletal 19 (blasted)	A0A1D5PMQ5_CHICK	LOC420039	54	1	0	0	0	0	0	1	1	0	0
185	avidin isoform X1 (blasted)	A0A1L1RKY8_CHICK	LOC426220	18	1	0	0	0	0	0	1	1	0	0
186	GMP synthase	A0A1D5NU96_CHICK (+1)	GMPS	77	1	0	0	0	0	1	0	0	0	0
187	Mitogen-activated protein kinase	Q8UWG6_CHICK	MAPK1	42	0	0	0	0	0	0	0	0	1	2
188	heterogeneous nuclear ribonucleoprotein M (blasted)	F7B5K7_CHICK (+1)	HNRNPM	76	0	0	0	0	0	0	1	2	0	0
189	Histone H2A	A0A1D5PA20_CHICK (+1)		16	2	0	0	0	0	0	1	0	0	0
190	Protein transport protein Sec23A	A0A1D5P0E2_CHICK (+1)	SEC23A	86	0	0	0	0	0	0	1	4	0	0
191	Alpha-enolase	A0A1D5PSH6_CHICK (+2)	ENO1	47	1	0	0	0	0	0	0	1	0	0
192	Profilin	Q5ZL50_CHICK	PFN2	15	0	0	0	0	0	1	1	0	0	0
193	Ribosomal protein S11	Q98TH5_CHICK	cRPS11	18	0	0	0	1	0	0	1	0	0	0
194	60S ribosomal protein L7	A0A1D5PDK7_CHICK (+2)	RPL7	22	0	0	0	1	0	0	1	0	0	0
195	Ectopic P granules protein 5 homolog	A0A1D5PUX8_CHICK	EPG5	292	1	1	0	0	0	0	0	0	0	0
196	Tropomyosin alpha-1 chain	A0A1D5P342_CHICK (+1)	TPM1	29	0	0	0	0	0	0	2	1	0	0
197	Tubulin beta chain	A0A1D5P4N6_CHICK (+2)	TUBB6	50	0	0	0	16	0	0	0	0	7	0
198	Rho GTPase-activating protein 7	A0A1D5PBM9_CHICK (+1)	DLC1	126	1	0	0	0	0	0	0	0	0	0
199	Poly [ADP-ribose] polymerase	F1NL05_CHICK (+1)	PARP1	112	0	0	0	1	0	0	0	0	0	0
200	Gelsolin	A0A1D5PNS4_CHICK	GSN	91	0	0	0	0	0	0	2	0	0	0

					GST					Cldn8 C-Terminal Domain				
#	Identified Proteins (227/946)	Accession Number	Alternate ID	MW kDa	E1	E2 #1	E2 #2	E3 #1	E3 #2	E1	E2 #1	E2 #2	E3 #1	E3 #2
201	Mitochondrial ubiquinol-cytochrome-c reductase complex core protein i	D0VX31_CHICK (+1)		49	0	0	0	0	0	1	0	0	0	0
202	Fiilamin-A-interacting protein 1	A0A1D5PE44_CHICK	FILIP1	138	2	0	0	0	0	0	0	0	0	0
203	Elongator complex protein 3	A0A0A0MQ58_CHICK (+1)	ELP3	62	1	0	0	0	0	0	0	0	0	0
204	Deoxyuridine 5'-triphosphate nucleotidohydrolase	A0A1L1RUW7_CHICK (+1)	DUT	11	1	0	0	0	0	1	0	0	0	0
205	NAD kinase 2, mitochondrial	F1NJV0_CHICK	NADK2	49	0	0	0	0	0	1	0	0	0	1
206	Endoplasmin	A0A1D5PPN9_CHICK (+4)	HSP90B1	92	0	1	0	0	1	0	0	0	0	0
207	Nuclear pore complex protein Nup88	A0A1D5PER2_CHICK (+1)	NUP88	69	1	0	0	0	0	0	0	0	0	0
208	Myosin regulatory light chain 2, smooth muscle minor isoform	A0A1D5PNS5_CHICK (+1)	LOC770011	20	0	0	0	0	0	0	2	0	0	0
209	Casein kinase II subunit beta	CSK2B_CHICK	CSNK2B	25	0	0	0	0	0	0	2	0	0	0
210	Apoptosis-inducing factor 1	A0A1D6UPT4_CHICK (+3)	AIFM1	75	0	0	0	0	0	0	0	1	0	0
211	Ubiquitin carboxyl-terminal hydrolase 4	F1NE88_CHICK (+1)	USP4	107	0	0	0	0	0	0	0	0	0	1
212	Myosin light polypeptide 6	A0A1D5PEM4_CHICK (+2)	MYL6	17	0	0	0	0	0	0	1	0	0	0
213	Nucleolar and coiled-body phosphoprotein 1	A0A1D5PUU2_CHICK	NOLC1	72	0	0	0	0	0	0	1	0	0	0
214	Anamorsin OS=Gallus gallus GN=CIAPIN1 PE=4 SV=1	A0A1D5NU53_CHICK (+5)	CIAPIN1	21	1	0	0	0	0	0	0	0	0	0
215	NudC domain-containing protein 2	E1BUG9_CHICK	NUDCD2	18	0	0	0	0	0	1	0	0	0	0
216	Tumor necrosis factor receptor associated factor-5	Q805B1_CHICK	TRAF-5	64	1	0	0	0	0	0	0	0	0	0
217	Integrin alpha-2	A0A1D5PHA5_CHICK (+1)	ITGA2	131	1	0	0	0	0	0	0	0	0	0

					GST					Cldn8 C-Terminal Domain				
#	Identified Proteins (227/946)	Accession Number	Alternate ID	MW kDa	E1	E2 #1	E2 #2	E3 #1	E3 #2	E1	E2 #1	E2 #2	E3 #1	E3 #2
218	Chromodomain-helicase-DNA-binding protein 7	CHD7_CHICK	CHD7	338	0	0	0	0	0	1	0	0	0	0
219	F-actin-capping protein subunit beta isoforms 1 and 2	A0A1D5P9M3_CHICK (+1)	CAPZB	32	1	0	0	0	0	0	0	0	0	0
220	Thioredoxin-dependent peroxide reductase	A0A1D5PBY3_CHICK (+3)	Gga	24	1	0	0	0	0	0	0	0	0	0
221	Succinate dehydrogenase [ubiquinone] flavoprotein subunit, mitochondrial	A0A1L1RJF7_CHICK (+2)	SDHA	52	1	0	0	0	0	0	0	0	0	0
222	Malate dehydrogenase	E1BVT3_CHICK	MDH2	37	1	0	0	0	0	0	0	0	0	0
223	Plastin-2	F6RS71_CHICK (+1)	LCP1	70	1	0	0	0	0	0	0	0	0	0
224	Heat shock protein HSP 90-alpha	A0A1D5P5R0_CHICK (+2)	HSP90AA1	83	2	0	0	0	0	0	0	0	0	0
225	Probable D-lactate dehydrogenase	F1P277_CHICK	LDHD	53	0	0	1	0	0	0	0	0	0	0
226	Cysteine desulfurase	A0A1D5P7V7_CHICK (+2)	NFS1	48	0	0	0	0	0	1	0	0	0	0
227	Transitional endoplasmic reticulum ATPase	A0A1D5NTY5_CHICK (+4)	LOC107049323	89	0	0	1	0	0	0	0	0	0	0

Table Appendix B: Protein Information Identified by Mass Spectrometry for Cldn8 C-Terminal Domain Interacting Partners
These data describe the proteins identified by mass spectrometry to interact with either GST or Cldn8 C-terminal domain samples bound to HH8 chick extract. This table shows the identified proteins, their accession numbers, their alternate ID, their molecular weight, and the number of times the protein was seen in GST samples (experiments 1-3, including duplicates) and in Cldn8 C-terminal domain samples (experiments 1-3, including duplicates).

Appendix C: Mass Spectrometry Data for Cldn14 C-Terminal Domain HH8 and Day 4 Samples

				Cldn14 C-Ter + Day 4		Cldn14 C-Ter + HH8	
#	Identified Proteins	Accession Number	MW (kDa)	GST	Cldn14	GST	Cldn14
1	2,4-dienoyl-CoA reductase, mitochondrial	A0A1L1RTA1_CHICK	36	1	1		
2	14-3-3 protein epsilon	1433E_CHICK (+1)	29	1	3		
3	14-3-3 protein theta	1433T_CHICK	28	5	18		13
4	14-3-3 protein zeta	1433Z_CHICK	28	0	4		2
5	20-hydroxysteroid dehydrogenase	F1N8Y3_CHICK (+1)	30		6	10	39
6	39S ribosomal protein L44	E1C5L8_CHICK	36	1			0
7	40S ribosomal protein S3a	A0A1D5PY92_CHICK	30	11	7	0	2
8	40S ribosomal protein S4	F1NFC6_CHICK (+1)	30	10	7		4
9	40S ribosomal protein S6	F7BYQ2_CHICK (+2)	29	5	2		
10	40S ribosomal protein S7	A0A1D5PFB4_CHICK (+1)	28	7	4		1
11	40S ribosomal protein S8	A0A1D5PT58_CHICK (+1)	24	4	2	1	2
12	40S ribosomal protein S12	A0A1I7Q419_CHICK (+1)	14	3	2		
13	40S ribosomal protein S13	RS13_CHICK	17	2	5		1
14	40S ribosomal protein S23	F1NDC2_CHICK	16	1	1		
15	40S ribosomal protein S25	A0A1L1RVH6_CHICK (+1)	9	3	1	1	2
16	40S ribosomal protein S26	A0A1D5PIE9_CHICK (+1)	13	2	1		
17	40S ribosomal protein S27	A0A1D5NZ06_CHICK	9	1	3		1
18	40S ribosomal protein S29 (blasted)	E1C3G8_CHICK	7		1		1
19	60 kDa heat shock protein, mitochondrial	CH60_CHICK	61	5	11	0	10
20	60S acidic ribosomal protein P0	F1NB66_CHICK (+1)	34	7	7		2
21	60S acidic ribosomal protein P2	A0A1D5PMT8_CHICK	12	5	3		1
22	60S ribosomal protein L3	A0A1L1RUP9_CHICK	25	2	2	0	
23	60S ribosomal protein L6	F6UD95_CHICK (+1)	33	4	2		
24	60S ribosomal protein L7	A0A1D5PDK7_CHICK (+1)	22	2	1		
25	60S ribosomal protein L7a	A0A1D5PNE4_CHICK (+5)	29	2			
26	60S ribosomal protein L9 OS=Gallus gallus GN=RPL9 PE=4 SV=1	A0A1D5NVI1_CHICK	22	2	6		2

				Cldn14 C-Ter + Day 4		Cldn14 C-Ter + HH8	
#	Identified Proteins	Accession Number	MW (kDa)	GST	Cldn14	GST	Cldn14
27	60S ribosomal protein L10	A0A1D5PD44_CHICK	19	3	2		1
28	60S ribosomal protein L11	A0A1D5P3B1_CHICK	20	1	3		2
29	60S ribosomal protein L12	E1BTG1_CHICK	18	4	6	1	1
30	60S ribosomal protein L13	A0A1I7Q3Z6_CHICK (+1)	19	5	2		
31	60S ribosomal protein L17	A0A1D5P149_CHICK (+2)	25	4	1		0
32	60S ribosomal protein L18a	F1NPD3_CHICK	21	2	1		1
33	60S ribosomal protein L21	R4GIQ2_CHICK	19	1	1		
34	60S ribosomal protein L22	F1N9J4_CHICK (+1)	15	2	1		
35	60S ribosomal protein L23	E1BY89_CHICK	15	4	3		3
36	60S ribosomal protein L27	A0A1L1RLQ0_CHICK (+2)	14	4	3		1
37	60S ribosomal protein L27a (blasted)	F1NBX4_CHICK	13	0	2		2
38	60S ribosomal protein L30	A0A1D5PNW0_CHICK (+1)	10	2	1	0	
39	60S ribosomal protein L31	A0A1L1RT94_CHICK (+1)	13	1			
40	60S ribosomal protein L35	A0A1D5PFV4_CHICK (+3)	11	1			1
41	60S ribosomal protein L35a	A0A1D5NYM9_CHICK (+1)	12	2	2		
42	60S ribosomal protein L35a	A0A1D5NV37_CHICK (+1)	11	2	3		2
43	60S ribosomal protein L37a	A0A1L1S0Q5_CHICK (+2)	8	3	1		
44	78 kDa glucose-regulated protein	GRP78_CHICK	72	14	16	7	8
45	NudC domain containing 2	E1BUG9_CHICK	18		1		2
46	Poly(rC) binding protein 2	A0A1D5P893_CHICK	35	2	3	1	2
47	AAA domain-containing protein	A0A1D5PVA4_CHICK	67	6	2		
48	AAA domain-containing protein	F1NU79_CHICK	46	1	1		
49	ADP-ribosylation factor 1	F1NN08_CHICK (+1)	21	1	6		2
50	AKAP2_C domain-containing protein	E1C929_CHICK (+1)	94	21	13		
51	ANK_REP_REGION domain-containing protein	A0A1D5P991_CHICK (+1)	107	17	7		
52	ATP synthase subunit alpha	A0A1D5PN54_CHICK	60	4	7	1	7
53	ATP synthase subunit beta	A0A1D5PU77_CHICK (+1)	57	2	9		7

				Cldn14 C-Ter + Day 4		Cldn14 C-Ter + HH8	
#	Identified Proteins	Accession Number	MW (kDa)	GST	Cldn14	GST	Cldn14
54	ATP-citrate synthase	A0A1D5PSE5_CHICK (+2)	121		1		
55	ATP-dependent RNA helicase DDX1	F1NV49_CHICK	83		13	0	
56	Abhydrolase domain containing 10	A0A1D5PJ73_CHICK (+1)	30		12		13
57	Acetyl-CoA acetyltransferase, mitochondrial	E1C0Q5_CHICK	44	1	2		1
58	Acetyltransferase component of pyruvate dehydrogenase complex OS=Gallus gallus GN=DLAT PE=3 SV=1	E1C6N5_CHICK	67				3
59	Acidic leucine-rich nuclear phosphoprotein 32 family member B	A0A1L1RVX5_CHICK (+2)	30				4
60	Aconitate hydratase, mitochondrial	A0A1D5NWW1_CHICK (+2)	87	2		3	
61	Actin filament-associated protein 1	A0A1D5PJK9_CHICK (+4)	82	4	3		
62	Actin filament-associated protein 1-like 1	A0A1D5P574_CHICK	86	4	1		
63	Actin, alpha cardiac muscle 1	ACTC_CHICK	42	319	264		96
64	Actin, alpha skeletal muscle	ACTS_CHICK	42	307	255	45	93
65	Actin, cytoplasmic 2	ACTG_CHICK	42	453	451	83	150
66	Actin-binding LIM protein 1	E1BS96_CHICK	83	12	3		
67	Actin-related protein 2	ARP2_CHICK (+1)	45	14	13		1
68	Actin-related protein 2/3 complex subunit 3	E1C8Y3_CHICK	21	5	3		2
69	Actin-related protein 2/3 complex subunit 4	F1P010_CHICK	20	6	5		1
70	Actin-related protein 2/3 complex subunit 5	Q5ZMV5_CHICK	16	7	4		1
71	Actin-related protein 2/3 complex subunit 5	F1P1S6_CHICK	20	2	2		
72	Actin-related protein 2/3 complex subunit	Q5ZJI7_CHICK	42	17	9		2
73	Actin-related protein 2/3 complex subunit	A0A1L1RWT1_CHICK (+1)	41	6	2		
74	Actin-related protein 3	ARP3_CHICK	47	17	14	1	4
75	Actin-related protein 10	F1NG10_CHICK (+1)	46	4	3		
76	Adseverin	A0A1D5PBC3_CHICK (+2)	79	1			
77	Afadin, adherens junction formation factor	A0A1D5PJR8_CHICK	210	7	2		
78	Aldolase_II domain-containing protein	A0A1L1RWX3_CHICK (+2)	81	5	1		

				Cldn14 C-Ter + Day 4		Cldn14 C-Ter + HH8	
#	Identified Proteins	Accession Number	MW (kDa)	GST	Cldn14	GST	Cldn14
79	Aldolase_II domain-containing protein	F1NEA1_CHICK (+1)	79	3	1		
80	Alpha 1 (V) collagen	Q9IAU4_CHICK	184	4	3		
81	Alpha-actinin-1	A0A1D5PF13_CHICK (+1)	103	42	25		
82	Alpha-actinin-2	A0A1D5PNV5_CHICK (+2)	103	23	14		
83	Alpha-actinin-4	ACTN4_CHICK	104	86	71		
84	Alpha-actinin-4	A0A1D5PIX0_CHICK	102	80	68		1
85	Alpha-centractin	Q5ZM58_CHICK	43	3	1		
86	Alpha-tropomyosin 2	Q8AWI4_CHICK	33	43	45		19
87	Alpha-tropomyosin	Q90740_CHICK	33	55	55	9	30
88	Angiomotin_C domain-containing protein	E1C5Z2_CHICK	102	7			
89	Ankyrin-3	A0A1D5PIW9_CHICK	476	4	0		0
90	Annexin	A0A1C9KD18_CHICK (+1)	39	4			
91	Apolipoprotein A-I	A0A1L1RJF5_CHICK (+1)	32	11	10		6
92	Apolipoprotein B	F1NV02_CHICK	523	15	16	48	116
93	Apovitellenin-1	APOV1_CHICK	12	1	3	4	9
94	Arf-GAP with SH3 domain, ANK repeat and PH domain-containing protein 2	A0A1D5P5F3_CHICK (+1)	109	1	0	1	3
95	Arp2/3 complex 34 kDa subunit	F1P1K3_CHICK	34	10	5		0
96	Avidin	A0A1L1RKY8_CHICK	18			3	3
97	BTB domain-containing protein	E1BVH8_CHICK (+1)	30		2		
98	Beta-tropomyosin	Q05705_CHICK	29	31	28		9
99	Brain acid soluble protein 1 homolog	BASP1_CHICK	25	5	2		
100	CFR-associated protein p70	O57660_CHICK	83	1	0		
101	Calcium voltage-gated channel auxiliary subunit alpha2delta 3	F1NX89_CHICK	124	3	3	5	4
102	Caldesmon	CALD1_CHICK	89	42	38	0	
103	Caldesmon	A0A1L1RKY9_CHICK	59	45	35		
104	Calponin	E1BSX2_CHICK	37	12	14	4	

				Cldn14 C-Ter + Day 4		Cldn14 C-Ter + HH8	
#	Identified Proteins	Accession Number	MW (kDa)	GST	Cldn14	GST	Cldn14
105	Calponin	A0A1L1RRB3_CHICK (+2)	33	3	3	2	
106	Calponin-homology (CH) domain-containing protein	F1NS33_CHICK	65	13	8		
107	Capping protein (Actin filament) muscle Z-line, alpha 2	A0M8U0_CHICK (+1)	33	16	17	1	8
108	Carbamyl phosphate synthetase 1, partial (blasted)	E1BTX8_CHICK	223		1		
109	Carbonic anhydrase 2	A0A1D5P3R2_CHICK (+1)	31			1	
110	Cardiac troponin I	Q6S7R6_CHICK	24	4	1		
111	Casein kinase II subunit alpha	CSK21_CHICK	45	1	0		
112	Caspase-3	O93417_CHICK	32		8		8
113	Cell division control protein 42 homolog	A0A1L1RTL5_CHICK (+1)	15	1	1		
114	Centrosomal protein	A0A1D5PMR7_CHICK	88		1		
115	Centrosomal protein	E1BTL1_CHICK	124	2	1		
116	CgABP260	Q90WF0_CHICK	280		4	0	
117	Cingulin	H9KYY1_CHICK	138	14	14	1	
118	Claudin	E1C5Q7_CHICK	25		37		43
119	Cofilin-2	A0A1D5NYP3_CHICK (+1)	17	2			
120	Collagen alpha-1(I) chain	CO1A1_CHICK	138	6			
121	Collagen alpha-1(XI) chain	F1P4K9_CHICK	76	1			
122	Collagen alpha-2(I) chain	CO1A2_CHICK	129	1			
123	Complement C1q binding protein	F1NJF0_CHICK (+1)	24	0	2		3
124	Connectin (Fragment)	A6BM71_CHICK	905	1		0	
125	Coronin	A0A1D5PCT4_CHICK	64	18	15		2
126	Coronin	A0A1D5PVL9_CHICK (+1)	54	4	4		
127	Coronin	A0A1D5PY15_CHICK	40	5			
128	CortBP2 domain-containing protein	A0A1D5PTS2_CHICK (+1)	69	2			
129	CortBP2 domain-containing protein	A0A1D5PE44_CHICK	138	1			

				Cldn14 C-Ter + Day 4		Cldn14 C-Ter + HH8	
#	Identified Proteins	Accession Number	MW (kDa)	GST	Cldn14	GST	Cldn14
130	Cyclin-dependent kinase 1	F1NBD7_CHICK	35	2	3		3
131	Cytochrome c oxidase subunit NDUFA4	A0A1L1RIQ5_CHICK (+1)	12	1	1		1
132	Cytoplasmic activation-proliferation-associated protein 1	Q5XNV3_CHICK	78 k	4			0
133	Cytospin-A	A0A140T8H5_CHICK (+1)	128	26	13		
134	DEAD-box RNA helicase	A0A1D5PBA9_CHICK (+1)	67	14	6		
135	DEAD-box helicase 3,X-linked	Q5F491_CHICK	72	7	8	7	2
136	DH domain-containing protein	E1C588_CHICK	196	2		0	0
137	DNA damage-binding protein 1	A0A1D5PBI5_CHICK (+1)	127	0	19		2
138	DNA polymerase delta subunit 2 isoform X1 (blasted)	A0A1D5PTS1_CHICK	51		3		1
139	Death-associated protein kinase 1	A0A1D5NT66_CHICK (+1)	160	7	2		
140	Dedicator of cytokinesis protein 7	A0A1D5PGL5_CHICK	95	20	16		
141	Desmin	E1BZ05_CHICK	53	17	16	3	6
142	Destrin	Z4YJB8_CHICK	19	6	4	5	3
143	Dihydropyrimidinase-related protein 2	DPYL2_CHICK (+2)	62	1	2		
144	Doublecortin	A0A1L1RJP0_CHICK (+1)	38	4	2		
145	Drebrin	DREB_CHICK	72	63	67	8	11
146	Drebrin-like protein	A0A1D5PRY7_CHICK	45	11	5		
147	Dynactin subunit 2	DCTN2_CHICK	45		2		
148	Dynactin subunit 6	F1NAP2_CHICK	21	2	3		
149	Dynactin subunit	E1BQQ5_CHICK	52	5	3		
150	Dystonin	A0A1D5P0Y6_CHICK (+1)	670	1	0		
151	EF hand-containing protein 1	Q49B65_CHICK	27	1	4		
152	EF-hand domain-containing protein	A0A1D5P657_CHICK	127				4
153	Ectopic P granules protein 5 homolog	A0A1D5PUX8_CHICK	292	1		1	
154	Ekaryotic initiation factor 4A-II	A0A1D5PR64_CHICK	28	2	5		5
155	Elongation factor 1-alpha 1	EF1A_CHICK (+1)	50	24	28	15	17

				Cldn14 C-Ter + Day 4		Cldn14 C-Ter + HH8	
#	Identified Proteins	Accession Number	MW (kDa)	GST	Cldn14	GST	Cldn14
156	Elongation factor 1-beta	F1NYA9_CHICK (+1)	25				2
157	Elongation factor 2	A0A1D5PS29_CHICK	95	7	28	7	13
158	Elongation factor Tu, mitochondrial (Fragment)	EFTU_CHICK	38	8	8		2
159	Endoplasmin	A0A1D5PPN9_CHICK (+3)	92				2
160	Erythroid protein 4.1	R4GHW9_CHICK	97	10	4		
161	Eukaryotic initiation factor 4A-II	A0A1L1RUX2_CHICK	45	4	4	2	3
162	Eukaryotic translation elongation factor 1	Q6EE30_CHICK	50		2		2
163	Eukaryotic translation initiation factor 3 subunit F	A0A1D5PVL4_CHICK (+1)	35	2			1
164	Eukaryotic translation initiation factor 5A	A0A1L1RQA1_CHICK (+1)	15	0	9		8
165	Exportin-T	E1C593_CHICK	110	1			
166	F-actin-capping protein subunit alpha-1	CAZA1_CHICK	33	18	15	0	9
167	F-actin-capping protein subunit beta isoforms 1 and 2	A0A1D5P5A8_CHICK	30	20	28	4	15
168	F-actin-capping protein subunit beta isoforms 1 and 2	A0A1D5P9M3_CHICK (+1)	32	19	27	4	
169	FAM193_C domain-containing protein OS=Gallus gallus PE=4 SV=1	A0A1D5P4I8_CHICK	84	1		3	
170	FIST_C domain-containing protein OS=Gallus gallus GN=FBXO22 PE=2 SV=1	Q5ZLD9_CHICK	43		4		
171	Family with sequence similarity 98 member B	E1C7K1_CHICK	45		2		1
172	Fascin	A0A1D6UPS2_CHICK (+1)	64	122	75	24	46
173	Fatty acid synthase	FAS_CHICK	275	0	2		
174	Fibrillin-2	A0A1D5NXE0_CHICK	300	2	1		
175	Fibrinogen alpha chain	F1P4V1_CHICK (+1)	87	0	2		
176	Fibrinogen gamma chain	O93568_CHICK	50	1			
177	Fibronectin	F1NJT3_CHICK	273	39	21		

				Cldn14 C-Ter + Day 4		Cldn14 C-Ter + HH8	
#	Identified Proteins	Accession Number	MW (kDa)	GST	Cldn14	GST	Cldn14
178	Fibronectin type-III domain-containing protein	F1NLE3_CHICK	50		1		
179	Filamin	Q90WF1_CHICK	273	27	21		
180	Filamin-B	A0A1D5NYG3_CHICK	284	105	87		
181	Four and a half LIM domains protein 3	A0A1D5P5R5_CHICK (+1)	33		0		4
182	Fragile X mental retardation syndrome-related protein 1	A0A1D5PDA7_CHICK (+4)	73				3
183	GTP-binding nuclear protein Ran	A0A1I7Q3Y7_CHICK (+1)	23	6	4		4
184	GTPase cRac1B	A0A1D5PZA2_CHICK (+5)	22	1	2		0
185	Galectin	A0A1D5PBG4_CHICK (+1)	15	3	2		
186	Gallus Gallus mRNA encoding a tropomyosin (probably non-muscle), homologous to a human heat stable cytoskeletal protein having an apparent molecular weight of 36000 Dalton (hscp 36) (Fragment)	Q9PSS9_CHICK	9	3	2		
187	Gap junction alpha-1 protein	CXA1_CHICK (+1)	43	9	6		
188	Gelsolin	GELS_CHICK	86	67	68	5	14
189	Gelsolin	A0A1D5PH32_CHICK	82	67	64	4	12
190	Glutaredoxin domain-containing protein	A0A1D5NVZ3_CHICK (+1)	66		2	4	37
191	Glutaredoxin-3	F1NNP6_CHICK	37	0	2	1	1
192	Glutathione S-transferase 2	GSTM2_CHICK	26	33	88	54	94
193	Glutathione S-transferase 3	GSTA3_CHICK	26	40	60	17	33
194	Glutathione S-transferase	A0A1D5NT70_CHICK	25	36	64	24	53
195	Glutathione S-transferase	A0A0A0MQ61_CHICK	25	39	73	21	49
196	Glutathione S-transferase	GSTA1_CHICK	25	27	49	27	46
197	Glutathione S-transferase	GSTA2_CHICK	25	62	80	40	70
198	Glutathione S-transferase	A0A1D5PDF1_CHICK	25	79	166	90	132
199	Glutathione S-transferase class-alpha	Q9W6J2_CHICK	25	8	17	2	5
200	Glutathione peroxidase	Q8QG67_CHICK	19	1		0	

				Cldn14 C-Ter + Day 4		Cldn14 C-Ter + HH8	
#	Identified Proteins	Accession Number	MW (kDa)	GST	Cldn14	GST	Cldn14
201	Glutathione peroxidase	A0A1D5NV92_CHICK (+2)	16	3			
202	Glutathione reductase	A0A1D5P338_CHICK (+1)	50			1	
203	Glyceraldehyde-3-phosphate dehydrogenase	F1NH87_CHICK (+1)	36	15	18	5	18
204	Glypican-4	A0A1D5PKI8_CHICK	85	3	2		
205	GrpE protein homolog	Q5ZHV6_CHICK	25	1	7	0	8
206	Guanine nucleotide-binding protein G(i) subunit alpha-2	A0A1D5PH67_CHICK (+1)	41	3	3		
207	HABP4_PAI-RBP1 domain-containing protein	F1NYE5_CHICK (+1)	45	2	1		
208	HP domain-containing protein	E1C5U6_CHICK	97	16	12		
209	HP domain-containing protein	E1C8N4_CHICK	206	69	62		
210	Heat shock cognate 71 kDa protein	A0A1D5PFJ6_CHICK	71	32	27	19	10
211	Heat shock cognate protein HSP 90-beta	HS90B_CHICK	83	10	5	2	3
212	Heat shock protein 10	F1NGP9_CHICK (+1)	11				1
213	Heat shock protein 70	Q7SX63_CHICK	70	17	14		
214	Heat shock protein HSP 90-alpha	A0A1D5P5R0_CHICK (+2)	83	9	12	1	4
215	Hemoglobin subunit alpha-A	HBA_CHICK	15	7	5		
216	Hemoglobin subunit alpha-D	HBAD_CHICK	16	5	7		
217	Hemoglobin subunit beta	A0A1D5PPV0_CHICK (+1)	17	11	12		
218	Hemoglobin subunit epsilon	HBE_CHICK	17	12	12	3	3
219	Hemoglobin subunit pi	HBPI_CHICK	16	13	13		3
220	Heterogeneous nuclear ribonucleoprotein A3	E1BZE6_CHICK	40	2			
221	Heterogeneous nuclear ribonucleoprotein H1-like protein	A0A1D5NY02_CHICK (+3)	54	3	3		
222	Heterogeneous nuclear ribonucleoprotein M (blasted)	F7B5K7_CHICK (+1)	76	11	5		
223	Histone H2A.J	H2AJ_CHICK	14	3	3	3	4
224	Histone H2B	A0A1D5PC92_CHICK (+3)	14	6	6	3	11

				Cldn14 C-Ter + Day 4		Cldn14 C-Ter + HH8	
#	Identified Proteins	Accession Number	MW (kDa)	GST	Cldn14	GST	Cldn14
225	Histone H3	A0A1D5PC18_CHICK (+4)	15	1	1	0	0
226	Histone H4 type VIII	H48_CHICK (+1)	11	8	6	6	7
227	Histone-lysine N-methyltransferase	H9L0M3_CHICK	333	1	1	1	1
228	Hydroxyacyl-CoA dehydrogenase trifunctional multienzyme complex subunit beta	E1BTT4_CHICK	51				3
229	Hypothetical protein CIB84_008831	A0A1D5PK33_CHICK (+1)	10	6	1		3
230	Hypothetical protein CIB84_008831	A0A1L1RSL1_CHICK	14	1	1	1	1
231	IF rod domain-containing protein	A0A1L1RKR4_CHICK (+1)	65	5	6	4	6
232	IF rod domain-containing protein	A0A1D5PMQ5_CHICK	54	4	8	2	9
233	IF rod domain-containing protein	A0A1D5PHS2_CHICK	41	14	12	12	27
234	IF rod domain-containing protein	A0A1D5PQ92_CHICK	26	6	8	5	8
235	Ig lambda chain C region	R9PXM5_CHICK (+1)	24			1	3
236	IgL	F1NSC8_CHICK	11			1	1
237	Immunoglobulin lambda light chain	F1NSC7_CHICK	11			1	2
238	Importin N-terminal domain-containing protein	F1NBA8_CHICK	119	2	1		
239	Importin N-terminal domain-containing protein	F1NRZ6_CHICK	116	3	1		
240	Insulin-like growth factor-binding protein complex acid labile subunit	E1C5R1_CHICK	58		1	1	
241	Junction plakoglobin	A0A1D5PA91_CHICK (+3)	84	1	1		4
242	KH type-2 domain-containing protein	F1NPA9_CHICK	27	5	9	2	14
243	KOW domain-containing protein	F2Z4K6_CHICK	17	2	1		0
244	Karyopherin subunit beta 1	A0A1D5P1W7_CHICK	120	3	4		
245	Keratin 12	F1NDN6_CHICK	54	6	9	3	10
246	Keratin, type I cytoskeletal 14	A0A1D5NX48_CHICK (+2)	51	4	7	2	6
247	Keratin, type I cytoskeletal 19	F1NDN9_CHICK	46	14	17	7	27
248	Keratin, type II cytoskeletal	A0A1D5P5F5_CHICK	30	3	3	1	3

				Cldn14 C-Ter + Day 4		Cldn14 C-Ter + HH8	
#	Identified Proteins	Accession Number	MW (kDa)	GST	Cldn14	GST	Cldn14
249	Keratin, type II cytoskeletal cochleal	K2CO_CHICK	54	33	29	20	52
250	Kinesin-like protein KIF24	R4GIH5_CHICK	148	1			
251	Ku domain-containing protein	F1NZI1_CHICK	87		3		
252	LIM domain only protein 7	A0A1D5P121_CHICK (+3)	128	7	4	0	
253	LIM zinc-binding domain-containing protein	A0A1D5PTF4_CHICK	85	55	46	2	5
254	LIM zinc-binding domain-containing protein	R4GG61_CHICK	44	2	2		
255	LIM zinc-binding domain-containing protein	F1NIU4_CHICK	109	2	2		
256	Lamin-B2	LMNB2_CHICK	68	2			
257	LanC-like protein 1	A0A1D5PYA4_CHICK	45		5	4	18
258	Leucine zipper protein 1	R4GHN9_CHICK	123	6	5		
259	Leucine-rich repeat flightless-interacting protein 1	F1NCG5_CHICK	46	3	6		
260	Leucine-rich repeat flightless-interacting protein 1	A0A1D5PMR9_CHICK	12	2	3		
261	Leucine-rich repeat flightless-interacting protein 2	A0A1D5P1C0_CHICK (+1)	48	7	8		1
262	LisH domain-containing protein	A0A1D5PUU2_CHICK	72	2			
263	Lymphocyte-specific protein 1	Q5F3Y0_CHICK	42	14	9		4
264	Lysozyme	B8YK79_CHICK (+1)	16	4	3	2	7
265	MSP domain-containing protein	A0A1D5PQJ6_CHICK	28	5	1		
266	Macrophage migration inhibitory factor	A0A1D5P337_CHICK (+2)	13		6		3
267	Malate dehydrogenase	E1BVT3_CHICK	37		1		
268	Microtubule-actin cross-linking factor 1	A0A1D5PAS4_CHICK (+4)	617	9	2		
269	Mitochondrial transcription factor A	A0A1L1RW12_CHICK (+2)	16				4
270	Mitochondrial ubiquinol-cytochrome-c reductase complex core protein i	D0VX31_CHICK (+1)	49		6		
271	Mitogen-activated protein kinase	Q8UWG6_CHICK	42		2		
272	Multifunctional protein ADE2	PUR6_CHICK (+1)	47				3
273	Myosin heavy chain, cardiac muscle	F1NM49_CHICK	224	140	136		

				Cldn14 C-Ter + Day 4		Cldn14 C-Ter + HH8	
#	Identified Proteins	Accession Number	MW (kDa)	GST	Cldn14	GST	Cldn14
274	Myosin light chain 1, cardiac muscle	F1P5V6_CHICK	22	38	43	6	15
275	Myosin light chain 1, skeletal muscle isoform	MLE1_CHICK	21	26	32		
276	Myosin light chain	F1NJ37_CHICK	21	52	52	6	9
277	Myosin light chain kinase, smooth muscle	A0A1L1RRF3_CHICK (+2)	217	27	20		
278	Myosin light polypeptide 6	A0A1L1RLN6_CHICK	17	46	58	12	26
279	Myosin light polypeptide 6	A0A1D5PEM4_CHICK	17	47	59	13	25
280	Myosin motor domain-containing protein	A0A1D5PXU1_CHICK	101	29	25		
281	Myosin regulatory light chain 2, smooth muscle major isoform	MLRM_CHICK	20	25	37	8	18
282	Myosin regulatory light chain 2, smooth muscle minor isoform	A0A1D5PNS5_CHICK (+1)	20	32	46	10	22
283	Myosin regulatory light chain 2A, cardiac muscle isoform	F1NYU0_CHICK (+1)	19	4	4		
284	Myosin, heavy chain 1G, skeletal muscle	F1P3X1_CHICK	223	85	82		
285	Myosin-1B	MYH1B_CHICK	223	118	119		
286	Myosin-1B	R4GIG1_CHICK	223	124	123		
287	Myosin-7	A0A1D5P600_CHICK	222	78	61		
288	Myosin-9	MYH9_CHICK	227	466	469	45	1
289	Myosin-9	A0A1D5PM19_CHICK	227	466	471	45	
290	Myosin-11	A0A1D5P8H1_CHICK	228	283			
291	Myosin-11	A0A1D5P1M0_CHICK	225	277			
292	Myosin-11	E1BXA5_CHICK (+1)	229	285	312		
293	Myristoylated alanine-rich C-kinase substrate	A0A1D5PDE6_CHICK	28	9	12		
294	NEDD4-binding protein 3 homolog	N4BP3_CHICK	48	1			
295	Neurofilament light	A0A1L1RUS3_CHICK (+2)	60	26	12		
296	Neurofilament medium polypeptide	F1NUT7_CHICK	96	30	19		
297	Nexilin	A0A1D5PJN9_CHICK	81	3	6		

				Cldn14 C-Ter + Day 4		Cldn14 C-Ter + HH8	
#	Identified Proteins	Accession Number	MW (kDa)	GST	Cldn14	GST	Cldn14
298	Non-POU domain-containing octamer-binding protein	Q5ZIZ5_CHICK	54	17	8		
299	Nonmuscle myosin heavy chain	Q02015_CHICK (+1)	231	413	442	23	0
300	Nuclear pore complex protein Nup205	A0A1D5PG44_CHICK (+1)	232	5	3		
301	Nuclear protein matrin 3	Q8UWC5_CHICK	101	3	1		
302	Nucleolin	A0A1D5NZ30_CHICK (+1)	75	6	3		
303	Nucleophosmin	A0A1L1RJ18_CHICK (+1)	31	7	5		3
304	Nucleoside diphosphate kinase	R4GM98_CHICK	20			3	
305	Nucleoside diphosphate kinase	NDK_CHICK	17	6	5	10	1
306	Nucleosome-remodeling factor subunit BPTF	A0A1D5PE97_CHICK	325	12	2	19	2
307	Obscurin	A0A1D5P9K1_CHICK	969			0	
308	Ovalbumin	OVAL_CHICK	43	15	17	7	14
309	Ovotransferrin	E1BQC2_CHICK	78		2		1
310	PDZ and LIM domain protein 7	PDLI7_CHICK	46	6	3		
311	PDZ domain-containing protein	F1NH40_CHICK	138	12	5		
312	PDZ domain-containing protein	A0A1D5PF01_CHICK	80	3	5		
313	PDZ domain-containing protein	E1BUP8_CHICK	311	2	2		
314	PH domain-containing protein	E1C7W8_CHICK	84	2			
315	PRKC apoptosis WT1 regulator protein	F1NA74_CHICK	36	5	2		
316	Palladin	F1P0G8_CHICK	89	4	3		
317	Paranemin	O57613_CHICK	193	22	18		
318	Paraspeckle component 1	PSPC1_CHICK	58	2	1		
319	Peptidyl-prolyl cis-trans isomerase	D0EKR3_CHICK	18		5		3
320	Pericentriolar material 1 protein	PCM1_CHICK	213	2	3		
321	Peroxiredoxin-1	PRDX1_CHICK	22	10	28	8	21
322	Peroxiredoxin-6	F1NBV0_CHICK	25		2	2	2
323	Plasminogen	F1NWX6_CHICK	91	0	1	1	2

				Cldn14 C-Ter + Day 4		Cldn14 C-Ter + HH8	
#	Identified Proteins	Accession Number	MW (kDa)	GST	Cldn14	GST	Cldn14
324	Poly [ADP-ribose] polymerase	F1NL05_CHICK (+1)	112	3	1		
325	Polyadenylate-binding protein	A0A1D5NYB2_CHICK (+2)	71	1	1		
326	Polypyrimidine tract-binding protein 1	A0A1L1S0D8_CHICK (+2)	60	1			
327	Polyubiquitin-B	A0A1D5NVA7_CHICK (+7)	11	3	2		2
328	Pre-mRNA-splicing factor ATP-dependent RNA helicase DHX15	F1NHI3_CHICK (+1)	88	1	1		0
329	Probable ATP-dependent RNA helicase DDX17	A0A1D5PD32_CHICK	73	7	3		
330	Profilin	Q5ZL50_CHICK	15		6		5
331	Prohibitin	PHB_CHICK	30	3	1		2
332	Prohibitin-2	PHB2_CHICK	33	3	3		1
333	Proliferating cell nuclear antigen	A0A1D5PDN3_CHICK (+1)	28		3		
334	Protein Shroom2	A0A1D5P807_CHICK	195	4	1		
335	Protein flightless-1 homolog	Q5ZLR0_CHICK	145	29	15	0	
336	Protein kinase domain-containing protein	A0A1D5PRN8_CHICK (+1)	53	4	2		
337	Protein phosphatase 1 regulatory subunit	F1NA71_CHICK	107	16	12		
338	Protein phosphatase 1 regulatory subunit	A0A1D5NZG0_CHICK (+3)	21	1			
339	Protein phosphatase 1, regulatory (inhibitor) subunit 9B	A0A1D5PQD8_CHICK	151	22	13		
340	Pterin-4-alpha-carbinolamine dehydratase 2	F1P3K7_CHICK (+1)	12				1
341	Putative uncharacterized protein	Q5F411_CHICK	60	2	2		
342	Putative uncharacterized protein	Q5ZMN6_CHICK	50	8	7	0	
343	Pyruvate kinase	F1NW43_CHICK	58		2		1
344	RNA polymerase II subunit A C-terminal domain phosphatase SSU72	SSU72_CHICK	23		2		9
345	RNA-binding protein 4B-like	A0A1D5NXB3_CHICK	41	5	1		
346	RNA-binding protein 14	A0A1D5NTG2_CHICK	77	2			
347	RNA-binding protein EWS	A0A1D5PQF4_CHICK	77		1		

				Cldn14 C-Ter + Day 4		Cldn14 C-Ter + HH8	
#	Identified Proteins	Accession Number	MW (kDa)	GST	Cldn14	GST	Cldn14
348	RRM domain-containing protein	A0A1D5P411_CHICK (+2)	51	4	1		
349	RRM domain-containing protein	Q5F4B6_CHICK	46			1	
350	Ras GTPase-activating protein-binding protein 1	Q5ZMN1_CHICK	52	2	1		
351	Ras-related protein Rab-1A	A0A1D5PE33_CHICK	23	3	2	1	3
352	Ras-related protein Rab-5A	Q5ZIP7_CHICK	24	1	2		
353	Ribonuclease/angiogenin inhibitor 1	Q5ZIY8_CHICK	50		2		8
354	Ribos_L4_asso_C domain-containing protein	A0A1D5NUQ4_CHICK (+7)	47	6	4		1
355	Ribosomal protein L15	F1NQG5_CHICK	24	2	1		
356	Ribosomal protein L18 (Fragment)	Q6EE60_CHICK	19	3			
357	Ribosomal protein	F6SU35_CHICK (+1)	25	5	1		
358	Ribosomal protein S11	Q98TH5_CHICK	18	3	5	0	4
359	Ribosomal protein S15a	A0A1L1RU99_CHICK (+1)	11	4	2		2
360	Ribosomal protein S16	R4GGJ0_CHICK	16	6	3		4
361	Ribosomal protein S19	A0A1D5PDV6_CHICK	15	2	3		2
362	Ribosomal_L2_C domain-containing protein	F1NIX0_CHICK	28	2	1		
363	Ribosomal_L14e domain-containing protein	A0A1D5PSZ9_CHICK (+3)	17	1	2		1
364	Ribosomal_L28e domain-containing protein	A0A1L1RLQ7_CHICK (+1)	14	3			
365	Ribosomal_S10 domain-containing protein	F1NH93_CHICK	13	1	1		1
366	RuvB-like helicase OS=Gallus gallus	F1N8Z4_CHICK	50	1	0		1
367	S5 DRBM domain-containing protein	E1C4M0_CHICK	31	4	3		2
368	S10_plectin domain-containing protein	E1C4N0_CHICK	19	3	2		1
369	S-adenosylmethionine synthase (blasted)	A0A1L1RNS1_CHICK	21		1		1
370	S-methyl-5'-thioadenosine phosphorylase	F1NCV7_CHICK	31		3		1
371	S-phase kinase-associated protein 1	SKP1_CHICK	19	0	2		2
372	SH3 domain-containing protein	F1NU55_CHICK	63	10	8		
373	SH3 domain-containing protein	E1BWI0_CHICK	325	7	3	0	3

				Cldn14 C-Ter + Day 4		Cldn14 C-Ter + HH8	
#	Identified Proteins	Accession Number	MW (kDa)	GST	Cldn14	GST	Cldn14
374	SLIT-ROBO Rho GTPase-activating protein 2	Q5ZLG7_CHICK	33	9	7	2	11
375	SLIT-ROBO Rho GTPase-activating protein 2	E1BZR0_CHICK	98	9	5		
376	Serine/threonine-protein kinase DCLK1	A0A1D5P0Z1_CHICK	81		1		
377	Serine/threonine-protein phosphatase 2A 55 kDa regulatory subunit B	A0A1D5PED5_CHICK (+2)	52	2	11		12
378	Serine/threonine-protein phosphatase	A0A1D5P888_CHICK	38	23	16		1
379	Serine/threonine-protein phosphatase PP1-beta catalytic subunit	PP1B_CHICK	37	20	13		
380	Serpin H1	SERPH_CHICK	46	4			
381	Serum albumin	ALBU_CHICK	70			1	1
382	Signal-induced proliferation-associated 1-like protein 1	E1BQZ3_CHICK	198	7	3		
383	Slow myosin heavy chain 1 (Fragment)	P79792_CHICK	32	10	11		
384	SoHo domain-containing protein	E1C009_CHICK	65	2	0	1	1
385	Solute carrier family 25 member 3	A0A1D5PS40_CHICK (+1)	40	2	0		1
386	Spectrin alpha chain, non-erythrocytic 1	A0A1D5PVG1_CHICK	286	298	255	4	
387	Spectrin alpha chain, non-erythrocytic 1	F1NHT3_CHICK	285	293	252		
388	Spectrin beta chain	A0A1D5PYZ8_CHICK	262	12	0		
389	Spectrin beta chain	A0A1D5PJY1_CHICK	274	265	189	0	
390	Splicing factor, proline- and glutamine-rich	F1P555_CHICK	70	22	18		
391	Stress-70 protein, mitochondrial	F1NZ86_CHICK	73	29	9	25	4
392	Structural maintenance of chromosomes protein	Q8AWB7_CHICK	143	2	1		
393	Surfeit locus protein 4	SURF4_CHICK	31	2	1		
394	Synaptopodin OS=Gallus gallus PE=4 SV=2	R4GI80_CHICK	99	2	1		
395	T-complex protein 1 subunit alpha	Q5ZMG9_CHICK	60	3	4		2
396	T-complex protein 1 subunit beta	A0A1D5NUC1_CHICK (+2)	58	1	1		1

				Cldn14 C-Ter + Day 4		Cldn14 C-Ter + HH8	
#	Identified Proteins	Accession Number	MW (kDa)	GST	Cldn14	GST	Cldn14
397	T-complex protein 1 subunit delta	Q9I8D6_CHICK	58	4	4		
398	T-complex protein 1 subunit gamma	A0A1D5P2D9_CHICK	61		1		
399	T-complex protein 1 subunit theta	TCPQ_CHICK	59	1	1		
400	T-complex protein 1 subunit zeta	F1NWH9_CHICK (+1)	58	2	5		0
401	TPR_REGION domain-containing protein	A0A1D5P9T4_CHICK (+1)	103	1	1		
402	Thioredoxin	THIO_CHICK	12	4	2	4	1
403	Thyroid adenoma-associated protein homolog	A0A1D5NZH4_CHICK (+1)	196	1		0	0
404	Tight Juntion Protein 1 (ZO-1)	A0A1D5PB11_CHICK	189	39	32		
405	Tight Juntion Protein 2 (ZO-2)	A0A1D5PA43_CHICK (+1)	133	17	13		
406	Transgelin-3	A0A1L1RNG7_CHICK (+1)	13	2			
407	Translocon-associated protein subunit delta	E1C218_CHICK	127	21	8	0	
408	Transportin 3	A0A1D5PDV1_CHICK	104	2	1		
409	Trimethyllysine dioxygenase, mitochondrial	TMLH_CHICK	49		13		17
410	Trinucleotide repeat-containing gene 18 protein	A0A1D5PVN8_CHICK	30	2	1		
411	Tropomodulin	Q91006_CHICK	40	17	15		1
412	Tropomodulin	E1BT74_CHICK	36	6	3		
413	Tropomodulin-3	A0A1D5PW62_CHICK (+1)	41	19	20	2	4
414	Tropomyosin alpha-1 chain	A0A1D5P342_CHICK	29	36	41		21
415	Tropomyosin alpha-1 chain	F1NM23_CHICK (+1)	33	55	55		29
416	Tropomyosin alpha-4 chain	A0A1L1RVU7_CHICK	29	50	49	8	25
417	Tropomyosin alpha-4 chain	A0A1D5P2B9_CHICK	29	51	51		25
418	Tropomyosin alpha-4 chain	A0A1D5P713_CHICK	29	29	22		10
419	Tropomyosin alpha-4 chain	F1NK75_CHICK	33	46	34		11
420	Tropomyosin beta chain	TPM2_CHICK	33	33	25		
421	Tropomyosin beta chain	A0A1D5P4H0_CHICK	33	34	27		9
422	Troponin C, slow skeletal and cardiac muscles	TNNC1_CHICK	18	5	7		

				Cldn14 C-Ter + Day 4		Cldn14 C-Ter + HH8	
#	Identified Proteins	Accession Number	MW (kDa)	GST	Cldn14	GST	Cldn14
423	Troponin I, slow skeletal muscle	F1NUT9_CHICK	19	14	8		
424	Troponin T, cardiac muscle isoforms	A0A1D5PBV6_CHICK (+3)	24	21	22		
425	Tubulin alpha chain OS=Gallus gallus	A0A1D5P198_CHICK	50	41	43	6	20
426	Tubulin alpha chain	A0A1D5NW27_CHICK	50	42	44		21
427	Tubulin alpha chain	A0A1D5PAR5_CHICK (+1)	50	21	19		10
428	Tubulin alpha chain	F1NMP5_CHICK	50	19	19	3	8
429	Tubulin beta chain	G1K338_CHICK	50	44	57		
430	Tubulin beta chain	F1NYB1_CHICK	50	57	70		32
431	Tubulin beta-2 chain	TBB2_CHICK	50	55	66		
432	Tubulin beta-5 chain	TBB5_CHICK	50	22	32		
433	Tubulin beta-7 chain	TBB7_CHICK	50	68	80	6	35
434	Tudor-interacting repair regulator protein	A0A1L1RIX9_CHICK (+1)	34	1	3		
435	Twinfilin	A0A1D5NTH5_CHICK	40	1	2		
436	Type I alpha-keratin 15	Q6PVZ2_CHICK	48	2	8	1	5
437	Type II alpha-keratin IIA	Q6PVZ5_CHICK	62	11	12	5	15
438	Type II alpha-keratin IIC	A0A146F047_CHICK (+2)	57	4	15	5	16
439	UBIQUITIN_CONJUGAT_2 domain-containing protein	F1NL19_CHICK	27				1
440	UBIQUITIN_CONJUGAT_2 domain-containing protein	Q5ZKN7_CHICK	18			2	
441	UBIQUITIN_CONJUGAT_2 domain-containing protein	A0A1L1S0T9_CHICK (+2)	27			0	2
442	Ubiquinol-cytochrome c reductase core protein 2	A0A1D5PEW4_CHICK (+2)	49	3	7		1
443	Ubiquitin carboxyl-terminal hydrolase	Q9PWC6_CHICK	109				7
444	Ubiquitin thioesterase	A0A1D5NTA0_CHICK	31		1		1
445	Unconventional myosin-I	E1C459_CHICK	116	3			
446	Unconventional myosin-Ib	A0A1D5PJ65_CHICK (+1)	132	42	38		
447	Unconventional myosin-Ic	F1NG39_CHICK	119	23	21	0	1

				Cldn14 C-Ter + Day 4		Cldn14 C-Ter + HH8	
#	Identified Proteins	Accession Number	MW (kDa)	GST	Cldn14	GST	Cldn14
448	Unconventional myosin-VI	A0A1D5PU33_CHICK (+2)	147	44	37		2
449	Unconventional myosin-Va	MYO5A_CHICK	212	79	73		0
450	Unconventional myosin-XIX	F1NN09_CHICK	47	3	1		
451	Unconventional myosin-XVIIIa	E1BY27_CHICK	232	123	114	1	0
452	VH1 protein	A0A1D5PQ15_CHICK (+8)	14				1
453	Vimentin	F1NJ08_CHICK	53	107	93	4	22
454	Vitellogenin-1	VIT1_CHICK	211		1	25	54
455	Vitellogenin-2	VIT2_CHICK	205	2		56	94
456	Vitellogenin-2	F1NFL6_CHICK	205	1	3	53	95
457	Vitellogenin-3 (Fragments)	VIT3_CHICK	38				9
458	Voltage-dependent anion channel	A0A1L1RLH6_CHICK (+2)	31	6	10	4	15
459	WD repeat-containing protein 89 i	F1NLN8_CHICK	43				2
460	WD_REPEATS_REGION domain-containing protein OS=Gallus gallus GN=DCAF7 PE=2 SV=1	Q5ZIT1_CHICK	39		1		
461	WD_REPEATS_REGION domain-containing protein OS=Gallus gallus GN=GNB4 PE=4 SV=2	E1BW98_CHICK	38		1		
462	WH2 domain-containing protein OS=Gallus gallus GN=JMY PE=4 SV=2	E1C822_CHICK	102	6	3		
463	WH2 domain-containing protein OS=Gallus gallus PE=4 SV=2	R4GH27_CHICK	58	9	5		
464	X-ray repair cross-complementing protein 5 OS=Gallus gallus GN=XRCC6 PE=4 SV=3	F1NED5_CHICK (+1)	70		2		
465	Xin actin-binding repeat-containing protein 1 OS=Gallus gallus GN=XIRP1 PE=4 SV=2	F1NUI2_CHICK	285	26	29		0
466	dUTPase domain-containing protein OS=Gallus gallus GN=DUT PE=2 SV=1	Q5ZKJ3_CHICK	18	2		1	
467	elongation factor Ts, mitochondrial (blasted) OS=Gallus gallus PE=4 SV=1	A0A1D5PZP4_CHICK (+1)	47		2		2

				Cldn14 C-Ter + Day 4		Cldn14 C-Ter + HH8	
#	Identified Proteins	Accession Number	MW (kDa)	GST	Cldn14	GST	Cldn14
468	myosin phosphatase Rho-interacting protein	A0A1D5PV45_CHICK (+1)	125	32	25		
469	plastin-3 (blasted) OS=Gallus gallus GN=PLS3 PE=4 SV=1	A0A1D5PE96_CHICK (+1)	71	1		0	
470	polymerase delta-interacting protein 2 (blasted) OS=Gallus gallus GN=POLDIP2 PE=4 SV=2	F1NNL9_CHICK (+1)	43		2		2
471	tRNA-splicing ligase RtcB homolog OS=Gallus gallus GN=RTCB PE=3 SV=2	F1NYI3_CHICK	55	1	7		6
472	voltage-dependent anion-selective channel protein 3 isoform X3 (blasted) OS=Gallus gallus GN=VDAC3 PE=4 SV=1	A0A1D5Q021_CHICK (+2)	32		1		2

Table Appendix C: Protein Information Identified by Mass Spectrometry for Cldn14 C-Terminal Domain Interacting Partners
These data describe the proteins identified by mass spectrometry to interact with either GST or Cldn14 C-terminal domain samples bound to HH8 or Day 4 chick extract. This table shows the identified proteins, their accession numbers, their alternate ID, their molecular weight, and the number of times the protein was seen in GST samples and in Cldn8 C-terminal domain samples for either HH8 or Day 4.